NTNU
Norwegian University of Science and Technology

Compact Subsea Separation Unit:

Nonlinear Model Predictive Control and Nonlinear Observers

Petter Norgren

Master of Science in Engineering Cybernetics

Submission date: December 2011
Supervisor: Lars Imsland, ITK
Co-supervisor: Gisle Otto Eikrem, Statoil

Norwegian University of Science and Technology
Department of Engineering Cybernetics

NTNU – Trondheim
Norwegian University of
Science and Technology

COMPACT SUBSEA SEPARATION UNIT:

NONLINEAR MODEL PREDICTIVE CONTROL AND NONLINEAR OBSERVERS

PETTER NORGREN

MASTER THESIS in ENGINEERING CYBERNETICS
Trondheim, December 2011

Supervisor: PROFESSOR LARS IMSLAND
Supervisor at Statoil: PHD GISLE OTTO EIKREM

NORWEGIAN UNIVERSITY OF SCIENCE AND TECHNOLOGY
Faculty of Information Technology, Mathematics and Electrical Engineering
Department of Engineering Cybernetics

NTNU
Norwegian University of Science and Technology

Master thesis in Engineering Cybernetics

Compact Subsea
Separation Unit:
Nonlinear model predictive control
and nonlinear observers

Faculty of Information Technology,
Mathematics and Electrical Engineering

Department of Engineering Cybernetics

Project written at NTNU, 2011

Printed by TAPIR-trykk

NTNU
Faculty of Information Technology, Mathematics and Electrical Engineering
Department of Engineering Cybernetics

PROJECT DESCRIPTION SHEET

Name of the candidate: Petter Norgren

Thesis title (Norwegian): Ulineær MPC og observere for et kompakt separasjonssystem

Thesis title (English): Nonlinear MPC and observers for a compact separation system

Background

A future subsea compact separation system, to be used at deep waters, is under development. The system will separate gas and liquid from the wells at the seabed and boost the gas and liquid up to the surface by use of a compressor and a pump. Since this system is much more compact than traditional separation processes, an advanced process control system is required. A laboratory test unit of this system has been developed and will be used as process in this project work. A dynamic simulator of this process is available, with a nonlinear model. An initial observer is implemented, but not used for control.

The compact process system requires a high speed MPC solution which makes computation time a significant aspect. The programming languages to be used are C++ and Matlab. Statoil's internal MPC tool Septic will be used for process control.

Work description

1. Do a literature study on observers/NMPC for nonlinear processes/models.
2. Set up a control structure involving nonlinear MPC which uses the estimated states/parameters from the observer. Discuss appropriate parameters to estimate online/offline to achieve offset-free (integral) control. If time permits, use process data to update the observer.
3. Run simulation study of different process disturbances, including evaluation of the numerical properties of the NMPC and observer(s).
4. Recommend start up and shut down sequences.
5. Discuss the performance of the control system and suggest further work.

Start date: 28 August, 2011 **Due date:** January, 2012

Supervisor: Lars Imsland
Co-advisor(s): Gisle Otto Eikrem, Statoil

Trondheim, __12.12.2011__________

______

Lars Imsland
Supervisor

Address
Sem Sælandsvei 5
NO-7491 Trondheim

Org.no. 974 767 880
E-mail:
postmottak@itk.ntnu.no
http://www.itk.ntnu.no

Location
O.S. Bragstads plass 2D
NO-7034 Trondheim

Phone
+ 47 73 59 43 76
Fax
+ 47 73 59 45 99

Phone: + 47 47 23 19 49

Abstract

In search of increased wealth and public prosperity, the oil industry have met new challenges in their quest for black gold. These challenges have driven Statoil's expertise to develop a compact subsea separation unit. The compact structure of this unit makes advanced process control a requirement. The study of this thesis will focus on configuring a NMPC with state process information supplied by a nonlinear observer. The study will be based on previous work on the Compact Separation unit. Statoil's internal MPC tool will be used for process control.

The state and parameter estimation performance of the implemented observers has been assessed with regards to both measurement noise and model/plant mismatches. This has been performed through simulations on the implemented model, but tests have also been conducted on an off-line data set from a test rig of the compact separation unit. The observers provided sufficiently accurate state estimates, with the exception being when the estimates were based on too severe measurement noise. The parameter estimation scheme proved to be suboptimal, but provided vital information during tests on the off-line data set.

The NMPC configuration developed during this project has been tested on several process disturbances, and have provided good results regarding regulation of the process within the desired control objectives. The configuration have proved to fulfill the performance criteria specified, both with the use of ideal process information and estimates supplied by the observers.

Digital-copy

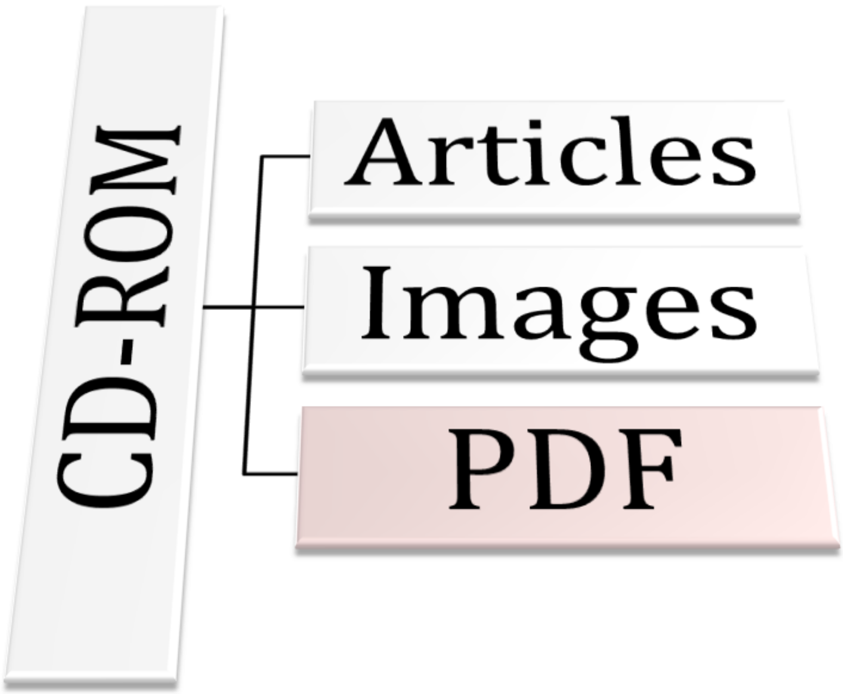

Preface

This thesis has been submitted as the diploma in my Master of Science degree in Engineering Cybernetics; and concludes five and a half years of hard work at the Norwegian University of Science and Technology.

I would like to thank my supervisor Lars Imsland at the department of Engineering Cybernetics as well as my co-supervisor Gisle Otto Eikrem for their help and support during this challenging work. The project on the Compact Separation unit have given me valuable experience into industrial MPC applications, and the knowledge that my work can help drive a challenging project forward has been a huge motivational boost.

I am also deeply indebted to my fellow students and friends, whom have provided invaluable suggestions through reviews, as well as formidable editing and support. Special thanks to:

Aleksander Børresen Eilertsen & *Linn Ingrid Berggård.*

Contents

List of Figures

List of Tables

List of Abbreviations

CV	Control Volume
CVR	Control Variables
DL	De-liquidizer
DVR	Disturbance Variables
EKF	Extended Kalman Filter
GLCC	Gas-Liquid Cylindrical Cyclone
GVF	Gas Volume Fraction
KF	Kalman Filter
LVF	Liquid Volume Fraction
MHE	Moving Horizon Estimation
MPC	Model Predictive Control
MVR	Manipulated Variables
NMHE	Nonlinear Moving Horizon Estimation
NMPC	Nonlinear Model Predictive Control
ODE	Ordinary Differential Equation

PDF	Probability Density Function
PS	Phase Splitter
SEPTIC	Statoil Estimation Prediction Tool for Identification and Control
TVR	Trend Variables
UKF	Unscented Kalman Filter

PART I

Introduction to the Compact Separation unit

Abstract – This part is an introduction to the report as well as to the Compact Separation process. The first chapter gives an overview of the report and the work previously conducted on the process. The next and last chapter of this part provides an overview of the process, explains the modeling and the simplifications made and also introduces the separation profiles.

The Norwegian oil adventure started in the late 1960s. Several different oil companies were given a license from the Norwegian government to start exploring for oil and gas on the Norwegian Continental Shelf. After several failed attempts, most of the large oil companies were on the verge of abandoning the possibility of ever finding oil in Norway. At the end of the summer of 1969, the oil company Phillips Petroleum decided to drill one last well on the Norwegian Continental Shelf. This final attempt stroke gold. The field now known as Ekofisk was discovered, an “elephant” was revealed. An “elephant” is the codename for an oilfield greater than 500 million barrels. This oil finding marked the start of the Norwegian oil adventure, and in the wake of this finding, both the Norwegian Petroleum Directorate and the government-owned oil company, Statoil, was founded[1].

Today, more than 40 years after Ekofisk was found, the oil and gas industry is experiencing new challenges. Many of the larger oil and gas fields are old and the efficiency at these fields is not what it used to be. New fields have been found, but many of these fields are relatively small and do not justify building of a complete new oil extraction installation. A solution would be to transport the oil and gas to an existing installation, but today’s multiphase technology does not fulfill the requirements to transport oil and gas over such vast distances. Another issue is the depths of the new fields. Much new subsea technology have been developed, however, these depths sets new and challenging requirements when it comes to robustness and size. The cost of new technology demands higher performance and better efficiency from these new developments compared to the old systems, thus more delicate control is required.

The issues described above drives the development of Statoil’s Compact Subsea Separation Unit, later referred to as the Compact Separation process. This system will be designed for very deep waters, and the compact structure of the unit will require more complex process control than traditional separation units.

[1]More information about the Norwegian oil history can be found at http://tekniskmuseum.no/gamlewebben/no/utstillingene/Jakten_oljen/historie.htm.

Chapter 1
Overview

The main purpose of the Compact Separation process is to separate the multiphase input flow into two single phases – liquid and gas. The pure liquid will be boosted to the surface using a pump, while the gas will be transported to the surface by the means of a compressor. The structure of the Compact Separation process will be further discussed in the next chapter.

1.1 Earlier work

The Compact Separation project started in 2007, and phase 1 of the project was completed in May 2011. Consequently, a lot of previous work has been conducted in regard to this project. The modeling of the Compact Separation process started with a summer project in 2007, and the modeling was further developed by [Ellingsen (2007)]. [Ellingsen (2007)] also conducted some initial research on the control strategy of the Compact Separation process, and concluded that model predictive control (MPC) would probably be the best control strategy, due to the complexity of the process.

In early 2008, [Nilsson (2008)] takes the development of the MPC strategy further by allowing nonlinearities in the model. This can lead to tighter and more accurate control. The concluding remark by [Nilsson (2008)] is that the introduction of nonlinear model predictive control (NMPC) to the Compact Separation process should be considered. [Grimstad (2008)] took the development of the model, as well as the NMPC algorithm, further and evaluated the performance of the NMPC when the Compact Separation process experiences hydrodynamic slugging[1] on the input. The control strategy was revised to perform better under steady state and under slugging sequences.

[Kristiansen et al. (2010)] report the test results from a high-pressure flow loop at SINTEF. The objective of these tests were to conduct proof of concept, and demonstrate the Compact Separation process. However, the test rig used was not a complete setup of the Compact Separation process, but rather a simplified version of the process. The simplifications in the process will be further discussed in the next chapter. The report concludes that the concept has been successfully demonstrated, and that further work on this project should be conducted. The report also concludes that MPC is the recommended control strategy.

However, according to PhD Gisle Otto Eikrem, co-supervisor of this project, the prediction step of the MPC was poor, and the success of the control system was due to the feedback of measurements. This result suggests that the model used for prediction is inaccurate and it is therefore desirable to implement nonlinear relationships in the controller.

During the summer of 2011, the author contributed to implementing a nonlinear observer scheme to estimate the states used by the NMPC for control purposes, however, this scheme was not used for control of the Compact Separation process[Steinshamn and Norgren (2011)].

[1]Hydrodynamic slugging is explained in Chapter 10 [p.75]

1.2 Contributions to the Compact Separation project

The work presented in this thesis will contribute to the Compact Separation project by carrying on the work on the implementation of the observers. This project will focus on the use of the implemented observers for control and evaluating the differences regarding robustness to measurement noise and model/plant uncertainties. A controller will also be configured to deal with appropriate process disturbances. The work has included extensive debugging, both in the implemented observers and in the process model used by the controller.

1.3 Report outline

Part I - Introduces the report and presents the model of the Compact Separation process with simplifications and potential problems.

Chapter 2 - Presents the mathematical model of the Compact Separation process, and the simplifications made.

Part II - Presents some brief theory on the different estimation and control techniques considered for the Compact Separation process.

Chapter 3 - Summarizes the background and some requirements for choice of a control algorithm.

Chapter 4 - Briefly presents theory, with pros and cons, for the different solutions to the NMPC scheme.

Chapter 5 - Discusses several schemes for estimating the states of a nonlinear process.

Chapter 6 - Discusses several schemes for estimation of uncertain parameters in a nonlinear process and some theory on parameter estimation.

Part III - Introduces different configurations used for control of the Compact Separation process.

Chapter 7 - Discusses the old strategy used for control.

Chapter 8 - Presents the new control strategy developed during this project.

Part IV - Presents the simulation results of the implemented controller and observers.

Chapter 9 - Gives the results of the observers performance, both with respect to the ideal process model and with respect to a off-line dataset.

Chapter 10 - Shows the results from the slugging case.

Chapter 11 - Shows the results from the start-up case.

Chapter 12 - Shows the results from the shut-down case.

Aftermath - Summarizes the project, discusses the results and what the next step should be.

Chapter 13 - Discusses the results of the work done through this project.

Chapter 14 - Concludes the performed work and suggests further work on the Compact Separation process.

Chapter 2
The Compact Separation process

2.1 Process description

An overview of the Compact Separation process is shown in Figure 2.1 [p.8] and, as can be seen from this figure, the gas-liquid separation is performed in two stages. The first, rough, separation is performed by a Gas-Liquid Cylindrical Cyclone (GLCC). The GLCC is a simple, low-weight and low-cost separator which is much more compact compared to the traditional gravity based vessel-type separator. The GLCC will only perform well on low flow rates, on high flow rates, the separation performed by the GLCC will be coarse. Therefore, a finer separation will be needed in order to reach the separation criteria set by the area of operation of the pump and compressor, as will be discussed later in this chapter.

From the GLCC there are two outlets, one liquid outlet and one gas outlet. Downstream the liquid outlet of the GLCC, a Phase Splitter (PS) is connected, while downstream the gas outlet a De-liquidizer (DL) is attached. The PS will perform a more precise extraction of gas from the liquid flow, while the DL will remove as much as possible of the liquid left in the gas flow.

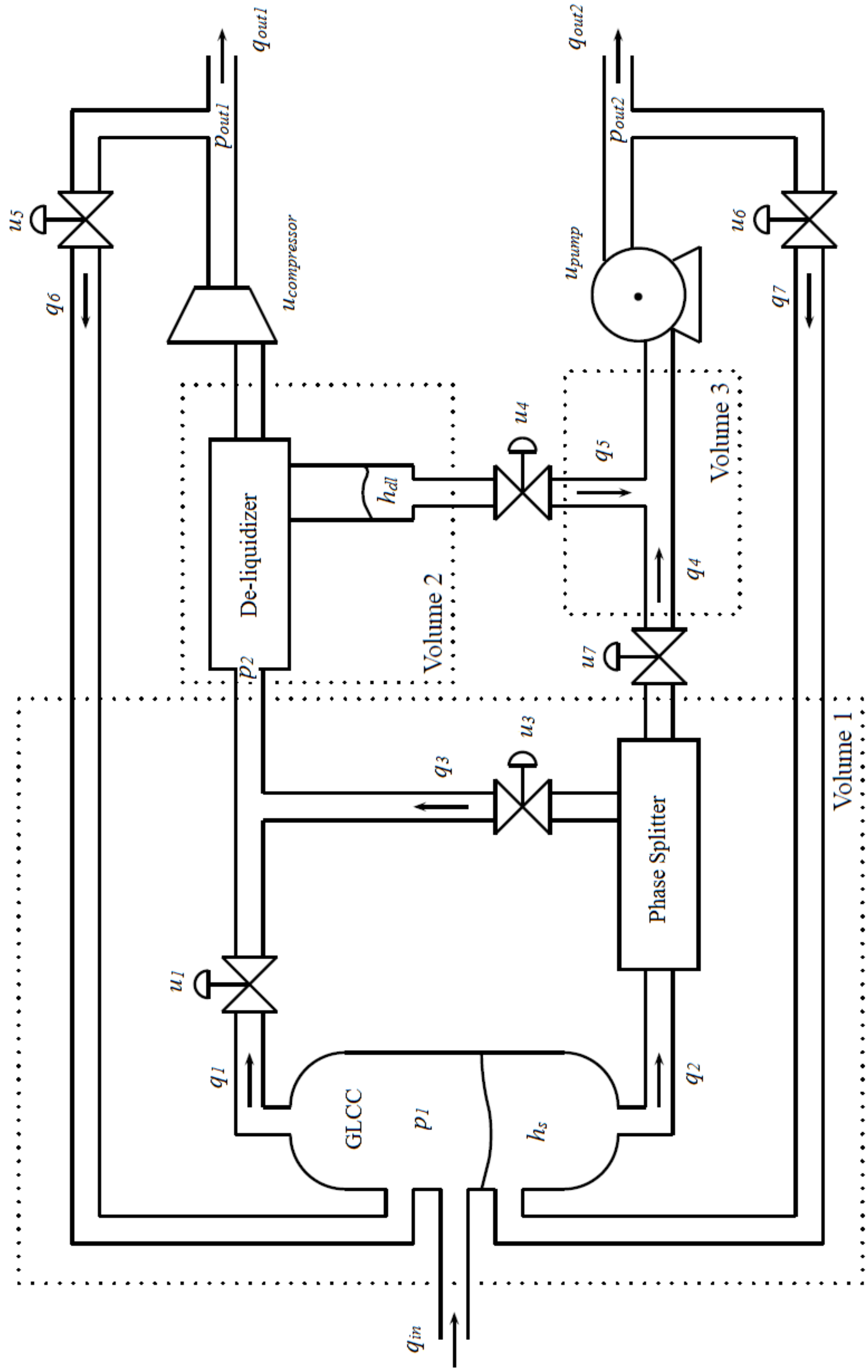

Figure 2.1: Overview of the Compact Separation process[Grimstad (2008)]

Both the DL and the PS are co-axial cyclones with a stationary swirl element and a centered gas extraction pipe[Kristiansen et al. (2010)]. This means that the separation is performed by rotating the unit and creating a centrifugal force, so the liquid will form an annular flow along the walls of the cylinder, while the gas will be concentrated in the middle[Grimstad (2008)].

Several valves have been placed on strategic places in the system, as can be seen from Figure 2.1 [p.8]. These valves will be the manipulated variables in the control system, and by controlling these valves the controller must assure that both the pump and compressor will be supplied with sufficiently pure liquid and gas respectively. This desire reasons to the superior performance of single phase pumps and compressors compared to their multiphase rivals. The single phase pump and compressor does, however, have an upper/lower bound on the gas volume fraction (GVF) in the flow; to avoid malfunction of the boosters, the control system must meet these control objectives.

In Figure 2.1 [p.8] it can also be seen that the Compact Separation process has two recirculation pipelines. With these recirculation pipelines, the control system will be able to provide the system with a certain minimum input flow rate. This is necessary, due to the pump and compressor's required minimum flow rate. Both the pump and the compressor might stall if their flow rates fall below this limit. Recirculating compressed gas in this manner will most likely cause issues with the thermodynamics of the system, since compressing gas leads to an increase in the temperature of the gas. However, neither the thermodynamics nor the recirculation pipelines are within the scope of this thesis and will therefore not be discussed further.

2.2 Process model

The model presented in this section has been developed in earlier work, and are presented by [Grimstad (2008)]. This model is explained in this chapter, and the simplifications made are discussed. In the earlier works presented at the start of the previous chapter, the focus was on the complete Compact Separation process, shown in Figure 2.1 [p.8]. During the summer of 2010, Statoil tested a linear MPC on a simplified setup of the Compact Separation process at SINTEF Multiphase Flow Laboratory in Trondheim, Norway. New tests has been scheduled for the summer of 2012 on this simplified test rig, and as noted in Chapter 1 [p.3], linear MPC proved to be inadequate.

As illustrated in Figure 2.1 [p.8] the process has been divided into separate control volumes (CV). The model presented in this chapter does not include the recirculation flows nor the pump; and the compressor has been replaced with a valve. As a consequence of removing the pump and the belonging recirculation flow, the third CV has been neglected to simplify the model. The resulting process is shown in Figure 2.2 [p.11].

These simplifications are obviously not realistic; a model based on these simplifications will not reflect the real process, however, the simplified model shown in Figure 2.2 [p.11] is an adequate description of the test unit at SINTEF[Kristiansen et al. (2010)]. Due to the new tests scheduled for the summer of 2012, this thesis will focus on the simplified Compact Separation process.

Differential equations

To model the Compact Separation system, the process has been divided into control volumes. With this approach, a mass balance for each CV can be expressed by using conservation of mass. The equation for conservation of

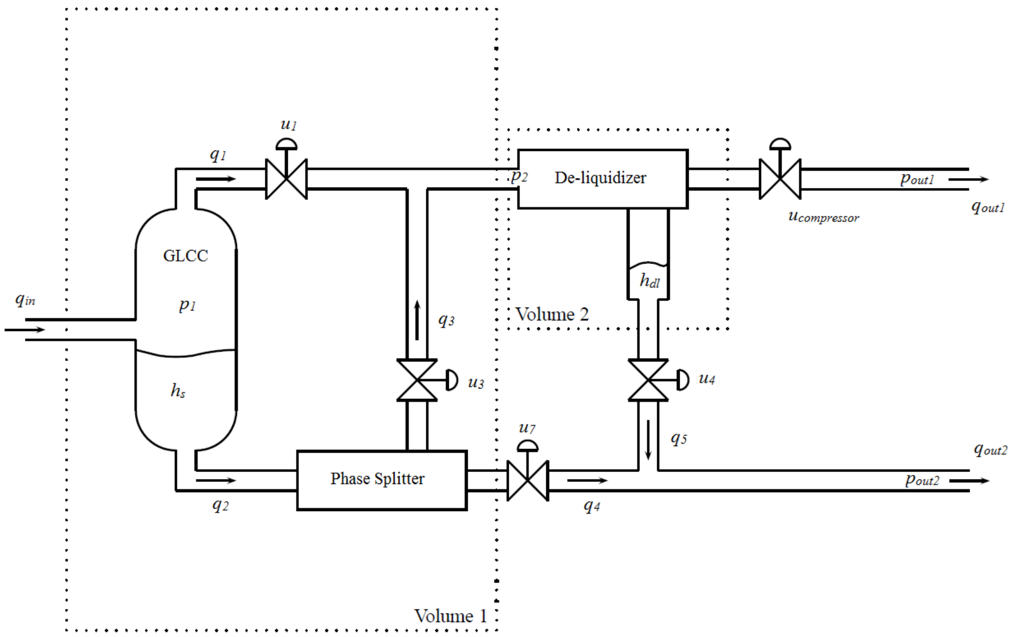

Figure 2.2: Overview of the simplified Compact Separation process

mass can be found in [White (2006)], and are shown in Equation 2.1 [p.11] below.

$$\dot{m} = w_{in} - w_{out} \tag{2.1a}$$

$$w = \rho q \tag{2.1b}$$

In Equation 2.1b [p.11], ρ is the density of the flow and q is volumetric flow rate. To introduce gas-liquid separation into the process the conservation of mass was split onto two separate equation-sets. One set conserving mass with regards to gas, and another with regards to liquids. The simplified Compact Separation process can thus be described by four differential equations, shown in Equation 2.2 [p.12]. The equations are subscripted, where the L stands for liquid, G is for gas; and 1 and 2 are separating between the two CVs.

$$\dot{m}_{1L} = w_{in1,L} - w_{out1,L} \tag{2.2a}$$

$$\dot{m}_{1G} = w_{in1,G} - w_{out1,G} \tag{2.2b}$$

$$\dot{m}_{2L} = w_{in2,L} - w_{out2,L} \tag{2.2c}$$

$$\dot{m}_{2G} = w_{in2,G} - w_{out2,G} \tag{2.2d}$$

The mass flow in the differential equations shown above consists of different volumetric flows with different density. To solve the differential equations above, knowledge about the quantity of gas and liquid in each flow is needed. The fraction of gas in the flow will be expressed by the gas volume fraction (GVF). The rest of the mass in the flow is defined as liquid, which in turn provides the liquid volume fraction (LVF). The LVF is therefore equal to 1 - GVF. The complete model dynamics for the Compact Separation process is given in Equation 2.3 [p.12].

$$\dot{m}_{1L} = \rho_L\Big[(1-\delta)q_{in} - (1-\alpha)q_1 - (1-\nu)q_3 - (1-\sigma)q_4\Big] \tag{2.3a}$$

$$\dot{m}_{1G} = \delta\rho_{in}q_{in} - \alpha\rho_1 q_1 - \nu\rho_1 q_3 - \sigma\rho_L q_1 \tag{2.3b}$$

$$\dot{m}_{2L} = \rho_L\Big[(1-\alpha)q_1 + (1-\nu)q_3 - (1-\eta)q_5 - (1-\mu)q_{out1}\Big] \tag{2.3c}$$

$$\dot{m}_{2G} = \alpha\rho_1 q_1 + \nu\rho_1 q_3 - \eta\rho_2 q_5 - \mu\rho_2 q_{out1} \tag{2.3d}$$

In Equation-set 2.3 [p.12], $\delta, \alpha, \sigma, \nu, \mu$ and η are the GVFs of different separations in the process. An explanation of the different separation degrees are given in Table 2.1 [p.13], and are further discussed in Section 2.3 [p.15].

In its current form, Equation 2.3 [p.12] has several variables. These variables are density, flow and separation degrees; and all of these variables

δ	–	GVF in input to GLCC.
α	–	GVF in gas outlet of GLCC.
β	–	GVF in liquid outlet of GLCC.
σ	–	GVF in liquid outlet of PS.
ν	–	GVF in gas outlet of PS.
μ	–	GVF in gas outlet of DL.
η	–	GVF in liquid outlet of DL.

Table 2.1: List of separation variables

must be modeled to complete the process model. To be able to model the flow between different control volumes, the pressure in the CVs must be modeled. [Grimstad (2008)] models the pressure in the CVs using the ideal gas law$_{\text{[White (2006)]}}$. The ideal gas law for the pressure in CV number x is given in Equation 2.4 [p.13], where R represents the universal gas constant[1].

$$p_x = \frac{m_{xG}RT}{MV_x} \tag{2.4}$$

The pressure inside CV1 and CV2 can now be modeled. The temperature of the system is assumed constant, which is not a reasonable assumption if the recirculation flows are taken into account, however, for the test rig, this assumption is acceptable. The molar mass, M, of the gas has also been assumed constant in the model. The average molar mass of a mixture can be calculated from knowledge of the quantity of the different molecules in the gas. By assuming this quantity is constant, the average molar mass of the gas can be assumed constant. The volume of the gas, V, is modeled using

[1] R has the value $8.314 J \cdot K^{-1} \cdot mol^{-1}$

the relationship shown in Equation 2.5 [p.14]. V_{CVx} is the total volume of control volume number x.

$$V_{xG} = V_{CVx} - \frac{m_{xL}}{\rho_L} \tag{2.5}$$

With a model for the pressure in place, a model for the flow can be expressed. [Grimstad (2008)] models the flow as a function of the valve openings, as shown in Equation 2.6 [p.14].

$$q = C(u)\sqrt{\frac{\Delta p}{\rho_{eff}}} \tag{2.6}$$

In Equation 2.6 [p.14], $C(u)$ is a function to restrict the flow based on the current valve opening, which is represented by u. Δp is the difference in pressure between the CVs that the flow is running to and from. ρ_{eff} is the effective density of the flow, and is a function of the separation degrees presented in Table 2.1 [p.13], denoted by S in Equation 2.7 [p.14]. C_{max} and K are constants that define the characteristics of the valve, i.e. the maximum flow rate and the minimum time used to open/close the valve$_{\text{[Grimstad (2008)]}}$.

$$C(u) = C_{max}\Big(K^{u-1} - K^{-1}\Big) \tag{2.7a}$$

$$\rho_{eff} = (1 - S)\rho_L + S\rho_x \tag{2.7b}$$

The mass of the gas in CV 1 and CV 2 is also used to model the density of the gas. The model of the gas density is shown in Equation 2.8 [p.14].

$$\rho_x = \frac{m_{xG}}{V_{xG}} \tag{2.8}$$

Disturbances

The variables δ, ρ_{in}, q_{in}, p_{out_1} and p_{out_2} in Equation 2.3 [p.12] are disturbances. This means that these variables can not be controlled, and they might be unpredictable. This is not entirely true for all the variables listed above. The input flow, as well as the GVF of the input flow, can be controlled on a certain level, since there must be some valves controlling the input to the system. However, defining these variables as disturbances means that the control system should assume that they are uncontrollable. This can for example be because of simplifications to the modeling, or computational complexity. Some variables, will be uncontrollable and uncertain, and must be defined as disturbances, like ρ_{in}.

2.3 Separation profiles

The only variables left to be modeled in Equation 2.3 [p.12], are the separation profiles. Modeling of the separation profiles is not easy, and they inhabit large nonlinearities. The separation profiles currently implemented will be presented in this chapter.

GLCC

The separation profile of the GLCC[2] is the simplest. When the flow rate into the GLCC is low, the GLCC will function as a small gravity separator. However, at high flow rates the separation degree of the GLCC will be more crude, thus making the separation profile of the GLCC a function of the fluid holdup time. The separation profile of the GLCC, based on the fluid holdup time, is shown in Equation 2.9 [p.17]. This model was found in the implemented computer code.

[2]GLCC: Gas-Liquid Cylindrical Cyclone

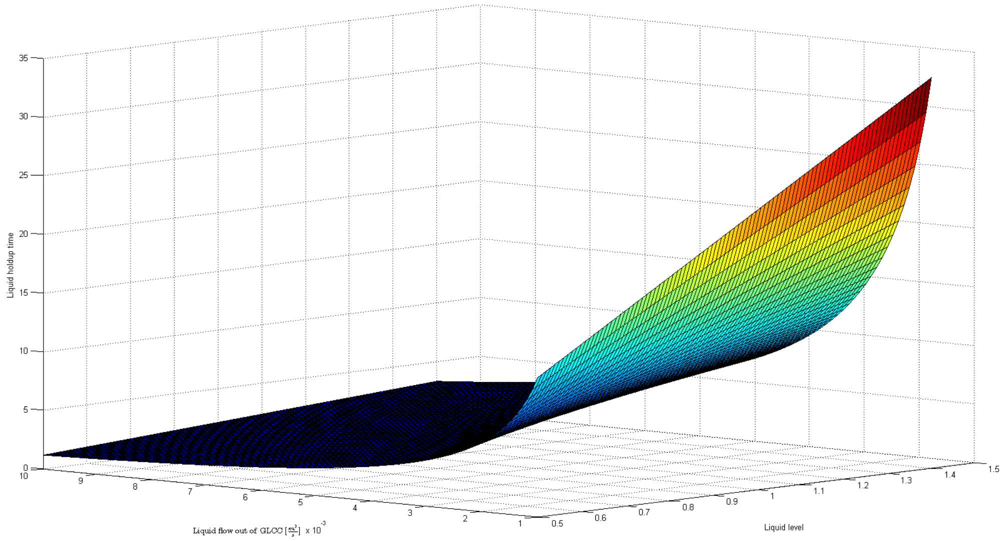

(a) Liquid holdup time vs. liquid flow out and liquid level in GLCC

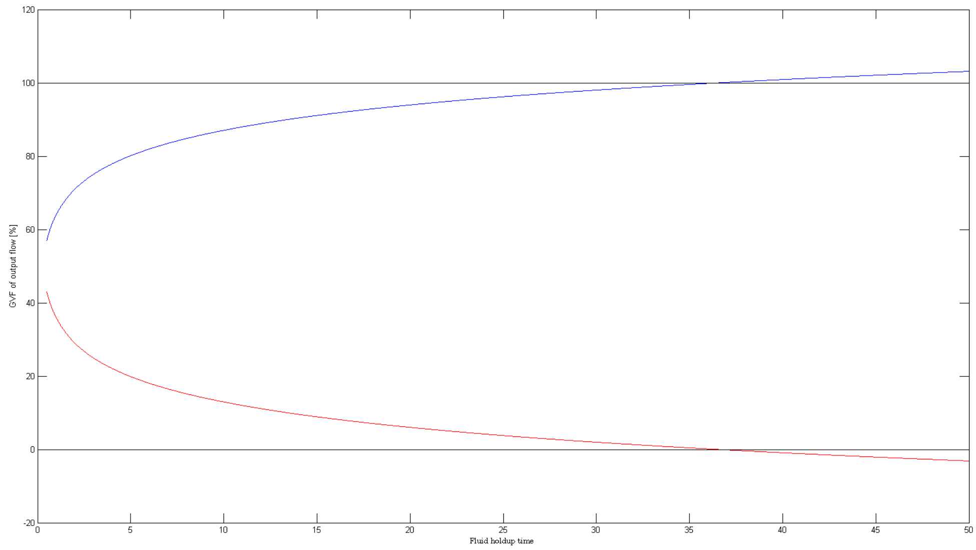

(b) Separation of gas and liquid vs. fluid holdup time

Figure 2.3: Separation profile of the GLCC

$$\alpha = 0.1 \cdot log\,(30\tau_{gas}) + 0.3 \tag{2.9a}$$

$$\beta = -0.1 \cdot log\,(30\tau_{liquid}) + 0.7 \tag{2.9b}$$

The holdup time will depend on the size of the GLCC, on the liquid level in the tank, and on the liquid and gas flow out of the GLCC at a given time. This way, a larger flow into the GLCC will give smaller holdup time in the GLCC. A lower liquid level in the GLCC will also result in a smaller holdup time, thus creating a cruder separation of liquid and gas. Figure 2.3 [p.16] illustrates the liquid holdup time versus liquid level and liquid flow out of the GLCC. This figure was created from Equation 2.9 [p.17] and from the equations defining the fluid holdup time, found in the computer code.

Phase Splitter

The separation profile of the PS[3] is more complex and contains more variables. The separation in the liquid outlet of the PS is based on the inlet conditions, which is the inlet flow and the GVF[4] of the inlet flow. The GVF of the liquid outlet will also depend on how much gas that is removed from the inlet flow.

The separation in the gas outlet of the PS also depends on the inlet conditions, but in a different manner than the liquid separation. The current separation depends on the separation degree from the previous time step, as well as the total inlet flow to the PS. The PS is designed to operate above a specific operating point with regards to flow rate; below this operating point, the PS will not be able to separate the gas and liquid properly in the

[3]PS: Phase Splitter

[4]GVF: Gas volume fraction

gas outlet. The liquid separation will not be affected by this operating point in the same manner. But since the PS is placed downstream from the GLCC, which operates best at small flow rates, the PS will only experience a small flow rate when the flow into the PS has a relatively low GVF. A small flow rate into the PS will therefore cause the flows out of both the PS outlets to contain mostly liquid. The controller must shut the valve between the PS and the DL when this happens to prevent a degradation of the separation through the DL – due to bad inlet conditions.

De-Liquidizer

The separation in the liquid outlet of the DL[5] tank is identical to the separation profile in the liquid outlet of the GLCC, presented in Equation 2.9b [p.17]. The liquid holdup time will, as with the GLCC, depend on the size of the tank and on the liquid flow out of the DL, both in the gas outlet and the liquid outlet.

In the gas outlet of the DL, the separation profile is calculated in a similar way as the separation profile of the flow in the gas outlet of the PS. The DL also has an operating point, and flows that falls beneath this operating point will not be separated properly. The separation of the fluids will also depend on the inlet flow and inlet GVF, as in the other separation profiles.

The separation profiles for the PS and the DL is much more complex than the separation profile for the GLCC. These separation profiles consist of a large number of variables, and this makes a graphical representation of these profiles hard. The modeling of the separation profiles are based on experiments and tests outside the scope of this thesis and will therefore not be discussed further.

[5]DL: De-liquidizer

PART II

Estimation and Control Theory

Abstract – This part presents theory on the chosen control strategy as well as theory on several nonlinear observers. The first chapter discusses the background for the implemented controller and why an observer must be introduced, while the next chapter presents theory on NMPC. The last two chapters present theory on nonlinear observers, with respect to state estimation and parameter estimation.

Controlling nonlinear systems is one of the biggest challenges in modern control theory. Almost all physical systems are nonlinear in nature, however, these systems are often linearized so the well known linear control theory may be applied. Due to the desired high performance control of many modern industrial processes, pure nonlinear control systems are becoming more and more popular.

Nonlinear control methods are often more suited to handle physical limitations and constraints than their linear counterpart. The reason for this is that a constrained system will be nonlinear, even if the constraints are linear themselves. Constraints are not always an important issue, but they can also be crucial for the robustness and reliability of the controller. Examples of this can be: An electro-motor having angular velocity limits, or a tank with a constraining volume. To ignore these constraints in the design of the controller, can in the worst case, lead to disastrous results.

A common problem with both linear and nonlinear control, is the issue of attaining information about the internal states of a given process. In a typical control system, some internal states can be measured, but it is often too expensive or too hard to measure all internal states. In some cases it might even be impossible.

This issue has led to the development of a branch of statistics and signal processing called estimation theory. This is the theory of how to estimate unknown states and/or parameters based on measurements, statistical data and often a process model. As with control theory, estimators have both linear and nonlinear versions. The Kalman filter and the moving horizon estimator are among the most famous and popular estimators today.

Chapter 3
Background

As noted in Chapter 2 [p.7], the test rig at SINTEF used a linear MPC solution for control. The Compact Separation process is inherently nonlinear, and therefore, it is desirable to implement a nonlinear controller. In Statoil's internal MPC tool, Statoil Estimation Prediction Tool for Identification and Control (SEPTIC), it is currently implemented a nonlinear MPC algorithm, but this controller, and the nonlinear separation profiles discussed in Chapter 2 [p.7], have not been thoroughly tested. Nor has the controller been tuned to satisfy the control objectives of the Compact Separation process.

Figure 3.1 [p.22] shows a block diagram of a typical control system with an observer in place. Advanced controllers, such as the NMPC, requires knowledge of all internal system states to be able to successfully control the system. All the internal states of a process is normally not available to the controller, the sensors will only measure a subset of the states or measure variables that are related to the states by some mathematical model. To gain access to all states, some sort of observer must be implemented with a model of the process. The observer does not need to have feedback from the process[1]. If this is the case, a small deviation between

[1]This is much like sitting in a room with with a wall-clock, but no windows; trying to predict the weather.

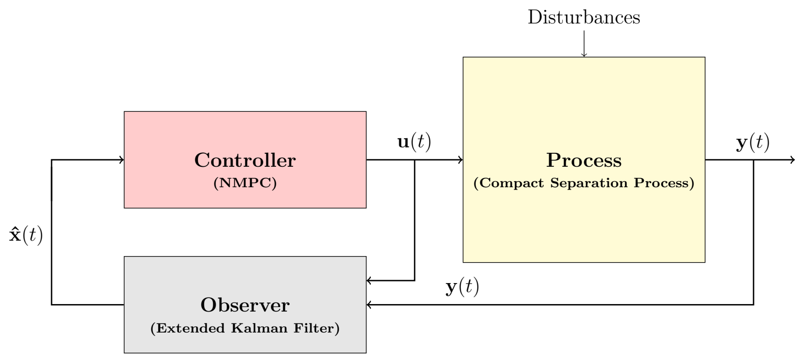

Figure 3.1: Overview of a typical control system[Steinshamn and Norgren (2011)]

the process model and the real process will cause the estimates to diverge from the real values. Therefore, feedback of measurements are almost always a requirement if the estimates are to be used in combination with the controller. However, using measurements are not without downsides. Measurements are always influenced by noise of some sort. This noise might for example be electric noise, caused by the transmission through copper wires, or it might be surface disturbances in a tank which will influence measurements of the liquid level. These problems have led to the development of several observer schemes, that combine knowledge of the process model and feedback of measurements, to get smooth and accurate estimates of the internal states. Examples of observer schemes that use variations of this method are the linear and nonlinear Kalman filter (KF) or the moving horizon estimation (MHE), which is actually a dual problem[2] of the MPC problem[Tenny and Rawlings (2002)].

The current version of SEPTIC has an observer, but this observer is not used for control of the process (the control system assumes perfect knowledge of all states). The observers that were implemented during the summer of 2011 are the unscented Kalman filter (UKF) and the extended Kalman filter (EKF)[Steinshamn and Norgren (2011)]. The differences between these two observer schemes, as well as a few other schemes will be presented later.

[2]For more information on dual problems visit en.wikipedia.org/wiki/Dual_problem

Chapter 4
Nonlinear MPC

Since the 90s, there has been an increased interest in nonlinear control. Many systems are inherently nonlinear in nature, and today's industry requires better control for economical and environmental purposes. The information in the current chapter has been found by reading the following articles: [Findeisen and Allgöwer (2002)], [Findeisen et al. (2004)] and [Marafioti et al. (2009)]. Nonlinear Model Predictive Control is a nonlinear control scheme that has received a lot of attention in the recent years. A reason for its success is its capability to handle the control problem in real-time, as well as its simple handling of physical constraints.

NMPC uses a model of the process-plant, with a set of internal process states, to predict the coming response of the open-loop system for a given prediction horizon; this horizon is named T_p. The optimal input for a given prediction horizon will be calculated from a control horizon, $T_c \leq T_p$. Note that the input is only optimal for that particular prediction horizon. Depending on the size of the prediction horizon, the input may have large deviations from the infinite horizon optimal input. The basic principle of model predictive control is shown in Figure 4.1 [p.24]. In this figure the control horizon is set equal to the prediction horizon, i.e $T_c = T_p$.

The first set of inputs calculated by the MPC will be used as inputs to

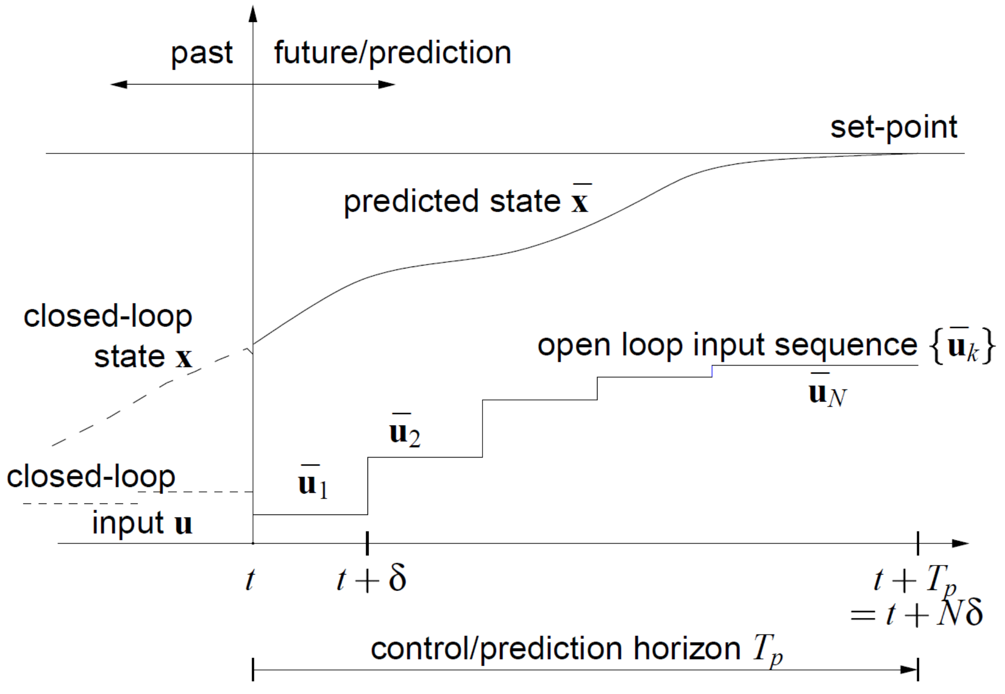

Figure 4.1: The basic principle of MPC[Findeisen and Allgöwer (2002)]

the process. When new measurements are available, at time $t+\delta$, the MPC will run the algorithm all over again and calculate a new set of inputs. δ is the sampling rate of the controller.

Equation 4.1 [p.24] shows the general discrete time state space system.

$$\mathbf{x}_{k+1} = \mathbf{f}(\mathbf{x}_k, \mathbf{u}_k) \tag{4.1a}$$

$$\mathbf{y}_k = \mathbf{h}(\mathbf{x}_k, \mathbf{u}_{k-1}) \tag{4.1b}$$

In Equation 4.1 [p.24], x_k is the state vector, u_k is the input vector and y_k is the measurement vector. With a basis in this discrete time system, the nonlinear MPC optimization problem can be states as:

$$\underset{u_0,u_1,\ldots,u_{n_p-1}}{\text{minimize}} \quad \sum_{k=0}^{n_p-1} G\left(\mathbf{x}_{k+1}, \mathbf{u}_k\right), \tag{4.2}$$

subject to:

$$\mathbf{x}_{k+1} - \mathbf{f}(\mathbf{x}_k, \mathbf{u}_k) = 0, \qquad k = 0, 1, ..., \tag{4.3a}$$

$$\mathbf{c}_x\left(\mathbf{x}_k\right) \leq 0, \qquad k = 1, 2, ..., \tag{4.3b}$$

$$\mathbf{c}_u\left(\mathbf{u}_k\right) \leq 0. \qquad k = 0, 1, ..., \tag{4.3c}$$

If it was possible to use an infinite prediction horizon – and if there were no model-plant mismatch or other disturbances, the input calculated by the MPC could be applied to the open-loop system over the whole control horizon. In real applications, neither of these assumptions are generally valid. Using an infinite prediction horizon is not possible when real-time processing is required – as it often is in a real control system. Even though many process models are developed before the real plant in industry, some model-plant mismatch generally occurs. Different types of both measurement and process disturbances are also common. Feedback is therefore a necessary requirement in real applications.

A problem with NMPC using finite prediction horizon is stability. The predicted open-loop and the real closed-loop behavior will be different, and ideally, it is desirable to use a NMPC scheme which guaranties stability regardless of tuning parameters. Several schemes have been proposed to guarantee stability, and most of these schemes achieve this property by adding suitable equality or inequality constraints to the standard NMPC setup. An example of a scheme that can guarantee stability is the scheme using a zero terminal constraint, or the scheme using a terminal region.

These schemes work by forcing each open-loop solution to end in a region where the system is stable, either a steady-state equilibrium point, or a region of attraction. Even if the schemes presented above can guarantee stability for the open-loop process model, this does not mean that the real system will necessarily be stable if there where to exist some model/plant uncertainties.

To address issues of robustness, at least three different NMPC schemes have been developed. The first solution is the min-max formulation, which modifies the cost function using the worst case disturbance. The second possibility uses the H_∞-problem in the in the NMPC framework, and the last solution optimizes a feedback controller at each sampling time. The first solution is very conservative, and might cause in-feasibility, since the worst case disturbance must be considered at all times. The H_∞-solution requires much computational time, and the same goes for the third solution. When disregarding the computational aspect, however, the third and last solution is very attractive since it is less conservative than the other solutions.

The stability analyses presented above assumes that all of the states are perfectly known. However, generally this is not the case, as previously discussed. When dealing with linear systems, the separation principle states that if the controller is stable and the observer is stable, then the combined system is also stable. This principle is not valid when dealing with nonlinear systems, and is a problem yet to be solved.

Chapter 5
State estimation

As noted before, all internal states of a process might not be available to the controller, or the measurements might be too noisy to be trusted in raw form. In this case, some sort of state estimation or filtering is necessary. This chapter will present a few observers, and their advantages and disadvantages when it comes to state estimation combined with NMPC.

5.1 Extended Kalman filter

The Kalman filter and its nonlinear extension has been in use in the industry since the 1970s and is still a popular state estimation tool. It has been well documented through the years, and there exists a lot of experience on the field of Kalman filtering. That fact and the simplicity of the nonlinear Kalman filter is the reason for its great success. However, the EKF algorithm is not without its disadvantages.

The principle of the EKF algorithm is shown in Figure 5.1 [p.28]. In the prediction step, the Kalman filter uses the previous state to predict the next state, and linearizes the nonlinear model to predict the covariance matrix. The prediction step is shown in Equation 5.1 [p.28].

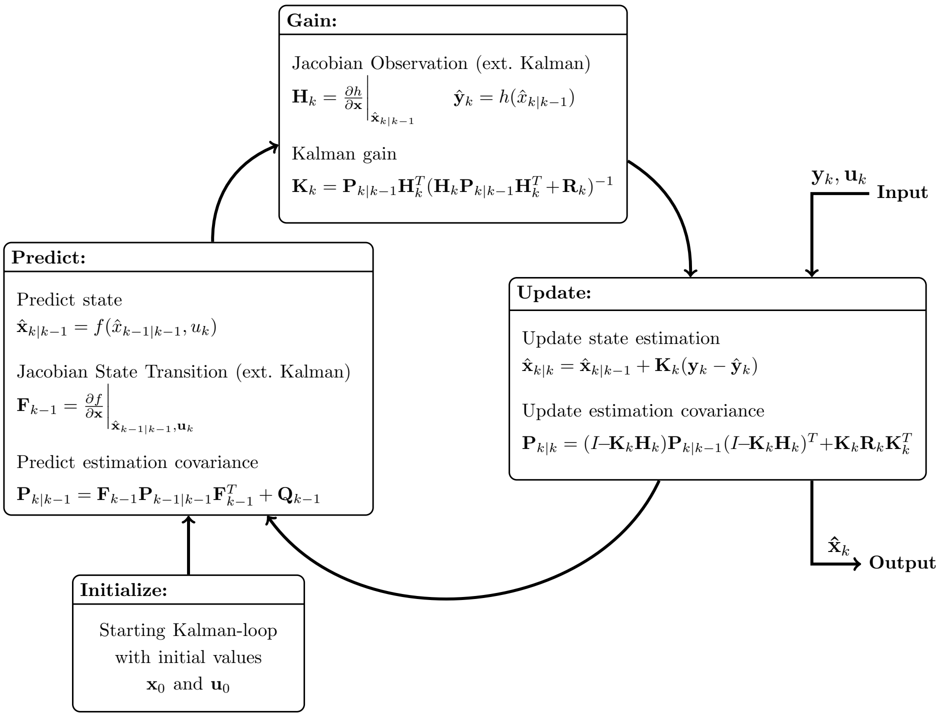

Figure 5.1: The extended Kalman filter algorithm$_{\text{[Steinshamn and Norgren (2011)]}}$

$$\hat{\mathbf{x}}_{k|k-1} = f(\hat{\mathbf{x}}_{k-1|k-1}, \mathbf{u_k}), \tag{5.1a}$$

$$\mathbf{F}_{k-1} = \frac{\partial \mathbf{f}}{\partial \mathbf{x}}\Big|_{\hat{\mathbf{x}}_{k-1|k-1}, \mathbf{u}_k} \tag{5.1b}$$

$$\mathbf{P}_{k|k-1} = \mathbf{F}_{k-1}\mathbf{P}_{k-1|k-1}\mathbf{F}_{k-1}^T + \mathbf{Q}_{k-1} \tag{5.1c}$$

In Equation 5.1 [p.28], $\hat{\mathbf{x}}_{k-1|k-1}$ is the old state vector estimate from the previous time-step and u_k is the input vector at the current time-step. $\hat{\mathbf{x}}_{k|k-1}$ and $\mathbf{P}_{k|k-1}$ is the a priori estimate of the state vector and the estimation covariance respectively, while $\mathbf{F_{k-1}}$ is the state Jacobian – based on the old state vector estimate; and finally $\mathbf{Q}_{k-1}$ is the covariance matrix of the process noise.

$$\hat{\mathbf{y}}_k = h(\hat{\mathbf{x}}_{k|k-1}) \tag{5.2a}$$

$$\mathbf{H}_k = \left.\frac{\partial \mathbf{h}}{\partial \mathbf{x}}\right|_{\hat{\mathbf{x}}_{k|k-1}} \tag{5.2b}$$

$$\mathbf{K}_k = \mathbf{P}_{k|k-1}\mathbf{H}_k^T(\mathbf{H}_k\mathbf{P}_{k|k-1}\mathbf{H}_k^T + \mathbf{R}_k)^{-1} \tag{5.2c}$$

$$\hat{\mathbf{x}}_{k|k} = \hat{\mathbf{x}}_{k|k-1} + \mathbf{K}_k(\mathbf{y}_k - \hat{\mathbf{y}}_k) \tag{5.2d}$$

$$\mathbf{P}_{k|k} = (I - \mathbf{K}_k\mathbf{H}_k)\mathbf{P}_{k|k-1}(I - \mathbf{K}_k\mathbf{H}_k)^T + \mathbf{K}_k\mathbf{R}_k\mathbf{K}_k^T \tag{5.2e}$$

Equation 5.2 [p.29] shows the update step of the EKF algorithm. $\hat{y}_k$ is the estimate of the current measurement, while $\mathbf{H}_k$ is the observation Jacobian. $\mathbf{R}_k$ is the measurement covariance and $\mathbf{K}_k$ is the Kalman gain. y_k is the current measurement vector, containing potentially noisy measurements collected from different sensors. Last, $\hat{\mathbf{x}}_{k|k}$ and $\mathbf{P}_{k|k}$ is the a posteriori estimate of the state vector and the estimation covariance.

The EKF scheme relies on linearization at each time step, to capture the nonlinearities of the system. If, however, the system has large nonlinearities between time samples, the EKF scheme will not provide a good prediction. The reason for this is that a lot of information about the process is lost during linearization. As a result of this loss of information, the EKF algorithm is not an optimal state estimator, however, the linear Kalman filter is. Another problem with the Kalman filter is that it does not handle physical constraints; neither hard, nor soft constraints. Hard constraints might be negative mass or size of a tank, while soft constraints can be a desired temperature or pressure range. Violating hard constraints can lead to infeasible solutions in the controller and unexpected behavior of the closed-loop system.

Due to the simplicity of the Kalman filter, and its superiority compared to moving horizon estimation (MHE) when it comes to run-time

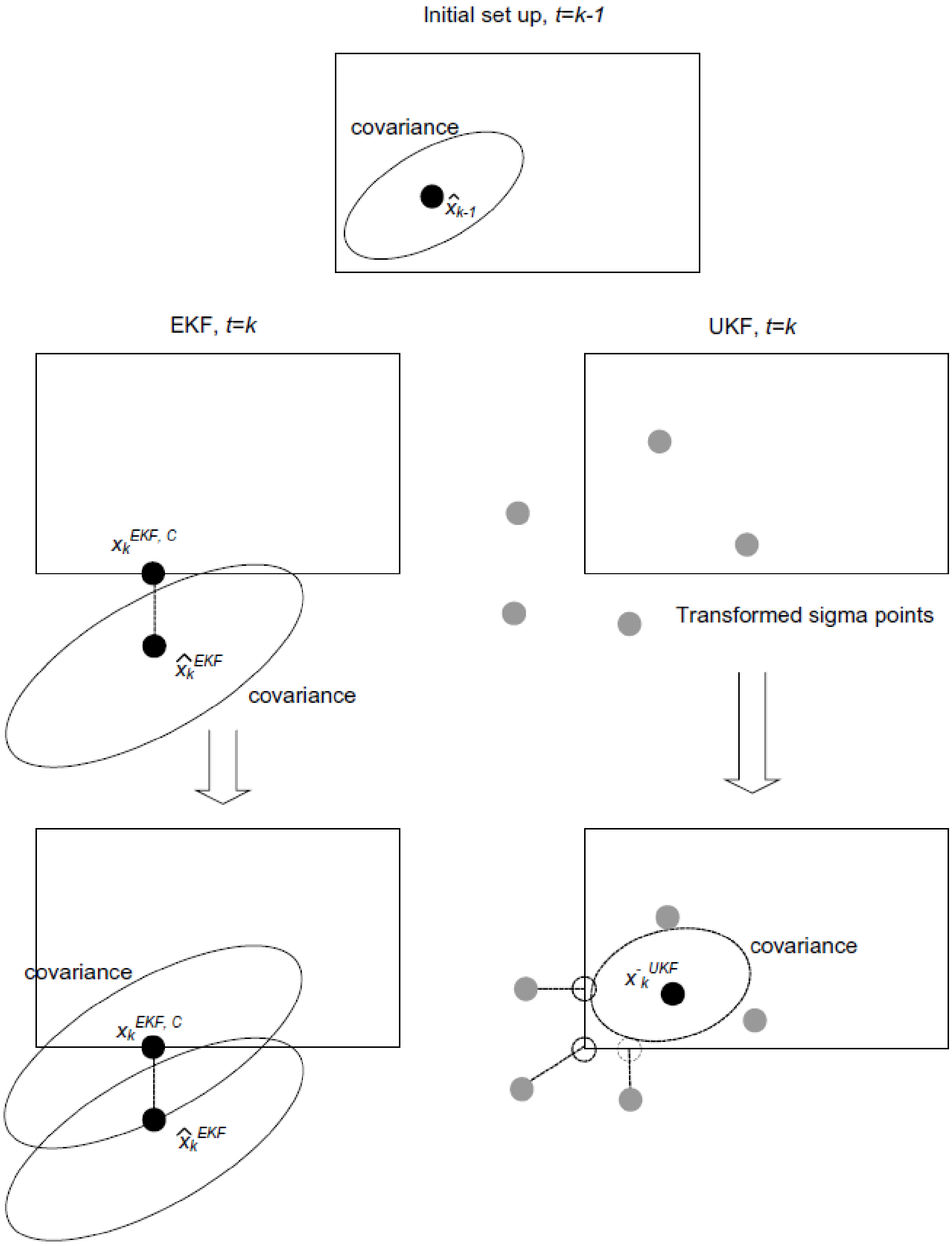

Figure 5.2: Illustration of constrained EKF vs. UKF[Kandepu et al. (2007)]

complexity, scientists have worked on solutions to the EKF's drawbacks. [Ungarala et al. (2007)] investigates an extension to the EKF algorithm that allows the EKF scheme to deal with constraints. They compare their new algorithm, the Constrained Extended Kalman Filter (CEKF), to the ordinary EKF and to the MHE algorithm, and show that the CEKF will perform similarly to the MHE, but the computational complexity of the CEKF are only marginally bigger than the EKF and a fraction of the complexity of the MHE.

5.2 Unscented Kalman filter

To deal with some of the drawbacks with the EKF algorithm, a new extension of the KF was proposed by [Julier and Uhlmann (1997)]. This new scheme would address the issues with the linearization part of the EKF. Local linearity is assumed when linearizing a nonlinear system. If this assumption is violated, it can result in a unstable filter. The new scheme would transform the information contained in the nonlinear model using a set of points, called *sigma-points*. The mean and covariance of the nonlinear model are captured precisely up to the second order[Julier and Uhlmann (1997)], which is more accurate than the EKF scheme. This new scheme is called the unscented Kalman filter (UKF), due to the nonlinear transformation called the unscented transformation. The UKF algorithm also has its advantages when it comes to implementation. There is no need to calculate the Jacobian matrices, and therefore it can be easier to develop a numerically stable estimator.

As noted in the previous section, the EKF algorithm can be extended to incorporate physical state constraints. [Kandepu et al. (2007)] modified the UKF scheme to handle constraints as well. Figure 5.2 [p.30] shows a graphical representation of how the EKF and the UKF captures the mean and covariance information. Both the constrained EKF and the constrained UKF algorithm uses so-called “clipping” to handle constraints. “Clipping” is originally from the way EKF handles constraints; the estimates are calculated and then checked against the constraints to see if any of the constraints are violated. If they are, the estimates are projected onto the boundary. The constrained UKF scheme works in a similar fashion, but an important difference is that the estimates are not clipped by the UKF scheme, instead the sigma-points are projected onto the constraint boundary. This way, the covariance will capture information about the constraints, and this will lead to a more accurate estimation. “Clipping” is illustrated in the last step in Figure 5.2 [p.30].

The last thing to note about the UKF scheme versus the EKF is the difference in run-time complexity. The run-time complexity of the EKF scheme will depend on the way the EKF algorithm is implemented. If the linearization is done analytically, then the EKF will be faster than the UKF. However, if the EKF is implemented using numerical linearization, as it often is when it comes to complex systems, the run-time complexity of the UKF will be comparable to the run-time complexity of the EKF.

5.3 Nonlinear moving horizon estimation

Moving horizon estimation have received much attention as an estimator in combination with MPC. This is mainly because of the constraint handling in MHE. MHE is one of the only estimators that handles constraints when computing the estimates. The main downside to MHE schemes are the computational complexity. MHE is a dual problem of the MPC, and just like the NMPC, nonlinear moving horizon estimation (NMHE) requires the solution of a nonlinear programming problem at each time step. Since NMHE is often used in combination with NMPC, the computational complexity of these algorithms together are often too restrictive and the sampling time of the control system can become too long.

The NMHE is a sub-optimal estimator, like the nonlinear KF's, that uses a finite moving window of both current and old measurements to update the state and the error covariance estimate[Johansen (2011)]. As with the NMPC algorithm, the NMHE performance will depend on the size of the window; the longer the history, the better the estimation. A longer window will on the other hand mean a bigger optimization problem, and thus, the computational complexity increases. If computational complexity was not an issue and unlimited memory was possible, the NMHE would be an optimal estimator. However, the NMHE can approximate an optimal estimator by tuning the arrival cost penalties[Tenny and Rawlings (2002)]. The arrival cost is a way to incorporate the information contained in the deleted measurements; an important issue when it comes to implementing NMHE.

5.4 Particle filters

Particle filters, also known as Monte Carlo methods, tries to estimate the probability density function (PDF) rather than the mean and the covariance. The UKF algorithm can be considered as a type of particle filter, but differs from the normal particle filters in some aspects. An example of a difference between the UKF and the normal particle filters is that the UKF is deterministic, while the normal particle filters uses randomly generated noise distributed by the known process noise PDF. Therefore "the particle filter can be considered a generalization of the UKF"[Simon (2009)]. Given enough particles, the particle filter will outperform the UKF, since the particle filter estimates the PDF, and the estimate of the PDF will converge to the real PDF when the number of particles goes to infinity.

[Daum (2005)] claims that for low dimensional problems the computational complexity of a well designed particle filter has approximately the same complexity as the EKF. However, for systems with high dimension, the computational complexity of the particle filter will become restrictive.

Chapter 6
Model identification

Even though many processes are modeled before they are even built, as with the Compact Separation process, the modeling seldom captures a complete and entirely accurate picture of the process. The reason for this is that some components may be difficult to model, the dynamics might be unknown or the behavior of different modules change from setup to setup. Moreover, the process dynamics of certain components might even change somewhat with time, and leave the model inaccurate. Therefore, to make the complete system more robust and to allow a more accurate control, it can be preferable to identify such uncertain process dynamics on-line.

6.1 The dual estimation problem

As discussed in the previous chapter, the system states generally need to be estimated. The problem of estimating both the states and the model parameters are often referred to as the *dual estimation* problem. Dual estimation works by alternating between using the model to estimate the states, and using the states to estimate the model. Basically, this process can be performed in two ways, either iterative or sequentially[Wan and Nelson (2001)]. A block diagram of the two methods of performing dual estimation can be seen in Figure 6.1 [p.36].

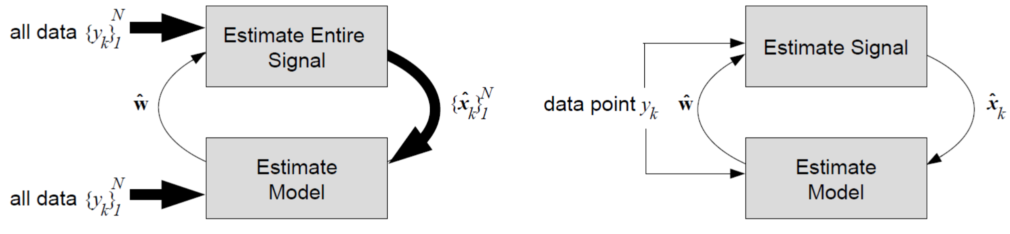

(a) Iterative (b) Sequential

Figure 6.1: Two approaches to the dual estimation problem[Wan and Nelson (2001)].

The iterative scheme works by estimating the states using the current model and the available measurements, and in the next step, the states and the measurements are used for updating the model. According to [Wan and Nelson (2001)], the iterative scheme is restricted to off-line applications. On the other hand, the sequential scheme works both for on-line and off-line applications – and works by using the individual measurements to estimate both states and model at the same time. The majority of research on dual estimation has been focused on linear models, but some papers have researched the possibility of using the EKF algorithm to dual estimation, such as [Khodadadi and Jazayeri (2011)], [Wan and Nelson (1997, 2001)], and [Wan et al. (2000)]. [Wan et al. (2000)] compare the EKF to the UKF with respect to dual estimation.

The dual EKF algorithm works by running two extended Kalman filters in parallel. One of the EKF's estimates the states, based on the old states and the old parameters, while the other EKF estimates the parameters using the same information. Both EKF's uses measurements for the correction step of the algorithm. A block diagram representation of the dual EKF algorithm is shown in Figure 6.2 [p.37].

Another version of a Kalman filter to solve the dual estimation problem

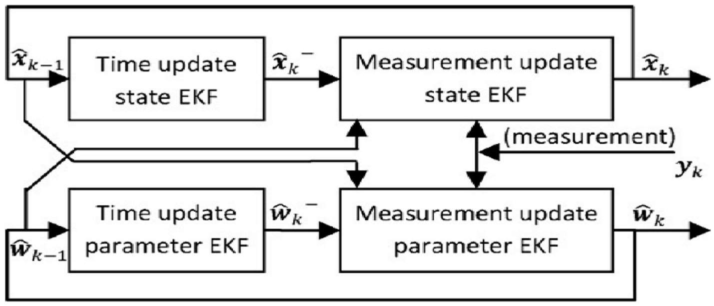

Figure 6.2: The dual EKF algorithm[Khodadadi and Jazayeri (2011)].

is the joint EKF algorithm. This version uses only one extended Kalman filter, and the state vector are the combined state and parameter vector. The resulting state vector z_k is shown in Equation 6.1 [p.37].

$$\mathbf{z}_k = \begin{bmatrix} \mathbf{x}_k \\ \mathbf{w}_k \end{bmatrix} \tag{6.1}$$

This method will result in a difficult optimization problem, caused by the high coupling between the states and the parameters. This was the algorithm implemented in the Compact Separation process during the summer project of 2011[Steinshamn and Norgren (2011)]. However, this algorithm sufferers from potential convergence problems[Khodadadi and Jazayeri (2011)]. These convergence problems are reduced with the dual EKF algorithm. Furthermore, the parameter estimating Kalman filter can be turned off when the states have converged; reducing the computational complexity of the entire system. Another solution to reduce the computational complexity is to increase the sample time of the second EKF, since the parameters are assumed to be constant.

The parameter estimation part of the dual EKF, are very similar to the ordinary EKF, shown in Chapter 5 [p.27], however, with some modifications.

The discrete time-update equations for the parameter filter are shown in Equation 6.2 [p.38]. The "noise" covariance is chosen as $R^r_k = (\lambda^{-1} - 1)P_{\mathbf{w}_k}$, where $\lambda \in (0, 1]$ is referred to as the forgetting factor[Wan and Nelson (2001)]. This way, the past data will be weighted less than new data. The equations given below are taken from [Khodadadi and Jazayeri (2011)].

$$\hat{\mathbf{w}}^-_k = \hat{\mathbf{w}}^-_{k-1} \tag{6.2a}$$

$$P^-_{\mathbf{w}_k} = P_{\mathbf{w}_{k-1}} + R^r_{k-1} = \lambda^{-1} P_{\mathbf{w}_{k-1}} \tag{6.2b}$$

And the measurement update equations are shown below, in Equation 6.3 [p.38].

$$K^{\mathbf{w}}_k = P^-_{\mathbf{w}_k} (C^{\mathbf{w}}_k)^T \left(C^{\mathbf{w}}_k P^-_{\mathbf{w}_k} (C^{\mathbf{w}}_k)^T + R^e \right)^{-1} \tag{6.3a}$$

$$\hat{\mathbf{w}}_k = \hat{\mathbf{w}}^-_k + K^{\mathbf{w}}_k \epsilon_k \tag{6.3b}$$

$$P_{\mathbf{w}_k} = \left(I - K^{\mathbf{w}}_k C^{\mathbf{w}}_k \right) P^-_{\mathbf{w}_k} \tag{6.3c}$$

ϵ_k and $C^{\mathbf{w}}_k$ are given in Equation 6.4 [p.38].

$$\epsilon_k = \left(\mathbf{y}_k - C\hat{\mathbf{x}}^-_k \right) \tag{6.4a}$$

$$C^{\mathbf{w}}_k = C \frac{\partial x_k}{\partial w} \bigg|_{\mathbf{w}=\hat{\mathbf{w}}_k} \tag{6.4b}$$

6.2 Observability

Observability theory on linear systems is well known, and given a linear system on the state-space form, it is easy to show if the system is globally observable or not. For theory on linear systems and observability, see [Hespanha (2009)]. Observability means that, given an arbitrary sequence of outputs from a system, it is possible to uniquely define the current state of the system.

Observability is generally a requirement to be able to estimate the unmeasurable states of a system, but checking the observability conditions of a nonlinear system is more tedious work. One approach to study observability of a nonlinear system, is to study the observability of the linearized system in the same manner as with linear systems. However, since the linearization is only valid in a region around the point the nonlinear system is linearized about, the observability analysis can only provide information about local observability. How large the region this analysis is valid in, will depend on the structure of the nonlinear system.

To study global observability, the local observability property must be studied at all the points the nonlinear system is linearized about. This can result in a very large complexity of the analysis. For a system with n_x states and n_u inputs, the dimension of the space where observability should be considered is $n_x + n_u$. With k number of samples of each state and input, this will result in a total of $k^{n_x+n_u}$ points where observability should be checked[Hammervold (2011)].

6.3 Parameter identifiability

There might be many uncertain parameters in a process model, however, it might not be possible to estimate them all. To be able to identify all the uncertain parameters, it is a necessary condition that the measurements contain enough information. Equation 6.5 [p.40] shows an arbitrary nonlinear system, where $\mathbf{x}$ is the state-vector, $\mathbf{u}$ is the input-vector, while $\mathbf{p}$ is the vector containing the uncertain parameters.

$$\dot{\mathbf{x}} = \mathbf{f}\left(\mathbf{x}, \mathbf{u}, \mathbf{p}\right), \tag{6.5a}$$

$$\mathbf{y} = \mathbf{h}\left(\mathbf{x}, \mathbf{u}, \mathbf{p}\right). \tag{6.5b}$$

In a system with n_x states, n_y measurements and n_p parameters, this will give a total of $n_x + n_y$ equations, and since the states of the system can be counted as unknown variables, we are left with a grand total of $n_x + n_p$ variables. Basic mathematics tells us that if we try to solve an equation-set with more unknowns than equations, we will not get a unique solution. Thus, the number of measurements, n_y, must be greater than or equal to the number of parameters, n_p, if we want to estimate the parameters.

The parameter identifiability analysis in a nonlinear system is complex, but by choosing $n_p \leq n_y$ the parameters will always be identifiable, as long as the Equations-set 6.5 [p.40] are solvable for the chosen parameters. The information in this section was found in [Hammervold (2011)].

PART III

Control Strategy

Abstract – This part presents the set-ups used to configure the NMPC algorithm. The first chapter introduces some of the tuning variables available in SEPTIC as well as some old configurations used to set up the controller in earlier work. The next chapter introduces the new control strategy developed during this project and the cases used to test the control algorithm.

When it comes to implementing and tuning controllers, there are many aspects that need careful consideration, such as physical and/or desired constraints that the control system must abide. Physical constraints on inputs can cause the controller to become unstable, if not accounted for when designed. Physical constraints cannot be violated in real life. For example, a pipe have only a given diameter – a pump has only a certain amount of effect. For example: A nuclear power plant is overheating and a pump is providing cold water to cool the plant down. The pump if operating at its limit (physical constraint), and there is therefore nothing one can do to make it deliver more water. The system becomes unstable at this point.

Desired constraints on the other hand, can be violated in real life, however, violation of these constraints might lead to damage of equipment, reduced productivity or even in extreme cases, loss of human life. This brings us to another aspect that must be analyzed when implementing a control system, namely priorities. It is obvious that constraints paramount to the safety of human life and equipment should be prioritized above constraints that, if violated, only will lead to reduced production. In order to fulfill this requirement, priorities can be divided into two groups, soft and hard constraints. Soft constraints are the constraints that can be violated without causing damage to equipment or humans; while hard constraints must be held in order to ensure that severe faults does not occur.

Not all control schemes have the capability of assigning priorities, and in these cases other strategies must be taken in order to assure the safety and continued operation of the system. This choice of control configuration will from now on be referred to as the control strategy.

Chapter 7
Old Control Strategy

Choosing a control strategy that will fulfill all hard constraints at all times – while considering that all the desired criteria's are met, is not always easy. A NMPC control scheme can have hundreds or thousands of tuning variables, depending on the complexity of the plant to be controlled. Identifying all hard constraints might not even be that simple, and sometimes all constraints of a system can be hard constraints.

The performance of a controller can often be affected by the current region of operation. A control scheme that is good in one region, might be inadequate in other regions. The Compact Separation process is meant to function on a wide variety of operating points: Cases that might prove especially difficult in this process can include shut-down, start-up and hydrodynamic slugging[1].

The main purpose of the Compact Separation process is to separate the gas and liquid from one multiphase input flow, into two single phase flows. The gas will be boosted to the surface using a single phase compressor, and must therefore contain as little liquid as possible, while the liquid will be boosted to the surface using a single phase pump, and must contain as little gas as possible. The single phase pump can tolerate about 3% gas in the

[1]Hydrodynamic slugging is explained in Chapter 10 [p.75].

liquid flow, and the compressor can handle about 3% liquid in the gas flow. If the GVF into the compressor or pump is below/above these limits, this will cause unnecessary wear and tear on the equipment, and will reduce the lifespan of the units.

This can indicate that the separation degrees into the pump and into the compressor should be considered as hard constraints. On the other hand, if the separation profiles are prioritized above the desired pressure in the two control volumes, and the only way to comply with the separation constraints is to decrease (or increase) the pressure in one of the CVs in such a way that no flow will flow through the system, then this might be even worse than if the separation constraints are violated for a short time. Therefore, both the differential pressure and the separation profiles will be considered as hard constraints, but care must be taken when tuning the algorithm. Avoiding liquid overflow in the GLCC and in the DL tank are also very important, and should be considered as hard constraints.

The control strategy from [Grimstad (2008)] is listed in Table 7.2 [p.46], and the control strategy used on the linear MPC, that was used for controlling the first tests on the test rig at SINTEF, is shown in Table 7.3 [p.48]. Before explaining the different control strategies, the SEPTIC MPC implementation must be highlighted.

7.1 SEPTIC tuning variables and priorities

SEPTIC contains a wide selection of tuning parameters. These parameters include priorities, penalties and high and low constraints. All variables are assigned a parameter type, such as manipulated variables (MVR), control variables (CVR), disturbance variables (DVR) and trend variables (TVR). The different types of variables can be assigned different types of constraints. For example, MVRs can be assigned ideal values or move penalties, while

1. Respect MVR rate of change limitations.
2. Respect MVR high/low limitations.
3. Respect hard CVR limitations.
4. Sort CVR/MVR specifications after the defined priorities.
5. Solve with respect to the specifications with lowest priorities first. If several specifications have the same priority, penalties and weighting will be used to find the most important specification.
6. Lock the solution with respect to CVR set point and MVR ideal value, and possibly expand the CVR limitations.
7. Start on point 5 again, until all specifications are handled.

Table 7.1: SEPTIC priority handling

CVRs can be assigned set points or set point deviation penalty. The weighting of the set point deviation is shown in Equation 7.1a [p.45] and the weighting of the input change is shown in Equation 7.1b [p.45]. Fulf and Span are tuning parameters to optimize the behavior of the control algorithm.

$$w = \left(\frac{\text{Fulf} \cdot (\text{predicted value} - \text{set point})}{\text{Span}}\right)^2 \tag{7.1a}$$

$$w = \left(\frac{\text{Move penalty} \cdot \Delta u}{\text{Span}}\right)^2 \tag{7.1b}$$

The priority scheme in SEPTIC will handle priorities in a certain manner, where hard constraints and physical limitations will be met first. The way the steady state solver deals with priorities are shown in Table 7.1 [p.45]. In the priority scheme used by SEPTIC, the lowest number (0) is the highest

Priority		Description	Penalty
0	u_i	Actuator constraints	
1	p_1	CV 1 pressure (High/Low)	1000
	h_s	GLCC tank liquid level (High/Low)	1000
	Δp_{12}	Differential pressure between CV 1 and CV 2 (High/Low)	100
	Δp_{23}	Differential pressure between CV 2 and CV 3 (High/Low)	100
2	q_{out_1}	Compressor anti-surge (Low)	10
	q_{out_2}	Pump minimum flow (Low)	10
3	p_1	CV 1 pressure (Set point)	10
	p_3	CV 3 pressure (Low)	10
	h_s	GLCC tank liquid level (Set point)	1
4	u_5	Gas recirculation (Ideal value)	10
	u_6	Liquid recirculation (Ideal value)	10
5	u_7	Control Valve (Ideal value)	1

Table 7.2: NMPC configuration in [Grimstad (2008)]

priority, while the highest number (99) is the lowest priority. The priority hierarchy, shown in Table 7.1 [p.45], was found in the SEPTIC documentation provided by Statoil.

7.2 Grimstad (2008) NMPC configuration

The control strategy of [Grimstad (2008)] is shown in Table 7.2 [p.46]. The min-max constraints of the actuators will always have the highest priority, due to the priority scheme in SEPTIC, shown in Table 7.1 [p.45]. Next, the control scheme will try to avoid damage to the equipment used in the Compact Separation process, by considering the CVRs with the highest priorities first. The high/low limits on the pressure is to keep the process operating within a desired operating area. The liquid level in the GLCC must have upper and lower bounds to avoid emptying or overflowing on bursts of liquid or gas bubbles. To ensure flow downstream the Compact Separation process the differential pressures between the different CVs must be positive, and above a certain level. The minimum flow of the pump and the compressor anti-surge constraints have a lower priority than the pressure and liquid level of the GLCC. This was justified by [Nilsson (2008)] to be due to the automatic shut-down procedure of the pump and compressor, which would shut them down before they ended up in a dangerous situation.

All the constraints discussed above are crucial for the operation of the Compact Separation process. Next step in the control scheme are the set points and the low level for the third control volume: These constraints will only be fulfilled if all the constraints with higher priority are fulfilled. Last is the ideal value of three of the control valves, to ensure that these stay completely closed when it is desired.

It is noteworthy that the control strategy in Table 7.2 [p.46] have neglected the high/low bounds on the GVF of the flow into both the pump

Priority		Description	Penalty
0	u_i	Actuator constraints	
1	σ	GVF in liquid flow out of PS (High)	100
	σ	GVF in liquid flow out of PS (Set point)	
	ν	GVF in gas flow out of PS (Low)	100
	ν	GVF in liquid flow out of PS (Set point)	
2	p_1	CV 1 pressure (High/Low)	10
	p_1	CV 1 pressure (Set point)	
	p_2	CV 2 pressure (High/Low)	10
	p_2	CV 2 pressure (Set point)	

Table 7.3: NMPC configuration on the SINTEF test rig

and the compressor. This control strategy assumes that the separations will be adequate over the whole operating area, however, this is not a reasonable assumption.

The control strategy presented in [Grimstad (2008)] is not directly applicable to the lab setup, due to the simplification of the process, and can therefore not be directly compared with the control schemes developed during this project. The control strategy of [Grimstad (2008)] is presented here to show a NMPC strategy that already has been tried, and what aspects must be considered when implementing a new control strategy.

7.3 SINTEF test rig MPC configuration

The actual MPC configuration used on the SINTEF test rig is shown in Table 7.3 [p.48]. Due to the simpler structure of the test rig versus the

CVR	High constraint	Low constraint	
Δp_{12}	4	0.5	[bar]
p_1	15	9	[bar]
p_2	12	8	[bar]
h_s	2	0	[meter]
h_{dl}	2	0	[meter]
GVF in q_{out_1}		97%	
GVF in q_{out_2}	3%		

Table 7.4: Control objectives in the Compact Separation process

complete Compact Separation process, the control strategy is also much simpler. Some new control variables have been introduced, however. The separation degrees of the different flows have been included as CVRs, and as can be seen from Table 7.3 [p.48] the control variables regarding the separation profiles have the highest priority – except for the hard constraints of the actuators. The pressure in the two control volumes are also set as CVRs.

The linear MPC configuration presented in Table 7.3 [p.48] is simple, but has certain drawbacks. The configuration presented in Table 7.2 [p.46] is more complex, and contains more CVRs. Some of these CVRs, as well as some of the MVRs, are not present in the simplified Compact Separation process (illustrated in Figure 2.2 [p.11]). Both the third control volume and the recirculation pipelines have been removed, and therefore all CVRs and MVRs belonging to these components are irrelevant to the case discussed here. This includes the CVRs Δp_{23} and p_3 and the MVRs u_5 and u_6. Both the pump and compressor are also removed and therefore the CVRs q_{out_1}

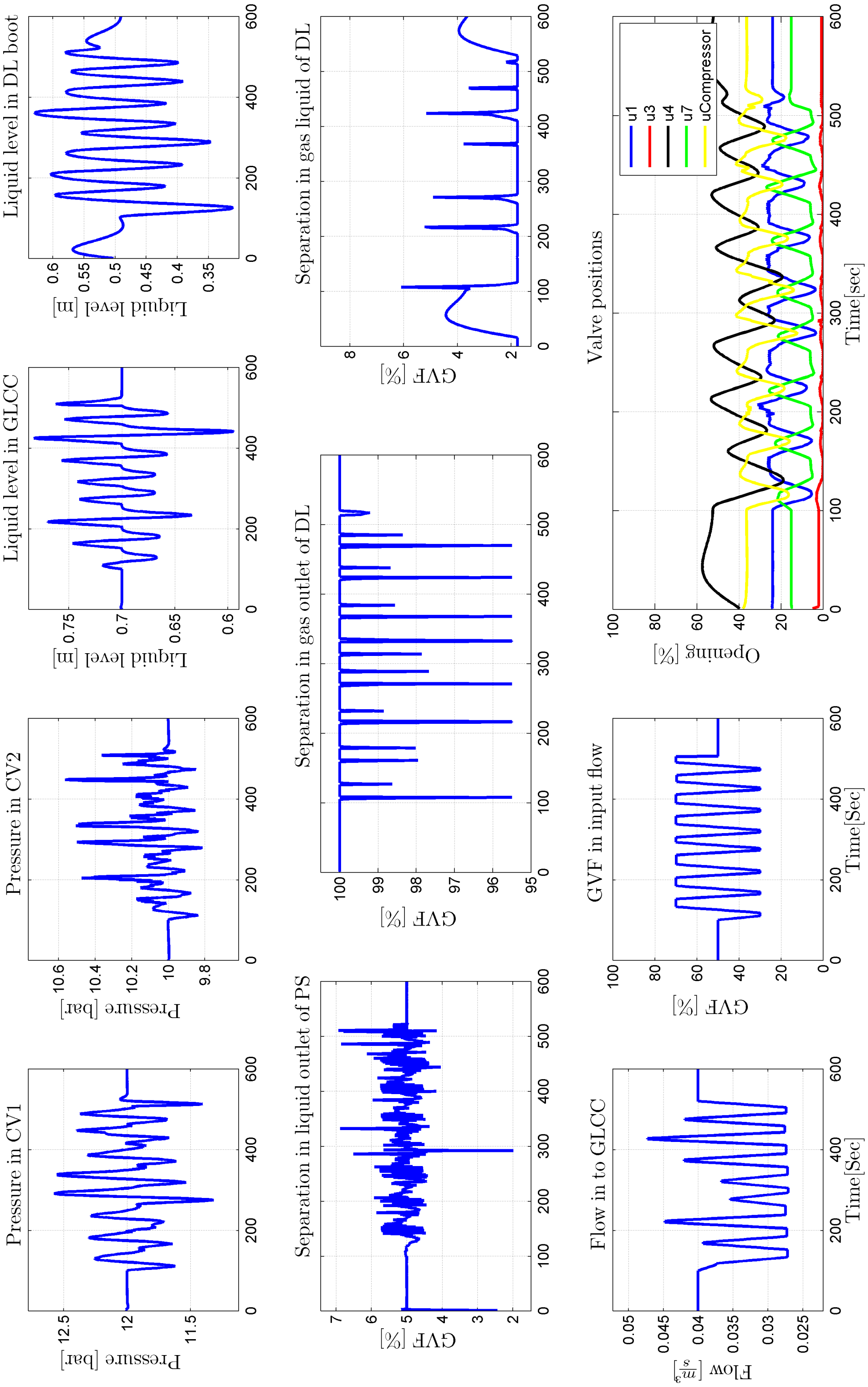

Figure 7.1: Simulation of the SINTEF test configuration

and q_{out_2} can be ignored.

Due to the fast dynamics of the process compared to the desired sampling time of the NMPC at 1 second, it is desired to control the liquid level of both the GLCC and the DL tank using PID-controllers with a higher sampling rate. Since it is not desirable to have two competing controllers controlling one valve, both the valve on the liquid outlet of the PS and the valve on the liquid outlet of the DL will be controlled solely by PID-controllers. The NMPC will therefore only have three MVRs left to control pressure and separation degrees in the Compact Separation process.

Table 7.4 [p.49] lists the control objectives in the NMPC algorithm. The differential pressure, Δp_{12}, has an important low value to ensure flow downstream the Compact Separation system. Too high differential pressure might cause a too large flow, resulting in a degradation of the separations through the in-line units. It is desirable to control the pressures in the system to stay within a certain operating point, therefore, high and low limits on the pressures have been introduced. The last control objectives that need to be satisfied are the maximum/minimum GVF of the flow into the pump and compressor. Neither pump, nor compressor are present in the test rig, however, gas-liquid separation is the main objective of the Compact Separation process. Since the recirculation pipelines should not be used to maintain the necessary separation degree, the simplified Compact Separation process should be able to perform as specified, without the recirculation pipelines. This means that the recirculation pipelines, when implemented, should only be used to ensure a minimum flow to the pump and the compressor.

In Figure 7.1 [p.50], some results from the simulation of the linear MPC configuration is shown. In this case the input to the GLCC was a slugging-case, with varying GVF and flow rate. When studying Figure 7.1 [p.50], some issues can be noted. The set point on σ, the separation in the liquid outlet of the PS, is set to 5% gas in the flow, and the highest GVF recommended for the pump was, as shown in Table 7.4 [p.49], 3%. The set point on 5% results in a average GVF of slightly more than 5%, and peaks almost up to 7%. A solution might be to use a lower set point, but this can result in more liquid in the gas outlet of the PS. The separation in the liquid flow out of the DL is, on average, below 3%, but this flow contributes so little compared to the liquid flow from the PS it is almost negligible.

The separation in the gas outlet of the DL does not have a set point, like the set point in the liquid outlet in the PS. The separation degree have some short transients to below 96%, with the recommended GVF into the compressor being 97%. These transients are, however, short, and the average separation is close to 100%, so the gas flow out of the Compact Separation process is sufficiently good.

Another problem with the configuration shown in Table 7.3 [p.48], is the lack of a set point on the differential pressure. During the tests at SINTEF, the Compact Separation process was used in a loop, and recirculated the fluids that were separated. This resulted in troubles with controlling the pressure in the Compact Separation process, and it was therefore desired to only control the differential pressure over the Compact Separation process. If the differential pressure is not controlled, this can result in a very high differential pressure, causing the test rig operator to become a very unhappy man or woman due to the high flow rates. Also, for optimal separation, the flow rates should be as small as possible, and therefore a high differential pressure in undesirable.

Chapter 8
New Control Strategy

The new control strategy developed through this project has been divided into three different configurations. The main configuration is for steady-state control and slugging cases, i.e. the normal operation of the system, while the other two are for start-up and shut-down sequences. Start-up and shut-down are two cases which are very different from the normal operation of the Compact Separation process, and since these two cases can be more or less planned, a new control strategy has been developed to meet the specific requirements of these cases. In the next sections, the idea and configuration behind each strategy is explained.

8.1 Steady-state and slugging

Ideally, the slugging sequence used to test the control strategy would be a square pulse, with varying amplitude and duty-cycle. This would be the ideal test sequence, since this is the worst-case slugging sequence that can possibly occur; and if the controller can handle this type of slugging, the controller will be able to handle all real slugging cases. However, using a square pulse as slug-case caused the controller to crash. The stiff dynamics of the system and the rapid change in the disturbance proved too much for

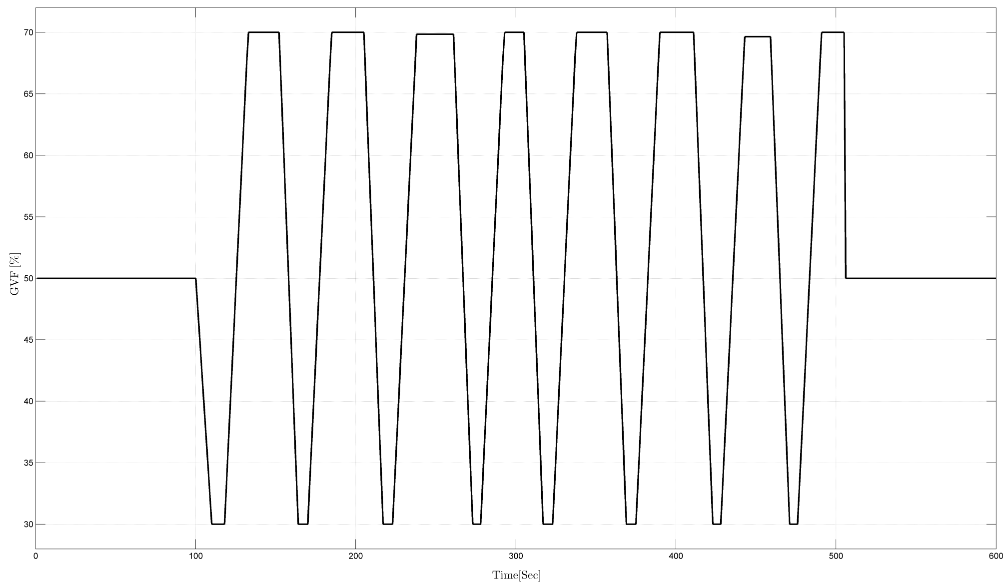

(a) GVF of the flow into the Compact Separation process

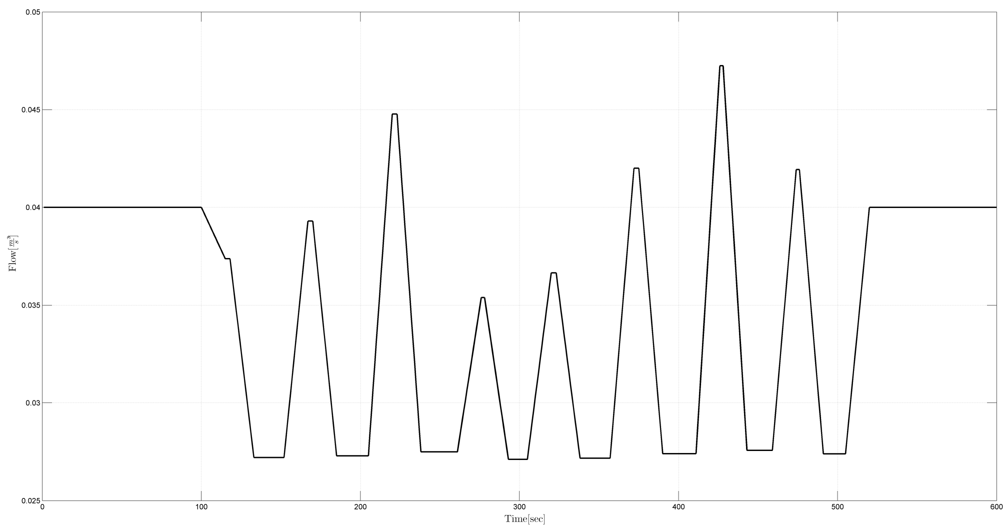

(b) Flow rate into the Compact Separation process

Figure 8.1: Slugging sequence used to test the NMPC

the ODE-solver[1] to handle. The slug sequence used to test the controller in this project is illustrated in Figure 8.1 [p.54]. The change in both the GVF of the input flow and the rate of the input flow are ramped up and down to a specified maximum and minimum value. The minimum time that the ODE-solver could handle was found to be between 15 and 20 seconds, and the maximum and minimum GVF possible was found to be 0.7 and 0.3. The NMPC configuration for the slugging and steady-state case is listed in Table 8.1 [p.56]. In all the cases presented below, the liquid level in both the GLCC and in the DL tank are controlled by PID-controllers. That is: u_4 and u_7 are controlled by PID-controllers, even if the controller being discussed is NMPC.

8.2 Start-up

When the Compact Separation process unit is installed, there will be a need for a controlled start-up procedure, and to control the system to its steady-state operating area. After a shut-down of the complete system there will also be a need to re-start the system; since start-up is a very extraordinary and tough case from a control perspective, this case is addressed separately.

Start-up of the Compact Separation process can cause problems if done too fast, because all valves are initially closed and there is a physical limitation to how fast a valve can be opened; therefore, overflows or controller instabilities can occur if the flow rate into the system is ramped up too fast. The separation degree out of the system is still an important control objective and should stay within the specified constraints, even through this special and challenging case. Three different start-up procedures are presented in the next subsections.

[1]ODE - Ordinary differential equation.

Priority		Set pt.	High/low	Penalty	Fulf	Span
0	$u_{compressor}$	-	1/0	1	1	0.1
	u_1	-	1/0	1	1	0.1
	u_3	-	1/0	2	1	0.1
1	Δp_{12} (low)	-	0.5	100	1	0.5
	Δp_{12} (high)	-	4	10	1	0.5
	σ (high)	-	0.03	100	10	0.1
	ν (low)	-	0.75	10	1	1
2	p_1 (low)	-	9	10	1	1
	p_1 (high)	-	15	10	1	1
	p_2 (low)	-	8	10	0.5	0.5
	p_2 (high)	-	12	10	0.5	0.5
3	p_1 (set point)	12	-	10	1	1
	p_2 (set point)	10	-	10	0.5	0.5
4	Δp_{12} (set point)	2.0	-	10	1	0.5

Table 8.1: New NMPC slugging configuration

Start-up using PID-controllers on all valves

This configuration does not use the NMPC at all. The NMPC is turned off, and each valve in the Compact Separation process is controlled by an individual PID-controller. The advantages of this method is the simplicity of the controller, and since the start-up procedure is a controlled disturbance, the behavior of the PID-controller is predictable. The PID-controller can be implemented in hardware, and is therefore a possible backup solution if the NMPC should fail for some reason.

Care must be taken when tuning the PID-controller, since a change in one of the valves will affect the rest of the system. In [Fjalestad et al. (2010)]

$u_{compressor}$	Controlled by a set point on 10 bar on CV 2.
u_1	Controlled by a set point on 12 bar on CV 1.
u_3	Controlled by a set point on 3% on σ.
u_4	Controlled by a set point on 0.5 meters on h_{dl}[2].
u_7	Controlled by a set point on 0.7 meters on h_s[3].

Table 8.2: PID-controller start-up configuration

it was proven that a too fast start-up or shut-down procedure would cause instabilities in the PID-controller. The input to the system should therefore be ramped up over a certain amount of time when starting up the system. An overview of the internal PID-controller configuration is given in Table 8.2 [p.57].

Start-up using NMPC on a planned start-up procedure

This subsection presents the start-up procedure using the same NMPC configuration as the one used to handle slugging, shown in Table 8.1 [p.56]. The planned start-up sequence is the same as the one used for the start-up with PID-controllers. The advantage of using this procedure is that there is no need to change control strategy, only a start-up sequence must be initiated.

Start-up using a modified NMPC configuration

The configuration presented here, is a modified NMPC configuration. The flow rate into the system, q_{in}, which is a disturbance in the original NMPC configuration, is now implemented as a manipulated variable. This way, the

[2]h_{dl}: Liquid level in DL tank.
[3]h_s: Liquid level in GLCC.

Priority		Set pt.	High/low	Penalty	Fulf	Span
0	$u_{compressor}$	-	1/0	5	1	0.1
	u_1	-	1/0	2	1	0.1
	u_3	-	1/0	5	1	0.1
1	q_{in} (ideal value)	0.04	-	1	10	0.01
	Δp_{12} (low)	-	0.5	100	1	0.5
	Δp_{12} (high)	-	4	10	1	0.5
3	p_1 (low)	-	9	10	1	1
	p_1 (high)	-	15	10	1	1
	p_2 (low)	-	8	10	0.5	0.5
	p_2 (high)	-	12	10	0.5	0.5
4	Δp_{12} (set point)	2	-	-	1	0.5
5	p_1 (set point)	12	-	-	1	1
	p_2 (set point)	10	-	-	0.5	0.5

Table 8.3: Modified NMPC start-up configuration

NMPC can control the start-up and plan it optimally, based on the current constraints and set points. Using this method one can hope to achieve a safer and quicker start-up than a planned disturbance can achieve. The controller could also be able to handle unexpected disturbances during start-up. Table 8.3 [p.58] shows the configuration for the modified NMPC start-up sequence.

8.3 Shut-down

Like the start-up case, shutting down the Compact Separation process is very hard from a control perspective. During the complete shut-down sequence, both pump and compressor will need a supply of sufficiently pure liquid and gas, and there must be no overflow. It is also desirable to leave the system in a safe state, so that the system can be started back up again without any complications. It might be necessary to shut the process down fast, if an emergency rises, but a too fast shut-down might cause problems with overflow and unstable controllers, as in the start-up case previously discussed. The next three subsections presents three different shut-down procedures.

Shut-down using PID-controllers on all valves

This configuration uses PID-controllers on all valves to shut the system down, just like in the PID-controller start-up procedure presented above. An overview is given in Table 8.2 [p.57]. The shut-down sequence is a pre-determined sequence, and must be planned with respect to how big changes in the input the controller can handle.

Shut-down using NMPC on a planned shut-down procedure

This approach uses the same configuration used for the slugging case, given in Table 8.1 [p.56]. The planned shut-down sequence is the same as the one used for shut-down with PID-controllers.

Shut-down using a modified NMPC configuration

As with the start-up case, an approach to a fully automated shut-down procedure was tried. The disturbance variable q_{in} is implemented as a MVR, and the NMPC can shut the system down in a controlled manner. To be able to shut the system down, the ideal value on the flow rate into the system has to be set to zero.

Priority		Set pt.	High/low	Penalty	Fulf	Span
0	$u_{compressor}$	-	1/0	2	0.33	0.1
	u_1	-	1/0	2	0.27	0.1
	u_3	-	1/0	5	0.55	0.1
1	q_{in} (ideal value)	0	-	1	10	1
	Δp_{12} (low)	-	0.5	100	1	0.5
	Δp_{12} (high)	-	4	10	1	0.5
3	p_1 (low)	-	9	1000	0.1	1
	p_1 (high)	-	15	10	0.1	1
	p_2 (low)	-	8	1000	0.5	0.5
	p_2 (high)	-	12	10	0.5	0.5
4	u_1	0	-	2	0.27	0.1
	u_3	0	-	5	0.55	0.1
5	$u_{compressor}$	0	-	2	0.33	0.1

Table 8.4: Modified NMPC shut-down configuration

It is desirable to shut the system down as fast as possible, because the reason for shut-down can often be an emergency. However, the system must not be shut down faster than it can handle, and the time used to shut down the Compact Separation process can be changed by tuning the penalty of deviating from the ideal value. Table 8.4 [p.60] shows the configuration for the NMPC shut-down sequence.

PART IV

Simulation Study

Abstract – This part presents the results from the work performed during this project. The first chapter studies the results from the evaluation of the different observers implemented. The next chapter will show results from the slugging case using the implemented NMPC configuration, while the last two chapters will present the results from the three different start-up and shut-down procedures.

Simulation is the process of experimenting with a designed model. The model can be either a representation of a real, physical system; or an imaginary one. To develop a model for a given process, assumptions are often made to simplify the dynamics of the system. This will, however, make the model less accurate, and it will differ from the process it is intended to describe. The purpose of simulating is to understand how a system works, and to understand the dynamics involved. One might simulate to verify that the developed model captures all aspects of a real life process, or to understand how a process might react to certain disturbances or manipulations.

Simulation is a word used in several different fields, and in this context simulation is defined as a computer simulation. This means that a computer will run a developed mathematical model, with a specified set of simulation variables, and through this, calculate predicted future values of the states in the process. The Monte Carlo method is counted as one of the first types of computer simulation. The Monte Carlo method is a method that uses a series of randomly generated samples to represent behavior that is hard to model. The Monte Carlo method was invented by John von Neumann, Stanislaw Ulam and Nicholas Metropolis during their work on the Manhattan Project in the 1940s. The project intended to simulate a nuclear detonation.

In addition to verification and understanding of physical models, simulations are extensively used to test whether a control system will perform as intended, to find bugs and errors in a program. It is often very important to find the majority of errors and to do tuning of a control system on a simulator to make the control system ready to be used on the physical system. The reason for this is that a control system that does not work on a real system, can often lead to both structural damage and injury to humans.

Chapter 9
Observer performance

Earlier, in Chapter 1 [p.3], it was mentioned that during the summer project of 2011, two different observers was implemented in SEPTIC, but these observers were not used for control of the Compact Separation process, since this was not a part of the assignment. To evaluate the performance of the implemented observers, both observer schemes were tested on three cases, namely slugging, start-up and shut-down. The results from the start-up and the shut-down, using states estimated by each implemented observer, can be found in Appendix A [p.119]. The slugging sequence, presented in Figure 8.1 [p.54], has been used through the first two sections of this chapter to test the observer performance. The observers have also been tested on an off-line process data set, taken from the test at SINTEF mentioned in Chapter 1 [p.3], to evaluate how good the performance of the two different observers are when the real process model is different from the model used in the observers.

9.1 State estimation

The most important task of the observer is to accurately estimate the internal states of the system model and to estimate disturbances, so the controller can base its decisions on the right information. If inaccurate estimates are

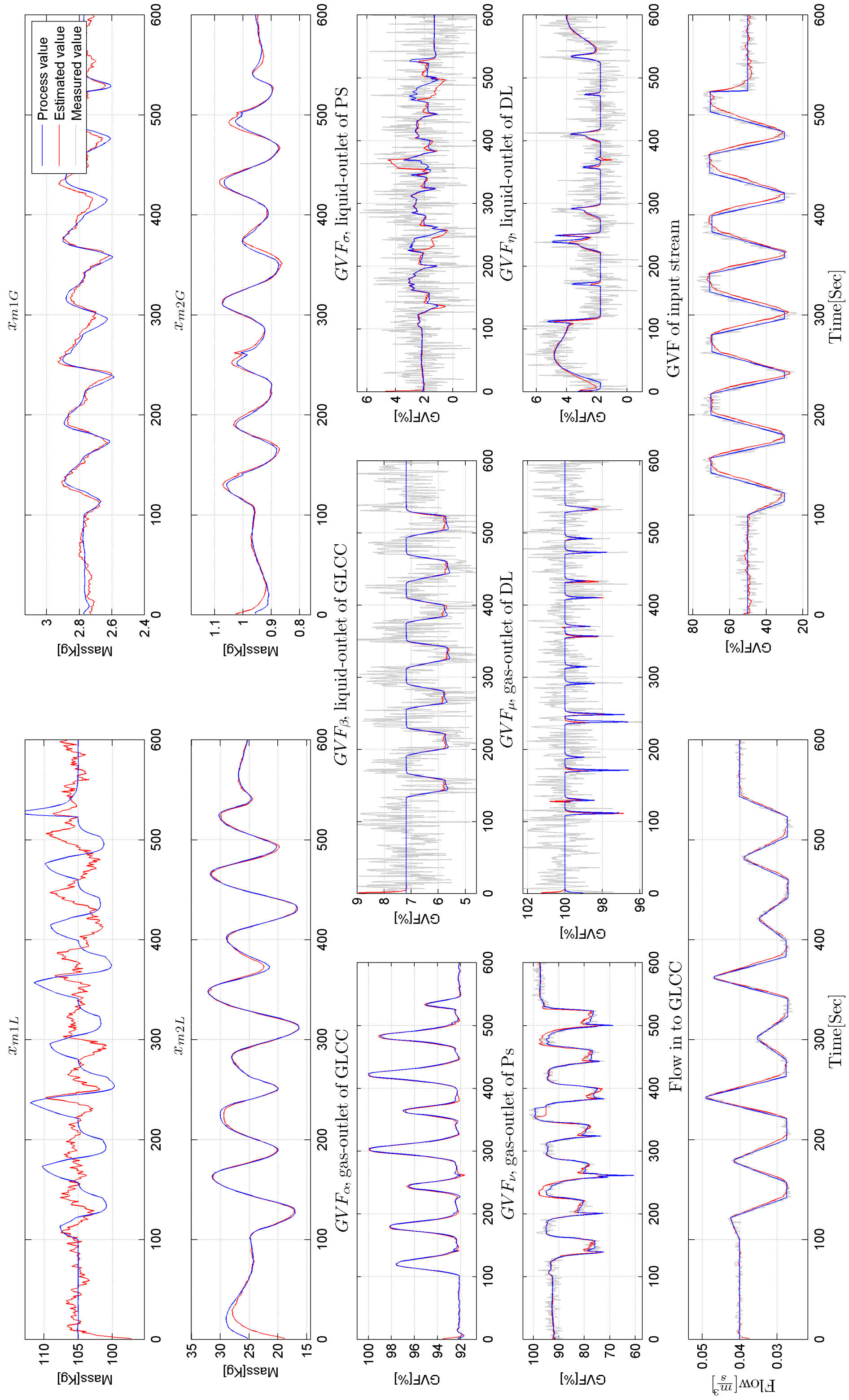

Figure 9.1: States estimated using EKF

delivered to the controller, this can lead to non-optimal control of the system, or in worst case – instability. Figure 9.1 [p.64] shows the real process states, as well as two of the real disturbances on the inlet of the system, versus the states and disturbances estimated by the extended Kalman filter. Three of the disturbances, namely the density of the input flow and the pressures on the two outlets, are excluded from this figure, since these disturbances are assumed constant. The same results using the unscented Kalman filter are presented in Figure 9.2 [p.66].

These plots show that the estimates of the states are good for most of the states, however, some states are more sensitive to noise than others. Gaussian white noise has been added to the ideal measurements, to simulate the effect of measurement noise. The noisy measurements are shown in Figure 9.1 [p.64] and in Figure 9.2 [p.66] as the measured value. The magnitude of the noise varies from measurement to measurement, since the different sensors will deliver different quality of measurements. For example, the multiphase meters used for measuring σ, ν and μ[1] are more accurate than the sensors used to the measure the liquid level in the GLCC and the DL tank. One reason for this is that the liquid measurements are influenced by waves in the tank, which makes the measurements noisy. Other reasons can be the quality of the sensor in use. The slug-sequence, which is the same as the one used in Chapter 10 [p.75], starts after 100 seconds. The reason for this, is to give the estimates time to converge before the hard control task starts.

From Figure 9.1 [p.64] and Figure 9.2 [p.66] it is obvious that the state that was most sensitive to noise was the mass of the liquid in control volume 1[2]. The mass of the gas in the same CV is also somewhat sensitive to noise,

[1] An overview of the separation profiles can be found in Table 2.1 [p.13].

[2] x_{m1L} and x_{m1G} is the mass of the liquid and gas in CV 1 respectively, while x_{m2L} and x_{m2G} represents mass of gas and liquid in CV 2.

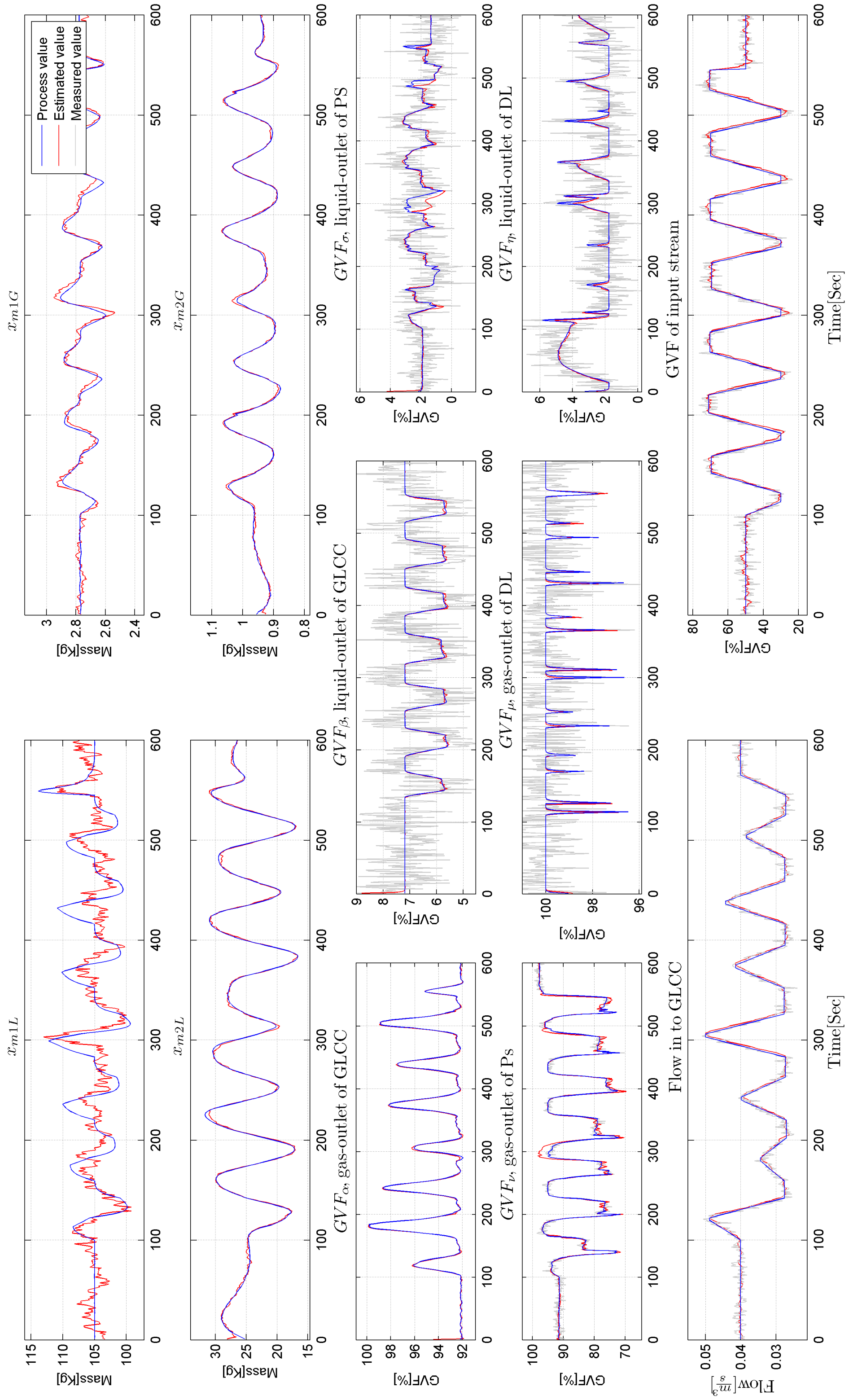

Figure 9.2: States estimated using UKF

but not as much as the mass of the liquid. One reason for this sensitivity is that this state depends on several noisy measurements, like the flow into the system and the liquid level; but the state itself is unmeasurable. The mass of the gas and liquid in the second CV was, however, not affected the same way.

When comparing the two observers, we can see that the UKF has more accurate estimates than the EKF, but it has the same sensitivities in the same states as EKF. During the simulation of the slug case, the UKF used about 0.1 seconds per run in average, with a worst case of 0.25 seconds; while the EKF used an average of 0.03 seconds per run and had a worst case run-time of 0.1 seconds. Both the accuracy differences and the run-time differences are consistent with the theory presented in Part II [p.19].

9.2 Parameter estimation

As discussed in Chapter 6 [p.35], it is desirable to estimate uncertain model parameters on-line. Therefore, the implemented observers have the capability of estimating the parameters of the uncertain separation profiles. For example, uncertain model parameters can be the constants in the separation profiles for the GLCC, Equation 2.9 [p.17], repeated below for simplicity.

$$\alpha = 0.1 \cdot log\left(30\tau_{gas}\right) + 0.3$$
$$\beta = -0.1 \cdot log\left(30\tau_{liquid}\right) + 0.7$$

By rewriting the equations for α and β, and by adding variables to the equations that can be used as states in the observer, the parameters of Equation 2.9 [p.17] can be estimated.

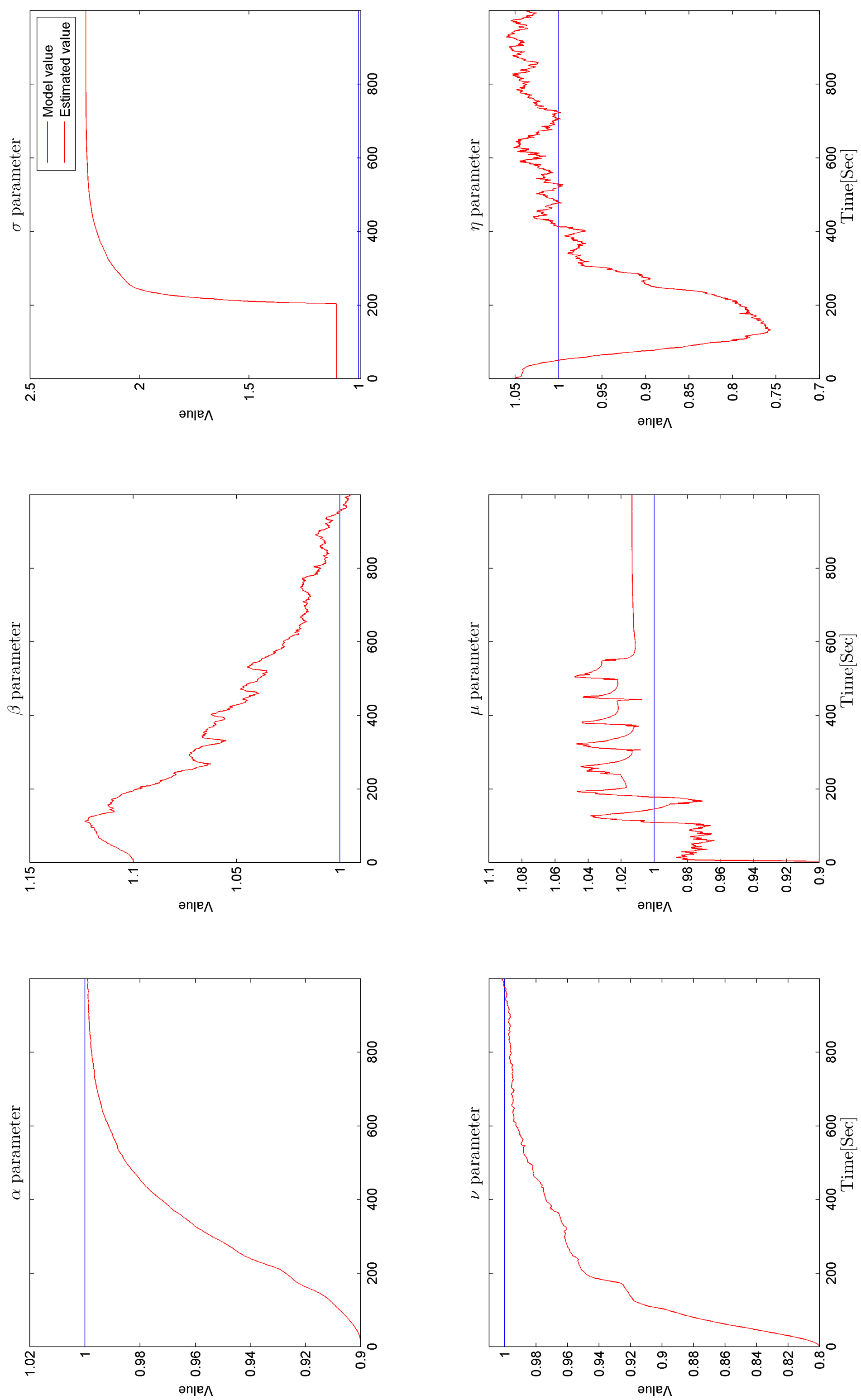

Figure 9.3: Estimates of uncertain model parameters

$$\alpha = a_1 \cdot log\,(30\tau_{gas}) + a_2 \tag{9.1a}$$

$$\beta = -b_1 \cdot log\,(30\tau_{liquid}) + b_2 \tag{9.1b}$$

Using this many parameters proved to be a too difficult task for the observers. The observer implemented in the summer project used 17 uncertain parameters, and 18 measurements. As discussed in Chapter 6 [p.35] the number of estimated parameters should always be less than the number of measurements, but the observers were still unable to estimate the parameters. This could be because the measurements do not contain enough information to estimate all the parameters, or the coupling between the state- and parameter estimation makes the optimization problem too difficult. Therefore, the new parameter estimation scheme only used a scaling of the separation profiles as the uncertain parameters, thus only 6 uncertain parameters were necessary. Changing the uncertain parameters is a way to check if the observer will be able to estimate the states even if the model used in the observer is not a perfect model of the process, as has been assumed until this point.

Figure 9.3 [p.68] shows the estimation of uncertain model parameters during a slugging case using EKF. As can be seen from this figure, the parameter estimation does not work perfectly. Most parameters converge, but one of the parameters, the scaling of σ, diverges. Figure 9.4 [p.70] illustrates how the state estimates evolve during the parameter estimation simulation. From this figure it can be seen that all the state estimates converge to the real state estimates, even if the scaling of σ diverges. This illustrates the problem that may arise due to the high coupling between the state and parameter estimation problem. Parameter estimation using UKF was also attempted, but a numerical issue made this impossible. This problem will

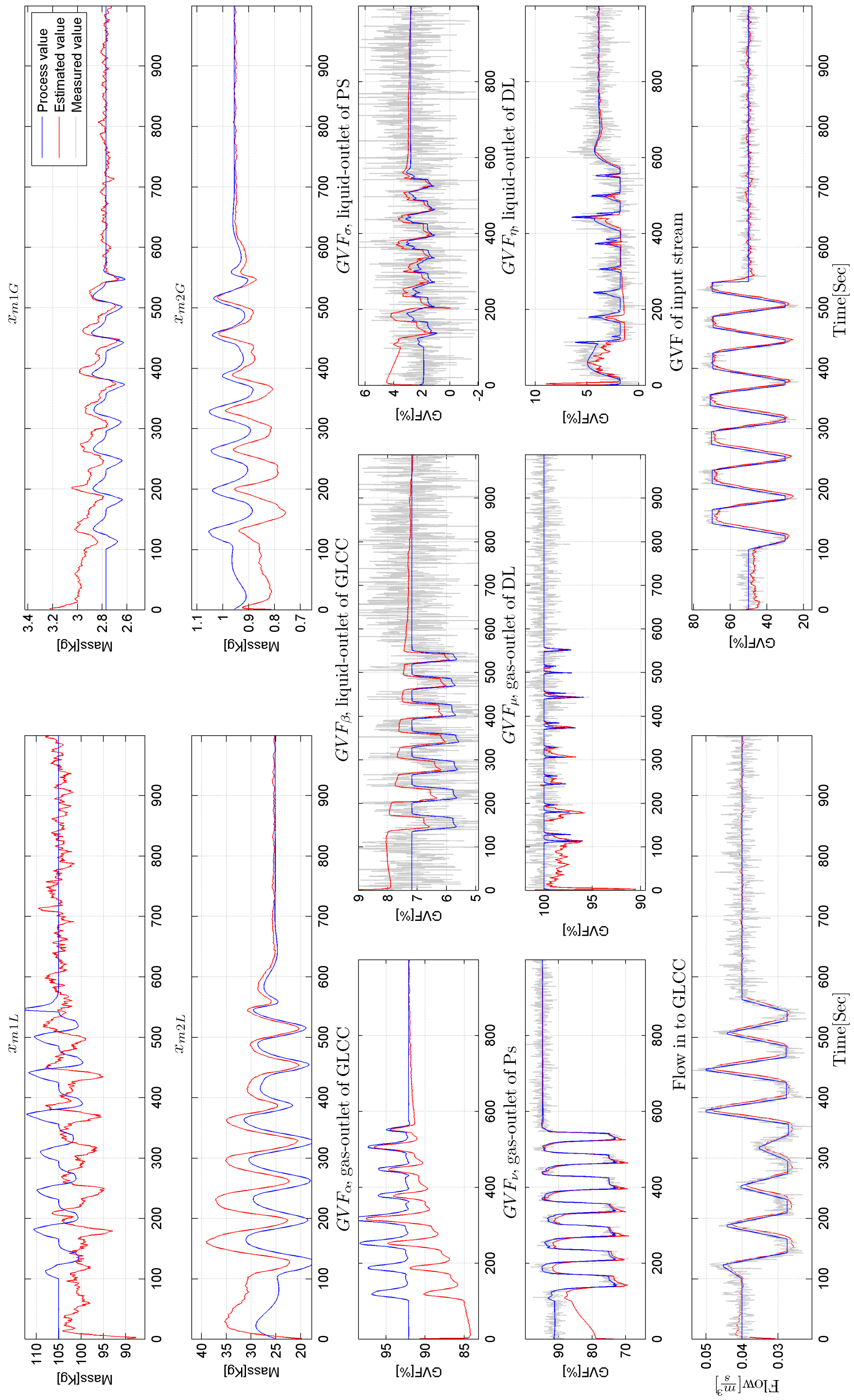

Figure 9.4: Estimated states with uncertain parameters

be discussed in Chapter 13 [p.95]. Due to this problem, only EKF was used in the next section.

9.3 Off-line process data set

So far, the model used as process has been the same as the model used for estimation. Even if the observer is able to handle some model/plant parameter mismatch, this does not mean that the observer will be able to handle the actual plant. The plant will have more model uncertainties, and the only data available to estimate the internal states and the process model parameters are noisy measurements.

Figure 9.5 [p.72] shows the observer performance with off-line data from the test rig at SINTEF as the measurements. In these plots, the values on the y-axis have been removed. The reason for this is to mask the test data, since these data are classified internal at Statoil, and the important aspects of this case are the smoothing and tracking capabilities of the observer.

Figure 9.5 [p.72] shows the performance of the EKF on the off-line data from the test rig. In order to get these results, the parameter estimation scheme had to be altered yet again. The scaling of σ was replaced with an offset parameter. Offset parameters were also introduced to remove bias on the estimates of the input flow rate and GVF. Figure 9.6 [p.73] shows the parameter estimation during the run on the off-line data set. Neither of the scaling parameters converge to a specific value during the 500 seconds long data set, but most of the states track and smooth the measurements well.

The state that inhibit the worst tracking performance is μ, but it gets closer in the end of the simulation. Using a constant scaling does not work well either, as can be seen from Figure 9.7 [p.74], which shows a run on the off-line data without parameter estimation (but the bias estimation of the disturbances were still used).

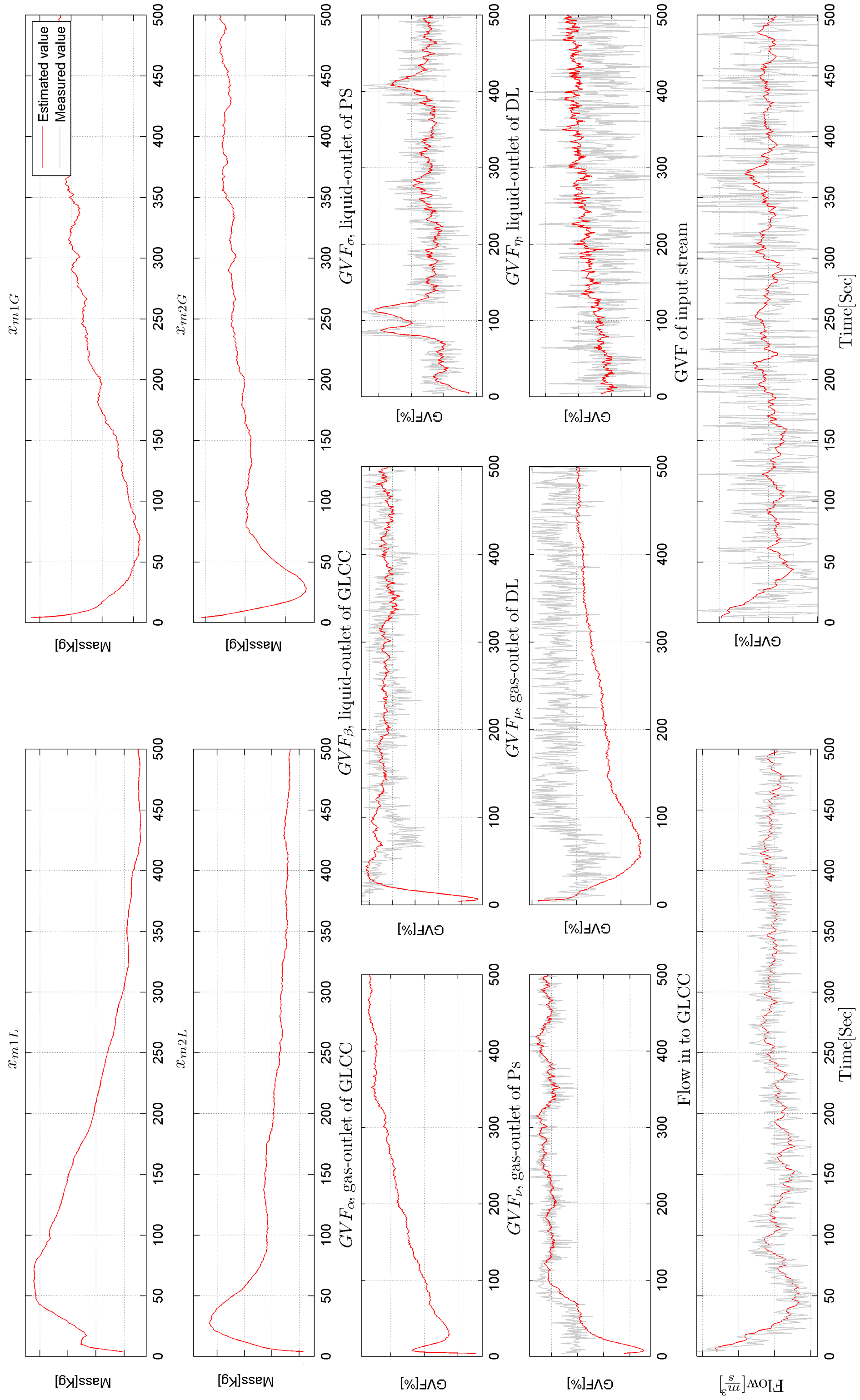

Figure 9.5: States estimated with EKF from offline data

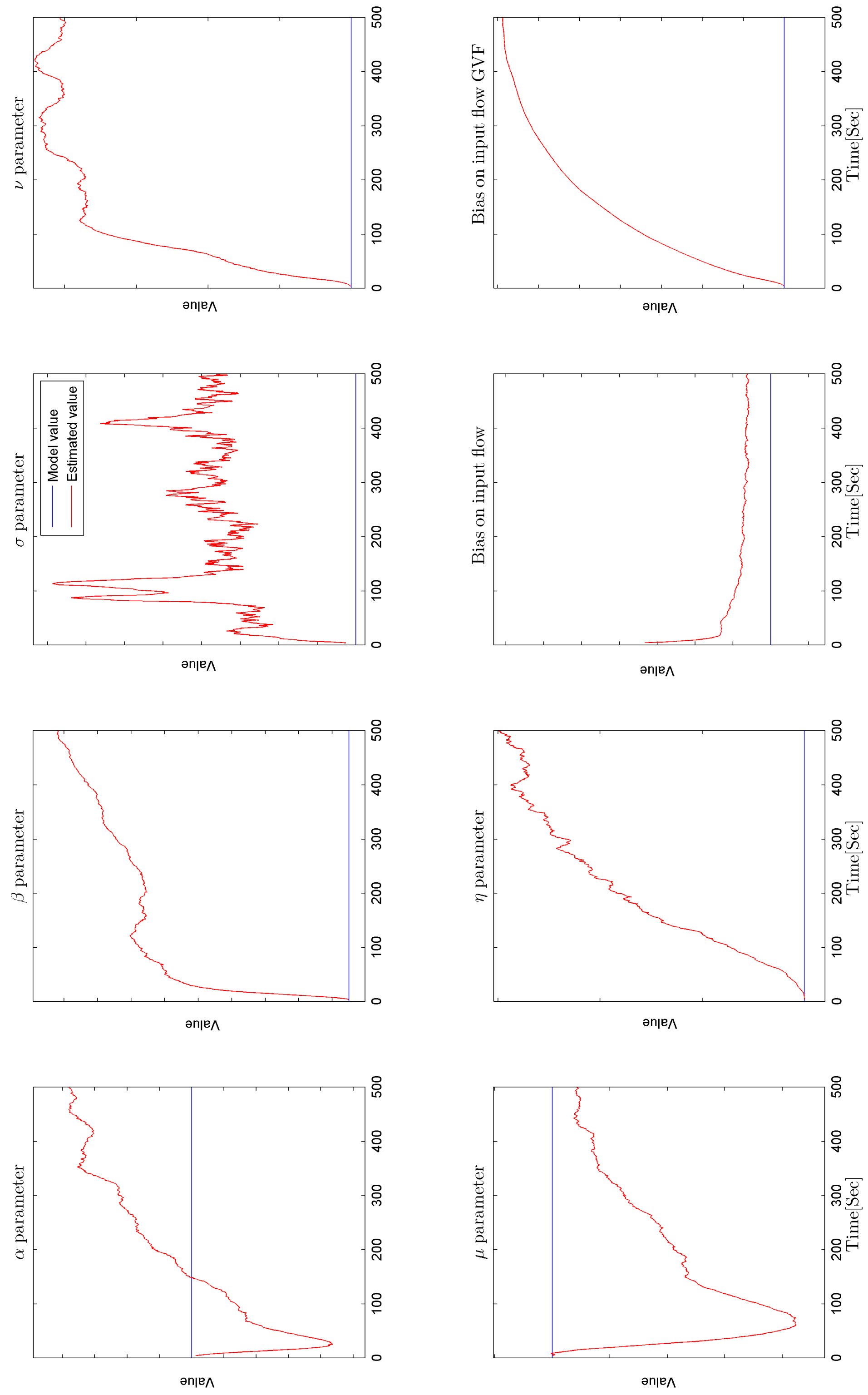

Figure 9.6: Parameters estimated with EKF from offline data

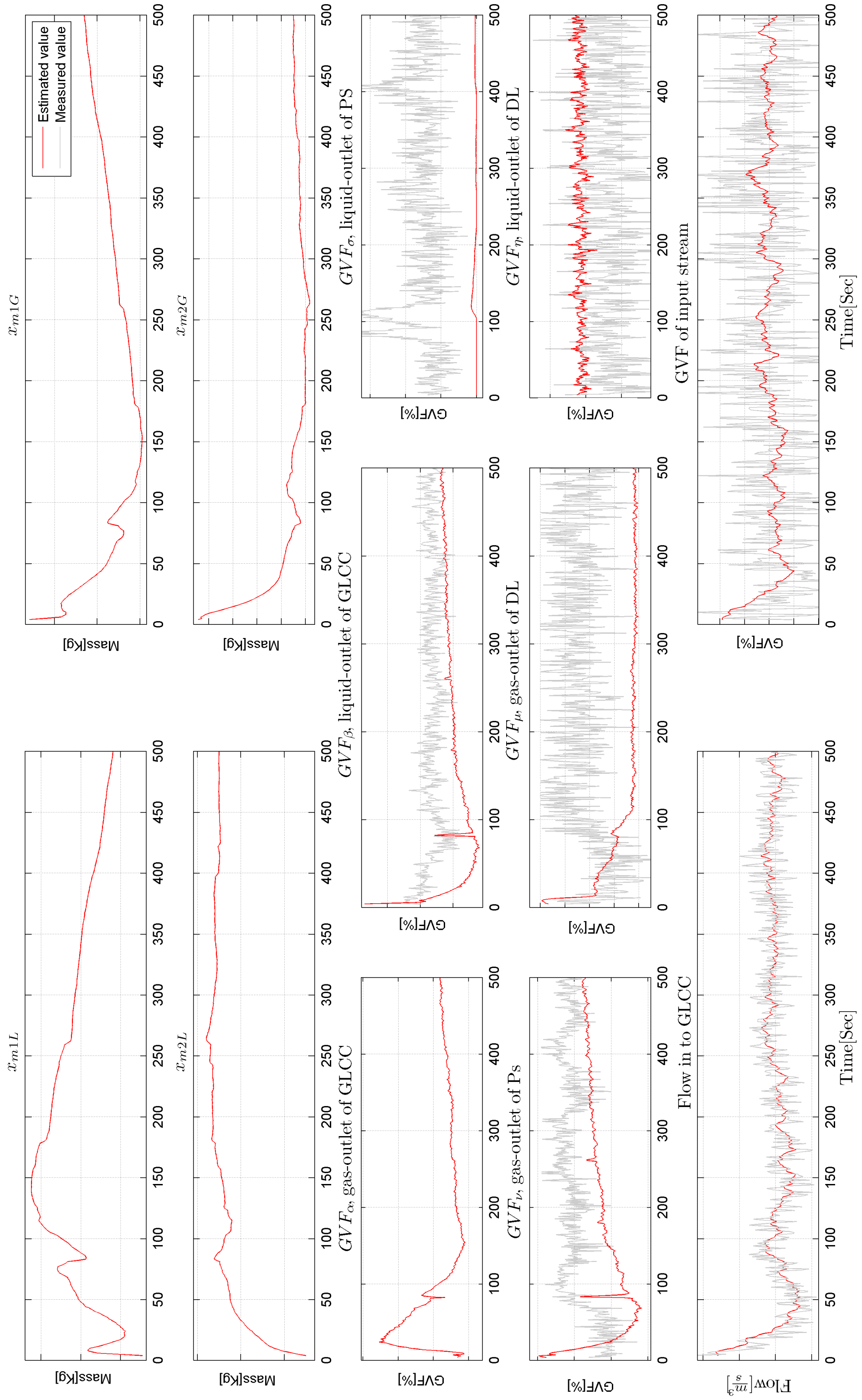

Figure 9.7: States estimated with off-line data without parameter estimation

Chapter 10
Case: Slugging

To test the implemented control strategy and to check if all constraints and control objectives can be held, even in tough cases, the control system must be tested using worst case scenarios. Hydrodynamic slugging, henceforth known as slugging, is a phenomenon that may arise in two-phase pipelines. When waves on the liquid surface grow to a height large enough to fill the pipe completely, a slug is formed. This occurs when gas flows at a higher rate than the liquid through the pipe. Figure 10.1 shows an illustration of a hydrodynamic slug.

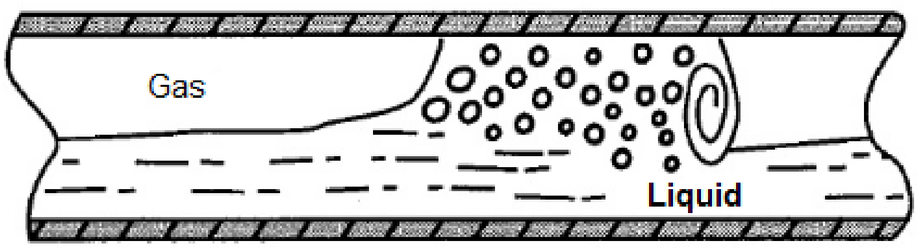

Figure 10.1: Forming of a hydrodynamic slug

Picture found on http://www.scribd.com/doc/50803045/2/Hydrodynamic-Slugging

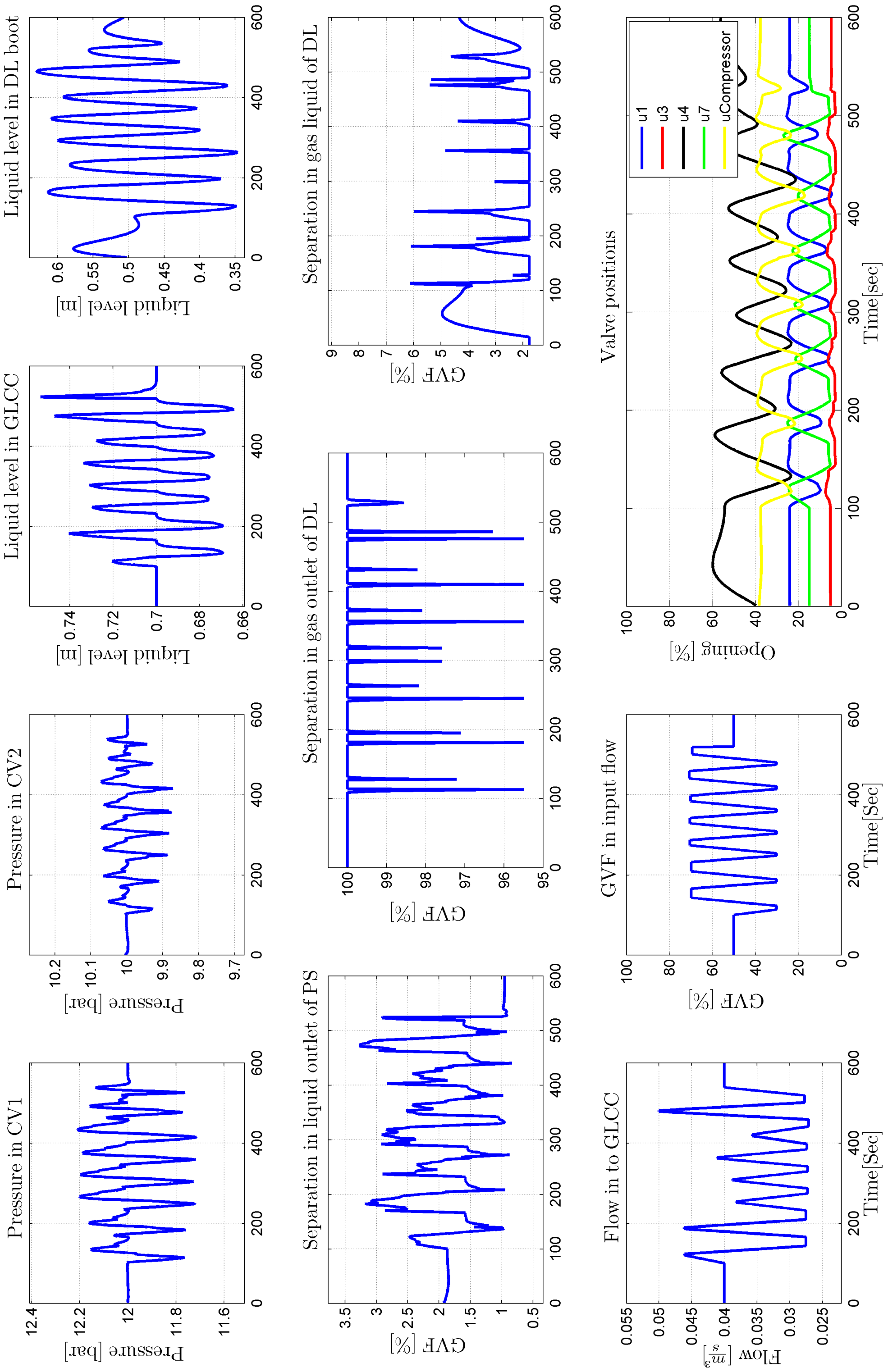

Figure 10.2: Slugging: NMPC with ideal states

Slugging is a tough case for the control algorithm, yet even through long slug cases, the algorithm should provide adequate control of the process. This means that even if the slugging goes on forever, the liquid tanks should not overflow and the GVF in the input flow to both the pump and compressor should be sufficiently low/high, such that the equipment is not damaged. The configuration used by the NMPC algorithm in the slugging case is shown in Table 8.1 [p.56], and the slugging sequence used to test the control strategy is shown in Figure 8.1 [p.54].

Figure 10.2 [p.76] illustrates the simulation of the slugging case. Only the states assumed important for the discussion of the NMPCs performance during the slug case is presented, due to a large number of measurements and states. During the duration of the slug case, the NMPC manages to deliver sufficiently pure gas and liquid flows out of the system. Both the liquid flow out of the PS, as well as the gas flow out of the DL, which are the main contributors to the liquid and gas flow out of the Compact Separation process, have certain transients in the GVF. However, these transients are short and the average GVF into both the pump and compressor are well within the desired control objectives, discussed in Chapter 7 [p.43]. The GVF of the liquid flow out of the DL will also contribute to the total liquid flow out of the Compact Separation process, but the flow rate in this output is very small compared to the liquid flow out of the PS. The GVF of the total liquid flow out of the system will therefore be mainly determined by the liquid flow out of the PS. As long as the GVF of the liquid flow out of the DL is below 5% on average, the effect of this flow on the total liquid flow will be neglected.

Figure 10.3 [p.78] illustrates a simulation with a slightly modified configuration. The linear MPC configuration used a set point of 5% on the GVF in the liquid flow out of the PS, σ. This was tested using the NMPC as well,

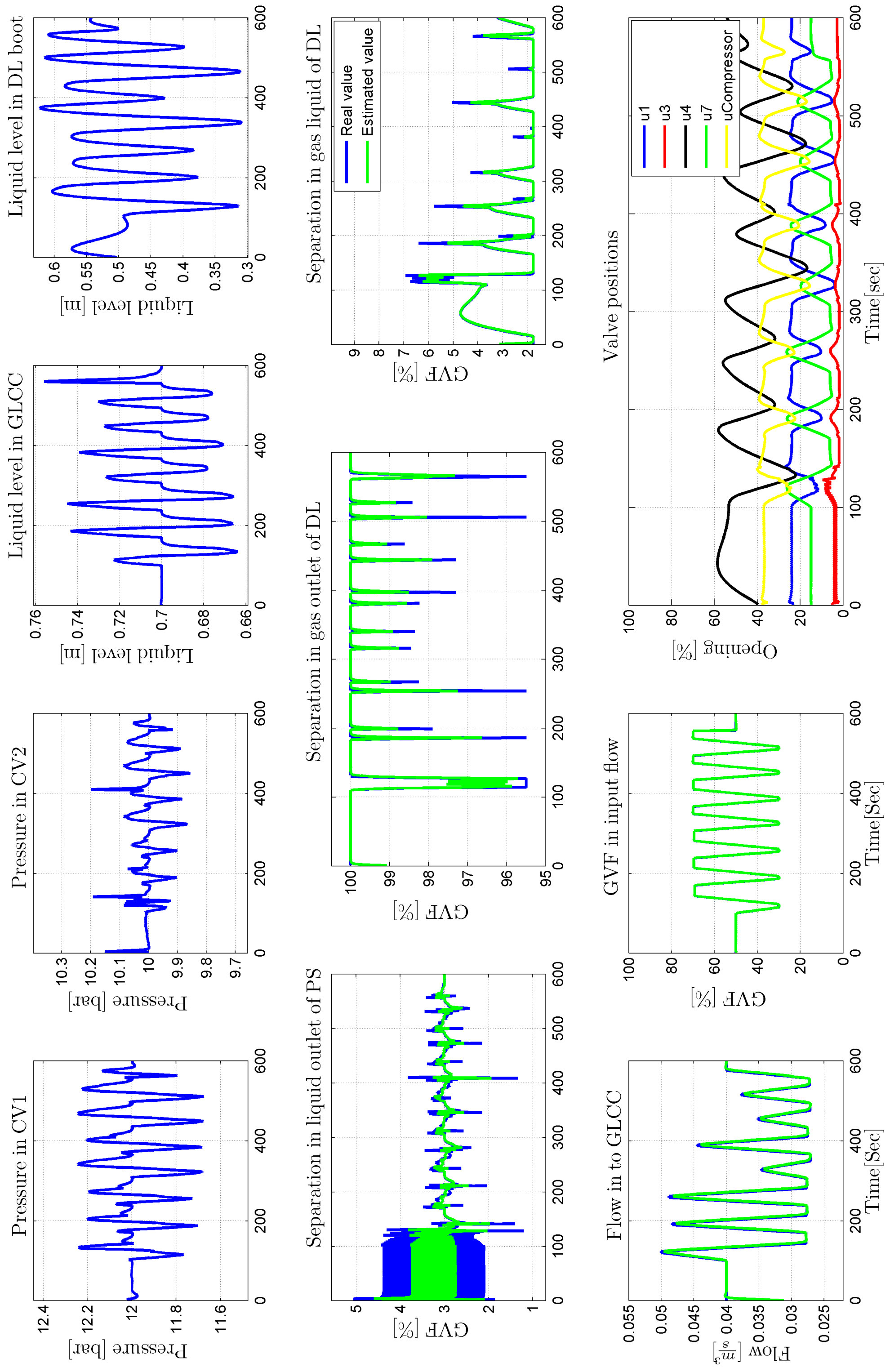

Figure 10.3: Slugging: NMPC with estimated states and set point on σ

but with a set point of 3%. In this plot, the NMPC uses estimated states from the observer, and before the slugging case started, this configuration resulted in large oscillations. The reason for this is that the estimates had not converged to the real values at the start of the simulation. Due to the problems with this configuration, the set point on σ was replaced with a high limit on 3%. This removed the oscillations, and resulted in a better liquid quality on average. The results from the simulation with the slugging configuration, where the NMPC uses estimated states from the EKF, is presented in Figure 10.4 [p.80].

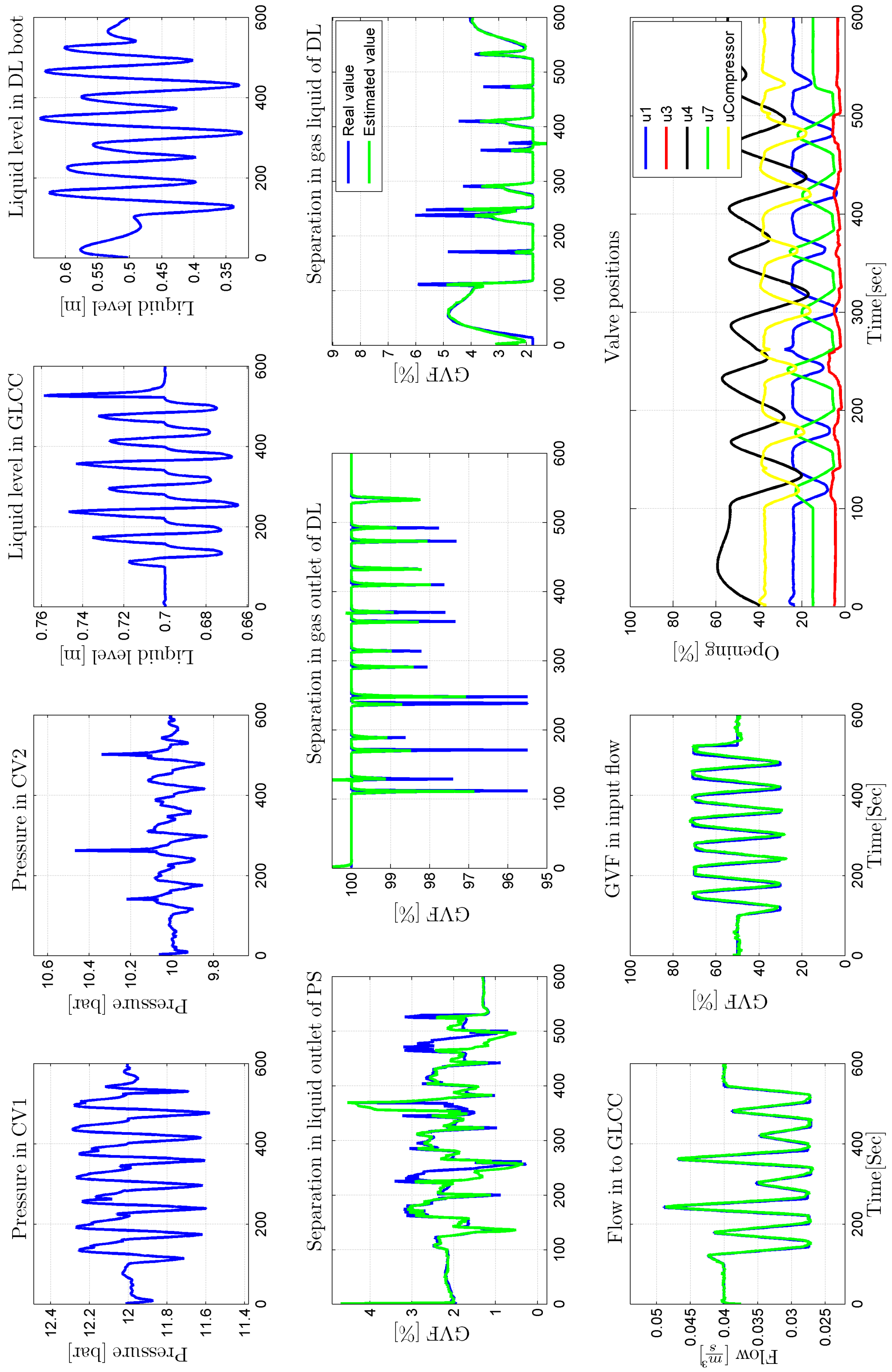

Figure 10.4: Slugging: NMPC with estimated states and high limit on σ

Chapter 11

Case: Start-up

Chapter 8, Section 8.2 [p.55], discussed the different configurations that have been tested to start the Compact Separation process – the simulation results from the different start-up configurations will be presented through this chapter.

The first control scheme tested was the basic PID-controller configuration, presented in Table 8.2 [p.57]. The results from this simulation are presented in Figure 11.1 [p.82]. From this figure it is obvious that the PID-controllers successfully manages to start the Compact Separation process, within the desired control objectives. In this start-up sequence, the flow rate into the system was ramped up from 0 to $0.04\frac{m^3}{s}$ in 20 seconds. While the flow rate was ramped up, the GVF into the system was changed. This was to simulate that, at the start of the sequence, the input flow was mostly gas and the liquid flow was increased until a certain point, before the gas was ramped up and the GVF ends at 50, i.e. 50 percent gas and 50 percent liquid in the input flow. This might not reflect the start-up at the test rig, where the gas must be started before the liquid[Kristiansen et al. (2010)], but pure gas into the system caused numerical issues with the ODE-solver.

The next start-up procedure tested was the NMPC with a planned start-up sequence. The results from this simulation is presented in Fig-

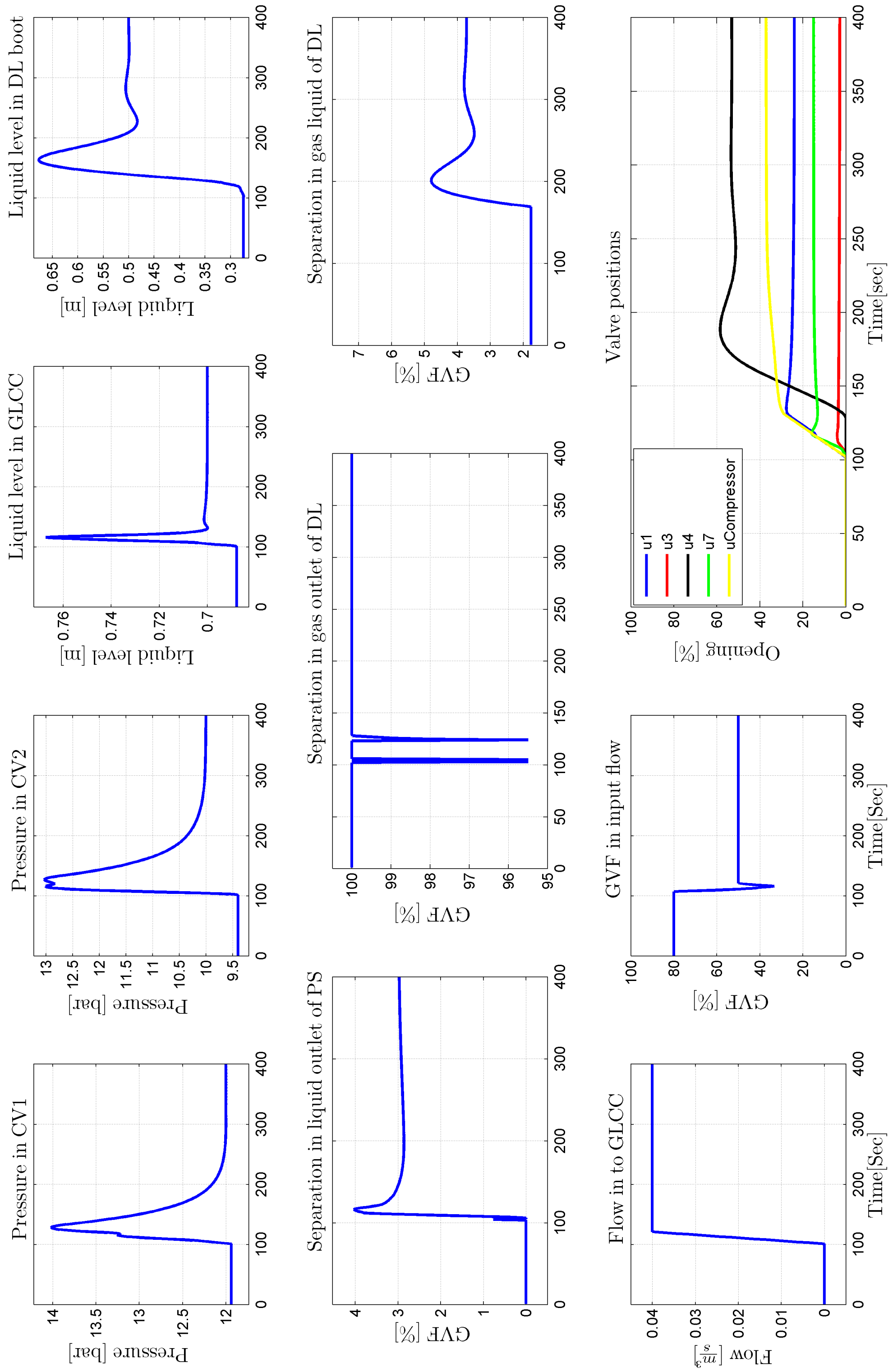

Figure 11.1: Start-up using internal PID-controller

ure 11.2 [p.84]. In this chapter, only the results with ideal states are shown, but in Appendix A [p.119], the results from the start-up procedures using estimated states are listed.

The planned start-up sequence used in this case was the same start-up sequence as the one used for the PID-controller start-up. As can be seen from the simulation results, the start-up was fast, and well within the constraints. 200 seconds after the start-up sequence begun, the system has reached steady-state.

The last start-up sequence, that was tested, was the fully automated NMPC start-up. The results are presented in Figure 11.3 [p.85]. The fully automated start-up procedure used longer time than the planned start-up. The start-up sequence could be tuned to go faster, but this resulted in numerical issues in the controller, and it was therefore hard to test a faster start-up. The GVF in the gas flow out of the DL experiences several overshoots with respect to the control objective, however, these overshoots are short and should not be considered to be a problem.

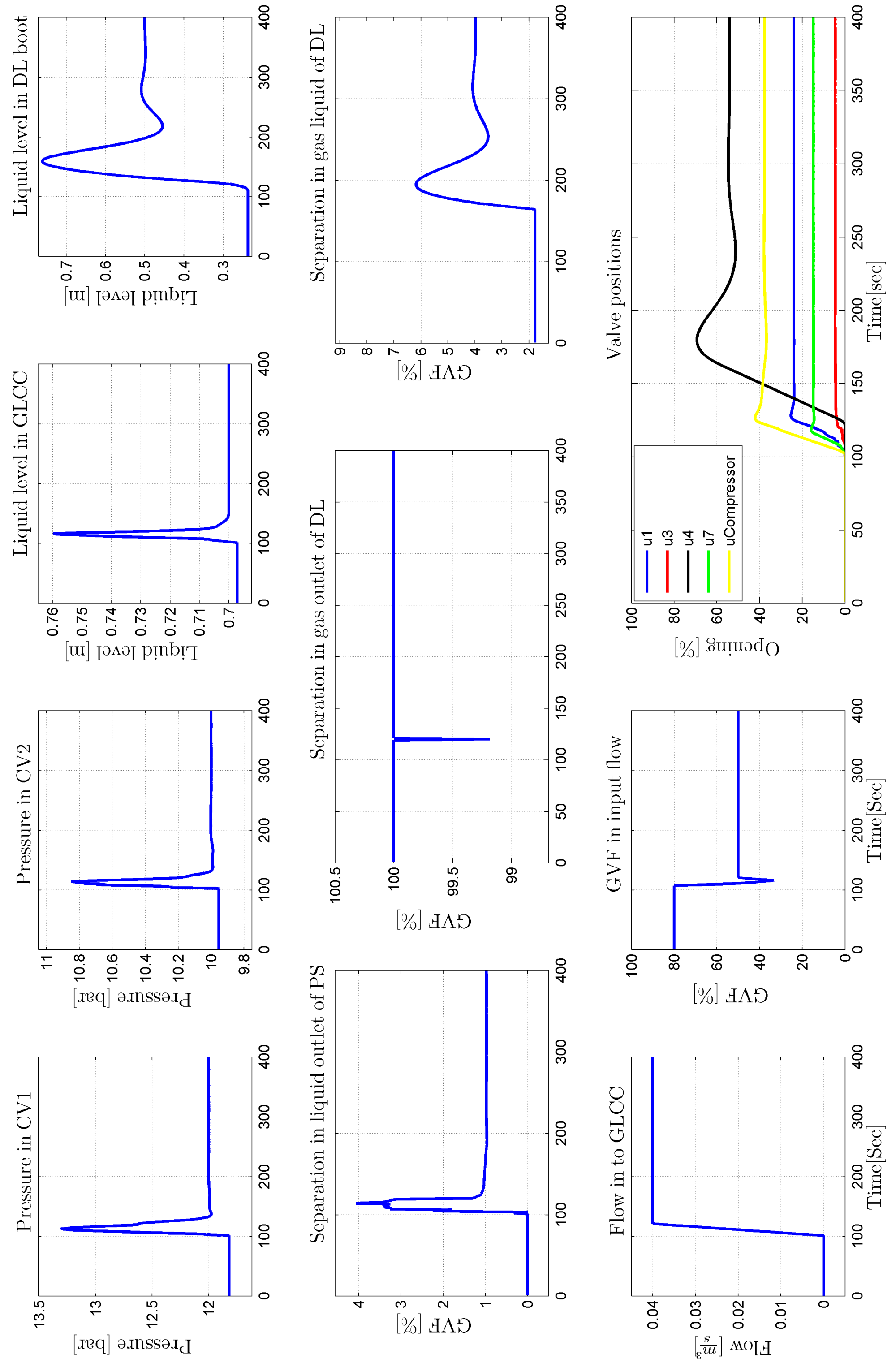

Figure 11.2: Planned start-up using NMPC with ideal states

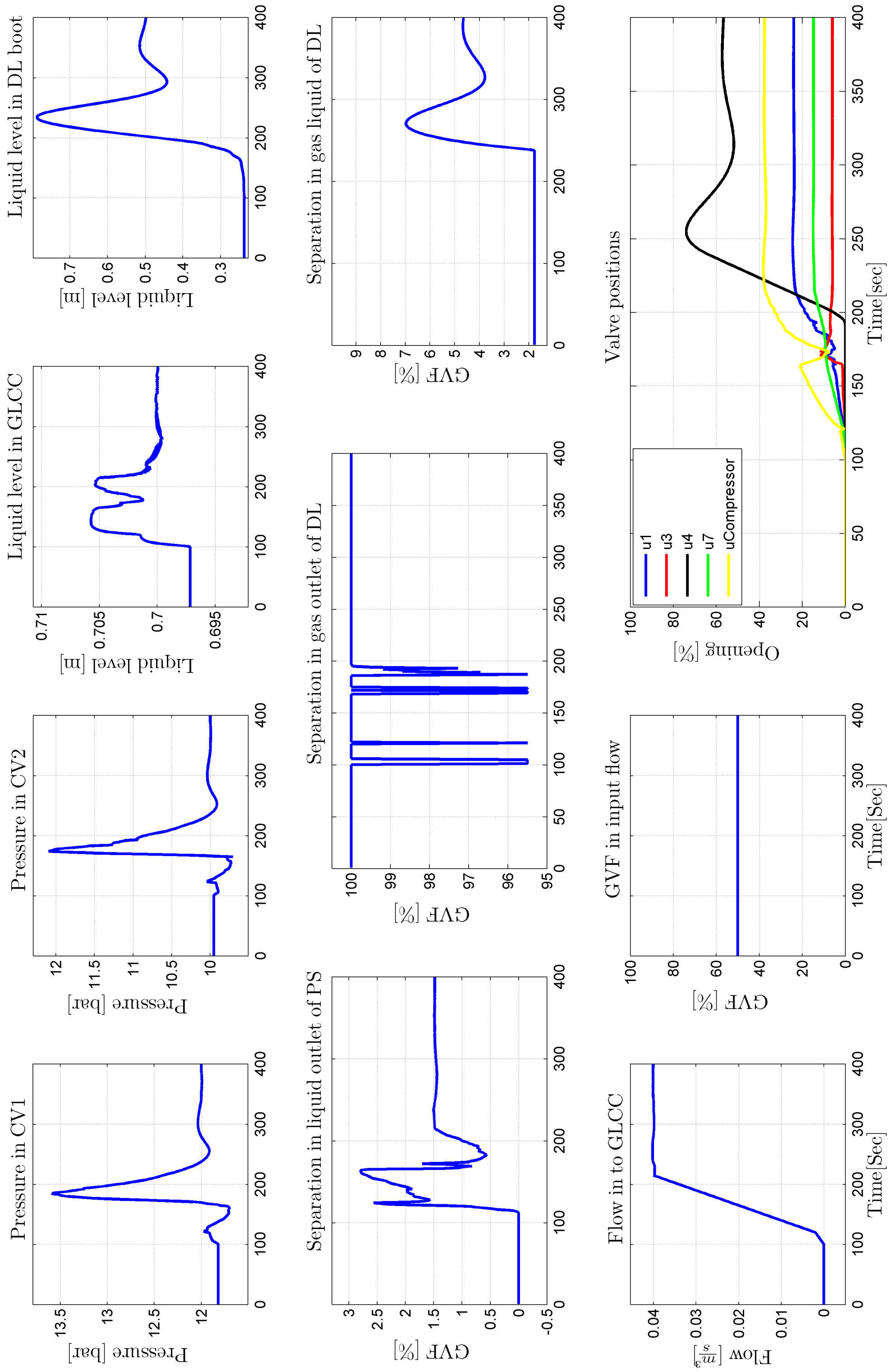

Figure 11.3: Start-up using NMPC with ideal states

Chapter 12
Case: Shut-down

As with the start-up case, several control configurations have been considered for shutting the Compact Separation process down. These configurations were discussed in Chapter 8, Section 8.3 [p.58].

The first shut-down procedure that was tested was the simple PID-controller configuration, presented in Table 8.2 [p.57]. The shut-down sequence used in this case was, as with the start-up, a preplanned sequence, where the flow rate into the system was ramped down. The GVF was also varied to simulate a possible shut-down procedure, where the gas flow into the system was reduced first. Then the liquid flow was reduced to a minimum (the solver did not manage zero liquid flow into the system), and the GVF was held constant at this level while the flow rate was ramped down the last part. The results from this case is presented in Figure 12.1 [p.88]. In order to get a sufficiently good shut-down, the shut-down sequence had to be longer than the start-up. While start-up could be managed in 20 seconds, the shut-down procedure had to be 50 seconds to be able to maintain differential pressure between the two control volumes. However, with a 50 seconds shut-down sequence, the shut-down of the process was performed within the desired control objectives.

The next case tested was the planned NMPC shut-down procedure.

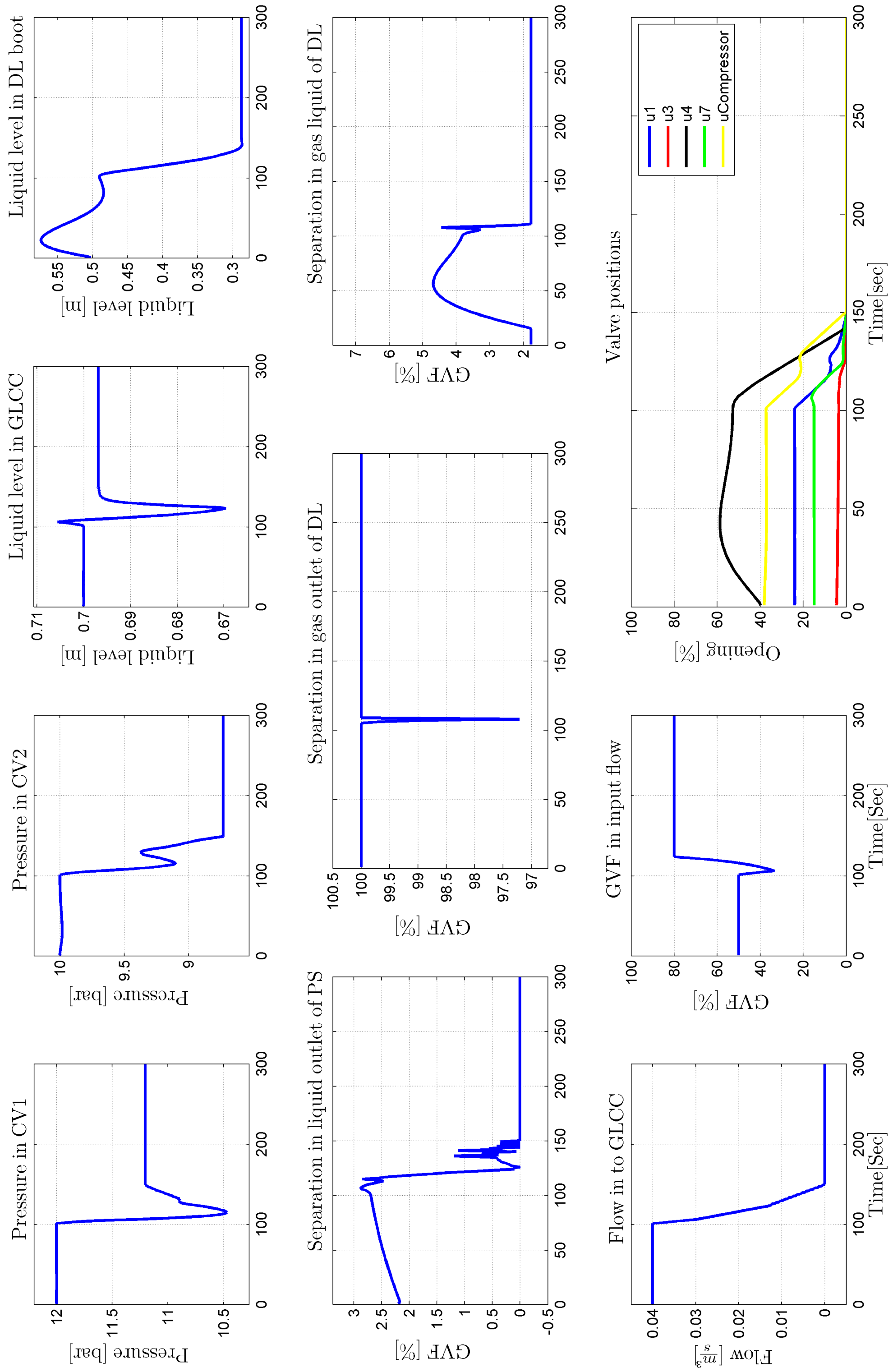

Figure 12.1: Shut-down using PID-controller

The shut-down sequence for this case is the same as for the PID-controllers. The results from the NMPC shut-down are presented in Figure 12.2 [p.90]. During the shut-down, the NMPC uses ideal states for control. The results from the shut-down procedure using estimated states are illustrated in Appendix A [p.119]. The NMPC manages to shut the Compact Separation process down successfully, and is within the desired constraints at all times – except for two transients in the GVF in the gas flow out of the DL.

A fully automated procedure was tested for shut-down as well, and the results from this simulation are presented in Figure 12.3 [p.91] for NMPC using ideal states for control. As with the fully automated start-up procedure, this method uses longer time to shut the system down than the planned sequences. The system is not completely shut down until 2 minutes have passed. The GVF in the liquid flow out of the PS has an overshoot that lasts for about 30 seconds. The reason for this is that the separation degrees are not used as CVR, since this caused numerical problems with the ODE-solver.

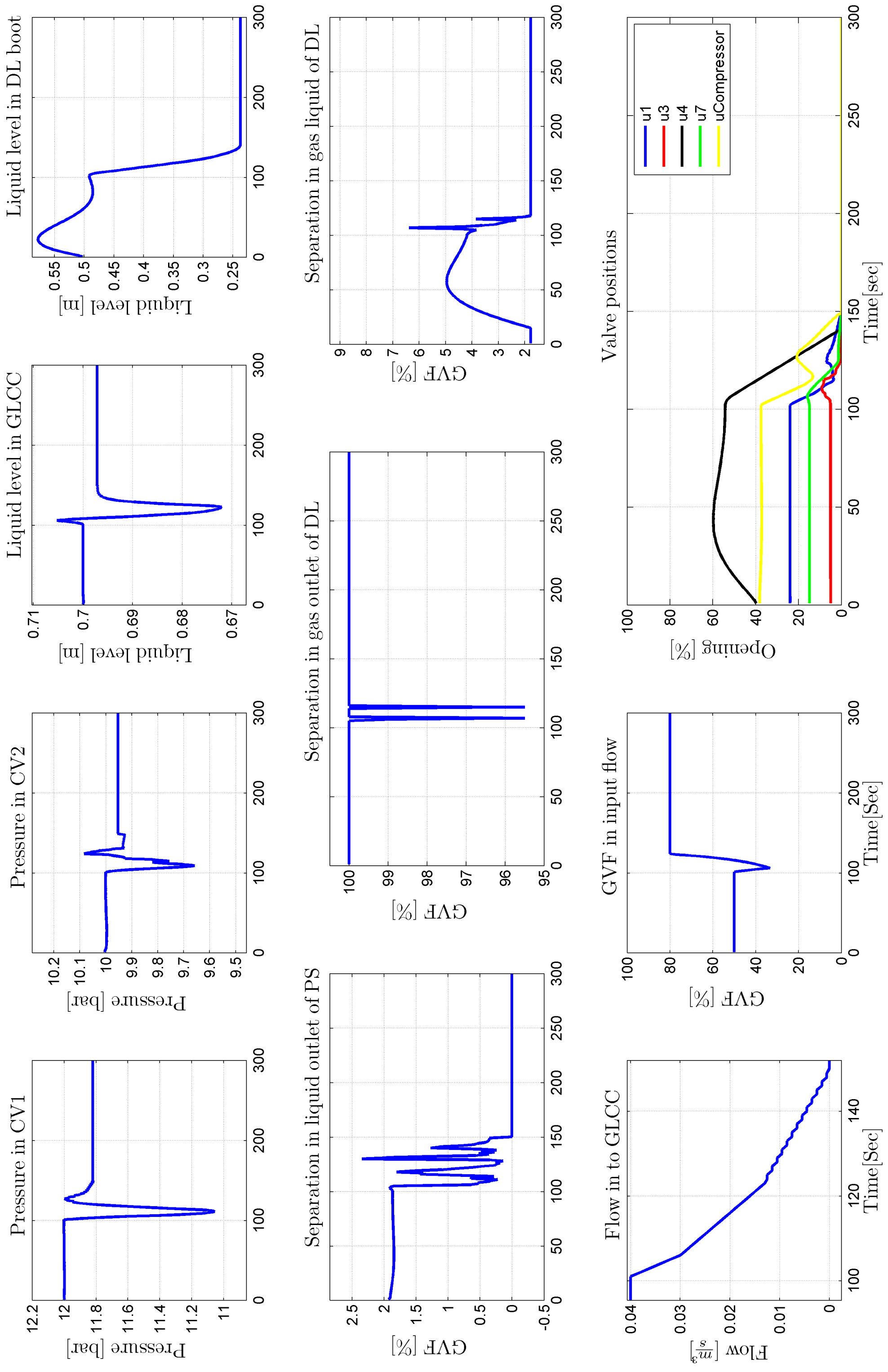

Figure 12.2: Planned shut-down using NMPC with ideal states

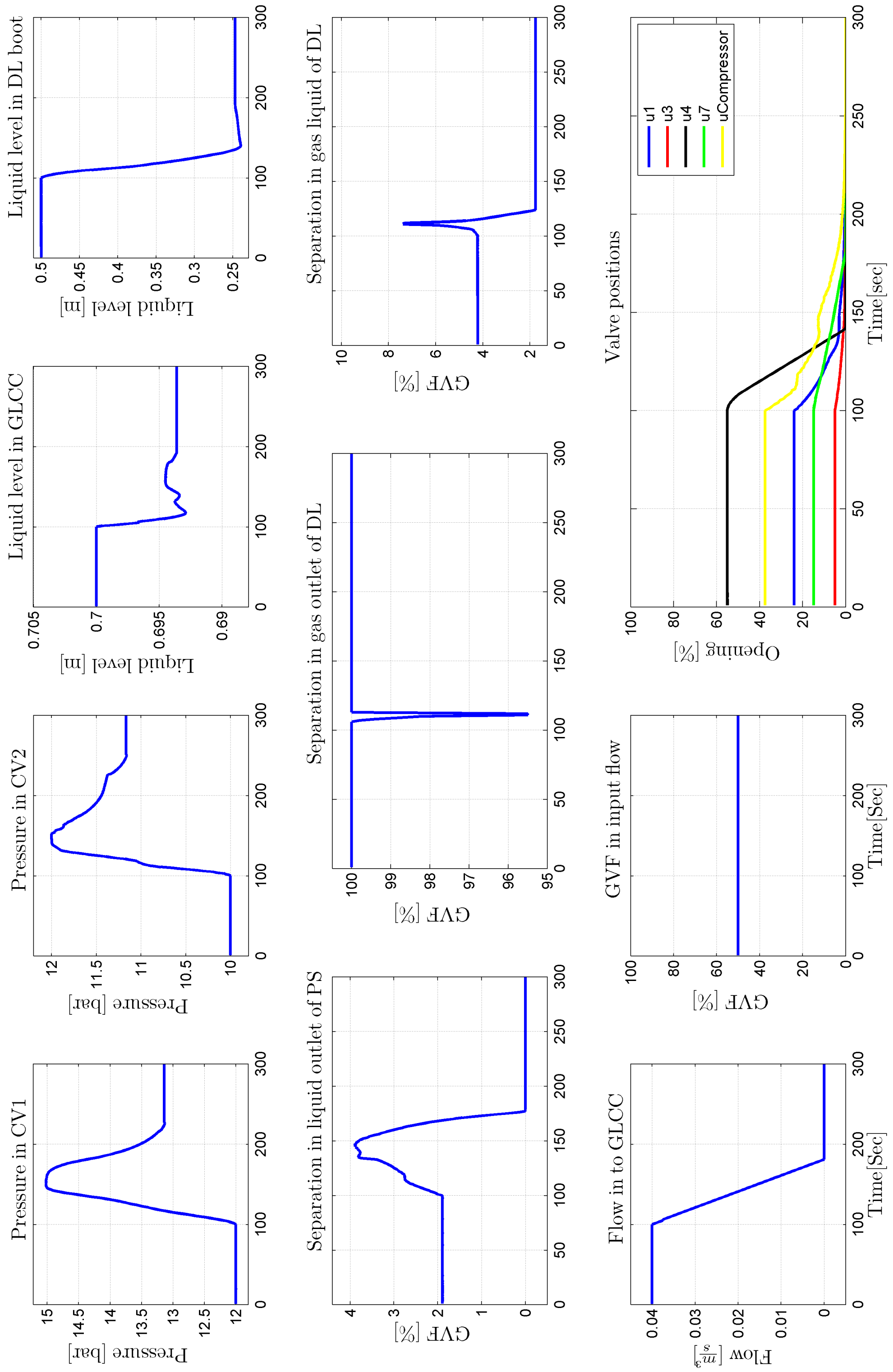

Figure 12.3: Shut-down using NMPC with ideal states

PART V

Aftermath

Abstract – The last part in this thesis will discuss the results presented in part IV [p.61], problems that have emerged during the work on this project and what the next step in the work on the Compact Separation process might be. The first chapter presents the discussion of results, while the next and final chapter will make some concluding remarks and suggest further work.

Chapter 13
Discussion

Through this thesis the Compact Subsea Separation Unit Statoil is currently developing, has been presented. The Compact Separation project has recently gone through a test demonstrating the concept, and the implemented control system was evaluated. Both basic control using PID-controllers and a linear MPC algorithm was tested. It was concluded that model predictive control was the preferred control strategy. The linear experimental models used to represent the gas-liquid separation proved inadequate for predicting future behavior of the process. Since the linear MPC approach underperformed, the next step was to assess the nonlinear version of MPC. To justify the more complex control structure of the NMPC, a more accurate and robust control must be provided. Unlike the linear MPC, the nonlinear MPC requires an observer to gain access to all internal process states and to reduce noise on the measured states. This thesis has therefore focused on implementing a nonlinear model predictive control strategy that uses the states and parameters estimated by an observer.

13.1 Process model

During the process of implementing the nonlinear MPC, several bugs in the implemented nonlinear separation profiles, as well as some bugs in the process model, were discovered and mended (and some new bugs were most likely introduced). These bugs include divide-by-zero and wrongly implemented equations. Exemplifying: In Equation 2.7b [p.14] ρ_L's and ρ_x's knowns were interchanged, i.e. $(1 - S)$ and S had switched places.

Another error was gas/liquid conservation through the Phase Splitter and the De-liquidizer. Conservation of mass is used to conserve gas and liquid in the different control volumes, but not through the in-line separation units. Through the PS this was not as problematic as through the DL, but the separation degrees on the outlet of the PS would not properly reflect the inlet properties of the flow. In the DL, the lack of gas/liquid conservation would cause the liquid gathered in the DL tank to flow back up and out of the gas outlet of the DL. This is not possible, due to the structure of the DL.

13.2 Observer performance

The implemented observers have not been used for control during the summer project. Nor have the observers been tested on different process disturbances, like slugging, start-up and shut-down sequences. The observer must provide accurate estimates in the whole region of operation of the process. The two implemented observers have a different structure, as discussed in Chapter 5 [p.27], and will therefore exhibit different properties and performance.

State estimation

Results from the state estimation using the extended Kalman filter and the unscented Kalman filter is shown in Figure 9.1 [p.64] and Figure 9.2 [p.66] respectively. As discussed in Chapter 9 [p.63], the estimation of the states using both observer schemes was generally good for most of the states. The hardest state to estimate was the mass of the liquid in CV 1. The mass of the gas in CV 1 was also a bit sensitive to noise, but not as much as the mass of the liquid. One of the reasons for the sensitivity in estimation of the liquid mass, was that this state was estimated from measurements of the liquid level in CV 1. This measurement was very noisy, since measurements of the liquid level was not only affected by electrical noise in the sensor, but also from waves on the liquid surface. Figure 13.1 [p.98] shows a simulation using significantly less noise on the liquid level in the GLCC. The noise was reduced from 10% to 2%, and the estimates of the liquid mass was significantly improved. The estimates of the mass of the gas in CV 1 does, however, have some overshoots, but this can be due to noise on another parameter.

The masses in the different CVs are not used directly by the controller to calculate new inputs since neither of these states are used as CVRs – meaning that this sensitivity will not affect the controller that much. It will, however, make the estimation problem harder; and is the reason for the over-/undershoots in σ and ν that can be seen in both Figure 9.1 [p.64] and Figure 9.2 [p.66].

Plots of the different start-up and shut-down procedures are presented in Appendix A [p.119], and from these results it can be seen that there is not much difference when it comes to controlling the Compact Separation process using either EKF or UKF as the applied observer. Since the controller is meant to run in real time, the relatively high run-time complexity of the UKF compared to EKF could be reason alone to choose the EKF.

Also worth noting, is that the PID-controllers use measurements that are not filtered by the observer. Therefore, the PID-controllers have only used the ideal measurements throughout this project. In a real application,

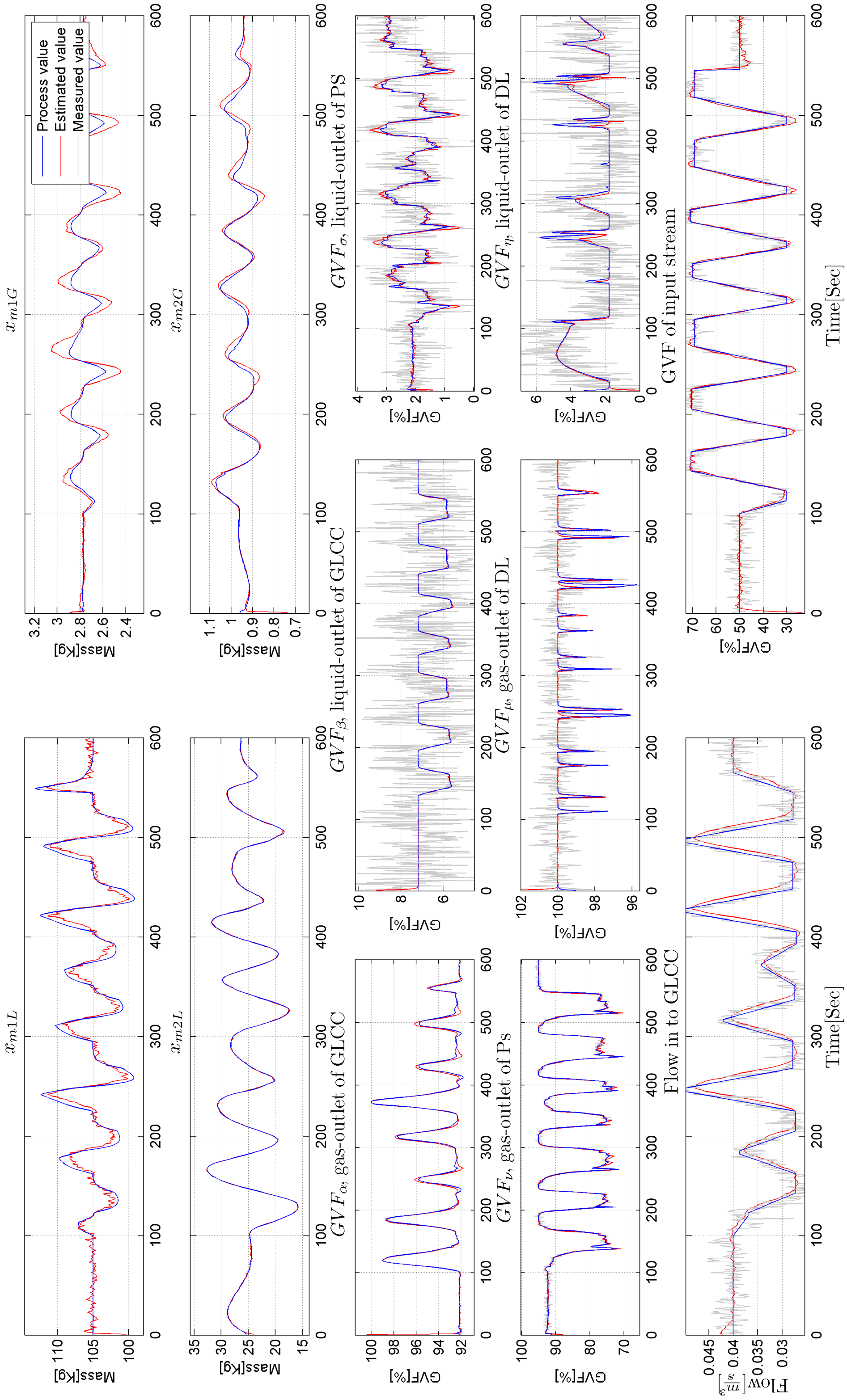

Figure 13.1: States estimated using EKF, less noise on liquid level in GLCC

the measurements used by the PID-controllers could be filtered by a Kalman filter, but since the PID-controllers are running every 0.1 seconds and the NMPC are running once each second – the Kalman filter might be unable to meet the time constraints of the PID-controllers. Another possibility could be to filter the measurements using a low-pass filter or another simple filtering algorithm.

Parameter estimation

Figure 9.3 [p.68] shows the result of trying to estimate the unknown model parameters using EKF. All parameters, except for the scaling of σ, converged during one slug-sequence simulation. At the end of the simulation the estimated states had also converged to the real process values, as can be seen from Figure 9.4 [p.70]. Even the GVF in the liquid flow out of the PS, σ, converged – even when parameters actually diverged.

Different observer setups to solve the dual estimation problem was discussed in Chapter 6 [p.35], and it was noted that the observers implemented in SEPTIC uses a so-called joint Kalman filter algorithm. This method estimates states and parameters using only one Kalman filter. The drawbacks of this was a high coupling between the states and the parameters, and an algorithm that could suffer from potential convergence problems. This might be an explanation for the difficulty in estimating both the parameters and the states – a possible solution could be to use the dual Kalman filter algorithm, discussed in Chapter 6 [p.35]. This algorithm uses one Kalman filter to estimate the states and one to estimate the parameters. This could lead to a smaller run-time complexity, since the state estimating Kalman filter will have fewer states, and the parameter estimating Kalman filter can run with a slower frequency, even on its own processor – if so is desirable. This scheme would also allow tuning of the two filters separately, which might reduce the parameter estimation's sensitivity in the tuning parameters – which also was a problem.

Estimation using off-line process data

Figure 9.5 [p.72] shows the results from the simulation where off-line process data has been used to update the observer. Without parameter estimation the observer was unable to track and smooth the measurements. The reason for this is the model/plant mismatch and trusting the model too much in the estimation. However, trusting the measurements too much would cause very noisy estimates.

Figure 9.6 [p.73] illustrates the parameter estimation during the same simulation as the state estimation discussed above. In order to get a good estimation, parameters estimating the bias had to be introduced on both the flow rate into the system as well as the GVF in this flow.

In Figure 9.7 [p.74] the parameter estimation has been turned off, except for the bias estimation on the input flow rate and GVF. The constant parameters used in this simulation were taken from the last values in the parameter estimation shown in Figure 9.6 [p.73]. The observer is not able to provide decent state estimates during this run, meaning that a different parameter estimation scheme should be chosen. The reason for this is that a good parameter estimation scheme should provide an estimate of the model parameters, not adjust the model to fit at the given time. This might not be possible if the structure of the real process is not similar to the model.

Scaling of the GVF of the liquid flow in the PS outlet turned out to provide too poor estimates. Therefore, a parameter estimating the bias was introduced instead. From Figure 9.6 [p.73] it can be seen that the estimate of the σ-parameter has the same shape as the measurement of σ. This indicates that the model of this separation profile is not a good reflection of the real process model.

Only the EKF was used on the off-line data as well as for parameter estimation during simulations, due to a numerical problem causing the whole application to crash when trying to estimate the states using UKF. This problem is further discussed in the subsection below.

Numerical evaluation

The implemented observer usually inhibits good numerical properties, but some issues must be addressed. The implemented observers are unconstrained and in certain cases, like in the initial start-up of the filter, the estimates can be outside the region of allowed values. This can cause the whole SEPTIC-application to crash. This mostly happened during the initial steps, but there is no guarantee that this cannot happen at any given time.

Another issue with the observers are a crash that may happen at any given time during the simulation. The reason for this crash was not found before the end of the project and has therefore not been fixed. During the summer project, an ODE-solver, different from the one used by SEPTIC to solve the MPC-problem, was implemented to run the model in the Kalman filter. This ODE-solver does not seem to be as robust as the solver used by SEPTIC and has been found to be the most likely reason for the observer crashing. The UKF algorithm was more sensitive to this problem than the EKF algorithm.

The ODE-solver used by the Kalman filters does not have the capability of iteration limits. This can potentially cause the observer to run forever – if it runs into a especially difficult case.

The numerical properties of the ODE-solver used in the NMPC was much more robust, even though this ODE-solver had problems when changing set points or disturbances too fast. Another problem was that not all cases could be simulated, such as start-up and shut-down using pure gas at the start/end of the sequence.

13.3 Control system performance

The control strategy was developed with a basis in the linear control strategy shown in Table 7.3 [p.48]. Several different control strategies were attempted during the work on this thesis, but the strategy that seemed to work best was the strategy shown in Table 8.1 [p.56] – which is a modified version of the old strategy. The main difference is the new control variable, namely the differential pressure between the two CVs. In a real application, the set points and the high and low constraints on pressure are important, because it is desirable to stay near a certain operating point. However, the test rig is a closed loop system where the gas and liquid separated through the Compact Separation unit are combined and recirculated again. This makes it more convenient to let the Compact Separation unit "follow" the pressure of the input to the rig. The differential pressure over the test rig could therefore become very large, which in turn would make the job hard for the operator of the test rig to control the feedback loop of gas and liquid. Actually, with respect to the gas-liquid separation, it would be desirable to minimize the differential pressure over the Compact Separation process, since a very small flow through the system would provide the best separation of gas and liquid. At very small flow rates, however, the production would be small – which is not desirable. If we think about future applications with pump and compressor in place, a certain minimum flow would be required to operate the system as well. Therefore, a minimum differential pressure between the different CVs are required.

Slugging

The results from the simulation study with the slug-case is presented in Chapter 10 [p.75] and the slug-sequence used to test the control system is shown in Figure 8.1 [p.54]. As mentioned earlier, it was not possible to use a square-pulse slugging sequence since this caused numerical problems in the ODE-solver. These numerical issues could also arise by rapid changes in the valve opening or by a too large change in set point. Therefore, when a change in the set point was required, this could be solved by ramping the set point up to the desired value. The change in valve openings could be reduced by punishing the use of the manipulated variables in the control strategy, thus allowing short-frequent disturbances to just pass through. Changes in disturbances are not generally something that can be controlled, but to simulate the slug-case, the disturbance had to be ramped up/down as well.

In the figures in Chapter 10 [p.75] the GVF of the output flows are plotted, along with other information. From these figures, it can be seen that the controller is able to handle a long slug sequence, both by using ideal states and by using states estimated by the observer. Using states estimated by the observer did, however, pose some restrictions on the choice of control strategy. The controller may become unstable due to inaccuracies in the estimates, and it is important to choose a control strategy that minimizes the probability of this happening. Figure 10.3 [p.78] illustrates a possible outcome where the controller becomes unstable due to inaccurate estimates. To solve this problem the high priority set point on σ at 3% was changed to a high priority high limit at 3%. This resulted in a more robust control strategy, and the average GVF in the liquid flow out of the PS where also lowered.

All the separations presented in Chapter 10 [p.75] experience certain transients. These transients occur when the total flow rate into either the De-liquidizer or into the Phase Splitter falls beneath a certain operating point. This happens since both the PS and the DL are designed to operate at a certain level, and when the flow rate into one of these units drops below this operating point, the quality of the separation of the unit decreases significantly. The control system uses a few seconds to adjust the valves when this happens – to compensate for the poor quality of the separation.

Start-up

The second case used to test the controller performance was the start-up strategy. The control strategy used in the slugging case was tested to start the Compact Separation process up from zero input flow and with all valves closed, to a desired working area. A preplanned start-up sequence was used to ramp up the input of the system, as discussed in Chapter 11 [p.81]. A PID-controller scheme was also tested to start up the system, using the same start-up procedure as the one used by the NMPC algorithm. Figure 11.1 [p.82] shows the result from the planned PID-controller start-up, while Figure 11.2 [p.84] shows the result from the planned start-up using NMPC with ideal states. Results from the start-up case, using states estimated by the observers, are shown in Appendix A [p.119]. These two schemes does not show too much differences; both controllers comply with the desired control objectives, also when the NMPC uses estimated states. In both the planned start-up control schemes, the input to the systems are ramped up in 20 seconds. Ramping up the input faster than this caused numerical problems for both the PID-controller and the NMPC. It is desirable to start the system as fast as possible – to maximize the production, but not faster than the control system can handle. In the two cases discussed above, the system reaches steady-state after about 200 seconds after start-up was initiated.

A modified control scheme was also tried to start the Compact Separation process up from zero input flow. The results from this simulation is shown in Figure 11.3 [p.85] for NMPC using ideal states. This control strategy performs within the given constraints, except for a few peaks – but the time used to start the system up using this controller is about 120 seconds. It was hard to avoid numerical problems with this configuration. Therefore, the GVF of the input flow could not be used as a manipulated variable in addition to the flow rate into the system – as was desired.

Shut-down

As with the start-up case, three different shut-down configurations were tested and are presented in Chapter 12 [p.87]. Both of the planned shut-down sequences, be it PID-controlled or NMPC, worked according to the specifications. However, the shut-down sequences could not be executed faster than 50 seconds – without causing numerical problems. The planned shut-down sequences also worked well when using estimated states in the NMPC, although the transients in the GVF in the gas flow out of the DL had a longer duration when the NMPC used states from the EKF; as can be seen from Figure 12.2 [p.90] compared to Figure A.5 [p.124] and Figure A.6 [p.125]. The planned shut-down with NMPC using states estimated by the UKF actually had one less transient than the ideal case. The differences between the ideal case and between the two observers, comes from the delay in the estimates when a change occurs.

Figure 12.3 [p.91] shows the modified NMPC shut-down configuration for ideal states. This configuration uses about 150 seconds before the system is completely shut-down; it was very hard to avoid numerical issues.The configuration was also extremely sensitive to changes in penalty on the deviation from the desired value on the valves – which was set to zero. A small change in this penalty could cause a too fast or too slow shut-down of a valve, which could cause the entire shut-down to fail. As with the start-up case, the shut-down sequence was unable to use the GVF of the input as MVR due to numerical problems.

A last thing worth noting about the fully automated shut-down and start-up procedure, is that to get the start-up and shut-down to work, the high and low limit on the separation of the flows out of the PS had to be removed. These control objectives were held most of the time nonetheless, but a disturbance on the input could cause this to change. Due to these limitations and due to the numerical sensitivity of the ODE-solver when using this strategy, it seems that the more robust start-up and shut-down sequence would be the planned NMPC or PID-controller start-up and shut-down. The PID-controller scheme is simple, however, the NMPC scheme would already be used for the normal operation of the plant – and model predictive control is preferred among operators due to the higher human-to-machine interface.

Chapter 14
Conclusions and further work

The complete Compact Separation process has been simplified to match the test rig used to demonstrate the concept of Compact Separation. Thus, making this thesis focus on the simplified Compact Separation process. However, the requirements for the test rig are still the same as for the complete system. Therefore, the simplified Compact Separation process should provide good separation – even during large process disturbances.

The performance of the implemented observers have been evaluated, and both the observers are able to estimate states with sufficient accuracy. However, some filtering should be provided on the liquid level measurements: Both with respect to the PID-controllers and the increase in accuracy this can provide. Too much noise can make the estimates noisy and unreliable, as have been proved in Chapter 9 [p.63].

The extended Kalman filter has also been successfully tested to track and smooth measurements from an off-line data set from the test rig and provided feasible estimates for the unmeasurable states. Unfortunately, the unscented Kalman filter was highly sensitive to a numerical problem with the ODE-solver used by the observers, and tests on the off-line data could not be performed using this observer scheme.

Parameter estimation has been tested on both the off-line data set and through simulations using EKF. Even though the parameter estimation scheme did not work optimally, it proved to be crucial with respect to estimation of states on the off-line data set – due to the model/plant mismatch.

The implemented NMPC configuration was tested on several different process disturbances, like start-up, shut-down and slugging. The NMPC configuration proved adequate and performed well on all the tested disturbances. The modified NMPC configuration was successfully used for start-up and shut-down, but in its current state, it has proved to be less robust than the normal NMPC configuration. Thus, the suggested normal NMPC configuration can be used for normal operation, including slugging sequences, and start-up and shut-down using preplanned ramping of the input gas and liquid flow.

14.1 Further Work

This section will present the problems with the implemented algorithms and models as they are today, and suggest further work to improve the Compact Separation process' control algorithm.

Model adjustment and parameter estimation

As discussed in Chapter 13 [p.95], the implemented parameter estimation scheme was not optimal; the parameters did not converge to a constant value representing a parameter defining the real process. Therefore, these estimated parameters would not provide a good representation of the model, if the parameter estimation was turned off, and the last values of the parameter estimation was used as the model parameters. A different setup, possibly with an increased number of parameters, should be implemented.

The model of the separation in the liquid flow in the outlet of the PS should be revised, as this model seemed to be the model that deviated most from the real process.

Filtering of measurements

The liquid level PID-controllers used ideal measurements for control. In a real application, the PID-controllers will only have access to noisy measurements, meaning some sort of filtering must be performed. Using the filtered measurements as input to the Kalman filter might also help reduce the noise on the mass of the liquid level in CV 1.

Observer implementation

Since the ODE-solver used in the observer have been found to be the most likely reason for the crashes of the observer, the ODE-solver should be changed. The fact that this ODE-solver does not have the capability of an iteration limitation supports the decision to change it, since it can lead to unacceptable behavior if the solver runs into a difficult case and is unable to deliver estimates to the controller.

The other problem that could cause the observer to fail, is its inability to constrain the states. In some cases, the estimates would be outside the feasible region, and this could cause the observer to fail. Therefore, implementation of a constrained observer should be considered.

Bibliography

Fred Daum. Nonlinear filters: Beyond the Kalman filter. *IEEE Transactions on Aerospace and Electronic Systems*, 2005.

Christian Ellingsen. Compact sub sea separation: Implementation and comparison of two different structures. Master's thesis, Norwegian University of Science and Technology, 2007.

Rolf Findeisen and Frank Allgöwer. An introduction to nonlinear model predictive control. *21st Benelux Meeting on Systems and Control*, 2002.

Rolf Findeisen, Frank Allgöwer, and Zoltan K. Nagy. Nonlinear model predictive control: From theory to application. *Journal of the Chinese Institute of Chemical Engineers*, 35:299 – 315, 2004.

Kjetil Fjalestad, Gisle Otto Eikrem, and Olav Kristiansen. Process control systems - CompactSep integrated process. Technical report, Statoil, 2010.

Bjarne Grimstad. Nonlinear MPC of a compact subsea separation plant. Master's thesis, Norwegian University of Science and Technology, 2008.

Andreas Hammervold. Model based estimation and control of BOS converter. Master's thesis, Norwegian University of Science and Technology, 2011.

João P. Hespanha. *Linear Systems Theory.* Princeton University Press, 2009.

Tor Arne Johansen. Introduction to nonlinear model predictive control and moving horizon estimation, 2011.

Simon J. Julier and Jeffrey K. Uhlmann. A new extension of the Kalman filter to nonlinear systems. *Signal processing, sensor fusion, and target recognition VI*, 1997.

Rambabu Kandepu, Bjarne Foss, and Lars Imsland. Applying the unscented Kalman filter for nonlinear state estimation. *Journal of Process Control 18*, 2007.

Hossein Khodadadi and Hooshang Jazayeri. Applying a dual extended Kalman filter for the nonlinear state and parameter estimations of a continuous stirred tank reactor. *Computers and Chemical Engineering*, 2011.

O. Kristiansen, G. S. Eidsmo, G. O. Eikrem, K. Fjalestad, Ø. Sørensen, and J. Morehouse. Integrated system, high - pressure SINTEF test results, CompactSep JIP phase 1 (revision 1). Technical report, Statoil, 2010.

Giancarlo Marafioti, Sorin Olaru, and Morten Hovd. State estimation in nonlinear model predictive control, unscented Kalman filter advantages. *Springer-Verlag*, 2009.

Jørn Sandvik Nilsson. Nonlinear MPC of a compact subsea separation plant. Master's thesis, Norwegian University of Science and Technology, 2008.

D. Simon. Kalman filtering with state constraints: a survey of linear and nonlinear algorithms. *IET Control Theory and Applications*, 2009.

Tarjei Steinshamn and Petter Norgren. Observer design for a compact separation process. *Summer Project 2011*, 2011.

Matthew J. Tenny and James B. Rawlings. Efficient moving horizon estimation and nonlinear model predictive control. *Proceedings of the American Control Conference, Anchorage, AK*, May 8 - 10:4475 – 4480, 2002.

Sridhar Ungarala, Eric Dolence, and Keyu Li. Constrained extended Kalman filter for nonlinear state estimation. *8th International IFAC Symposium on Dynamics and Control of Process Systems*, 2007.

E. A. Wan and A. T. Nelson. Dual Kalman filtering methods for nonlinear prediction, smoothing and estimation, 1997.

E. A. Wan, Rudolph Van der Merwe, and A. T. Nelson. Dual estimation and the unscented transformation. *Neural Information Processing Systems*, 2000.

Eric A Wan and Alex T Nelson. Dual EKF methods, 2001.

Frank M. White. *Fluid Mechanics*. McGraw-Hill, 2006.

Declaration

I herewith declare that I have produced this work without the prohibited assistance of third parties and without making use of aids other than those specified; notions taken over directly or indirectly from other sources have been identified as such. This paper has not previously been presented in identical or similar form to any other Norwegian nor foreign examination board.

The work presented in this thesis was conducted from August 2011 to December 2011 under the supervision of Professor Lars Imsland at the Norwegian University of Science and Technology and PhD Gisle Otto Eikrem at Statoil.

TRONDHEIM - NORWAY, 20th of December 2011

Reflection

Through this project I feel I've done more than just expand my theoretical skills. I feel I've learned how much trouble a small error can provide and how *frustrating* it can be when nothing works: But yet, the *experience* and *feeling* of solving a problem by never giving up – well worth every hour.

> *The dictionary is the only place where success comes before work.*
>
> – Mark Twain

Appendices

The appendix includes additional results not directly required in the discussion performed through the thesis. All the results presented in the appendices, as well as in the rest of the report, can also be found in digital form on the CD attached on page vii.

Appendix A
Additional plots

List of additional plots

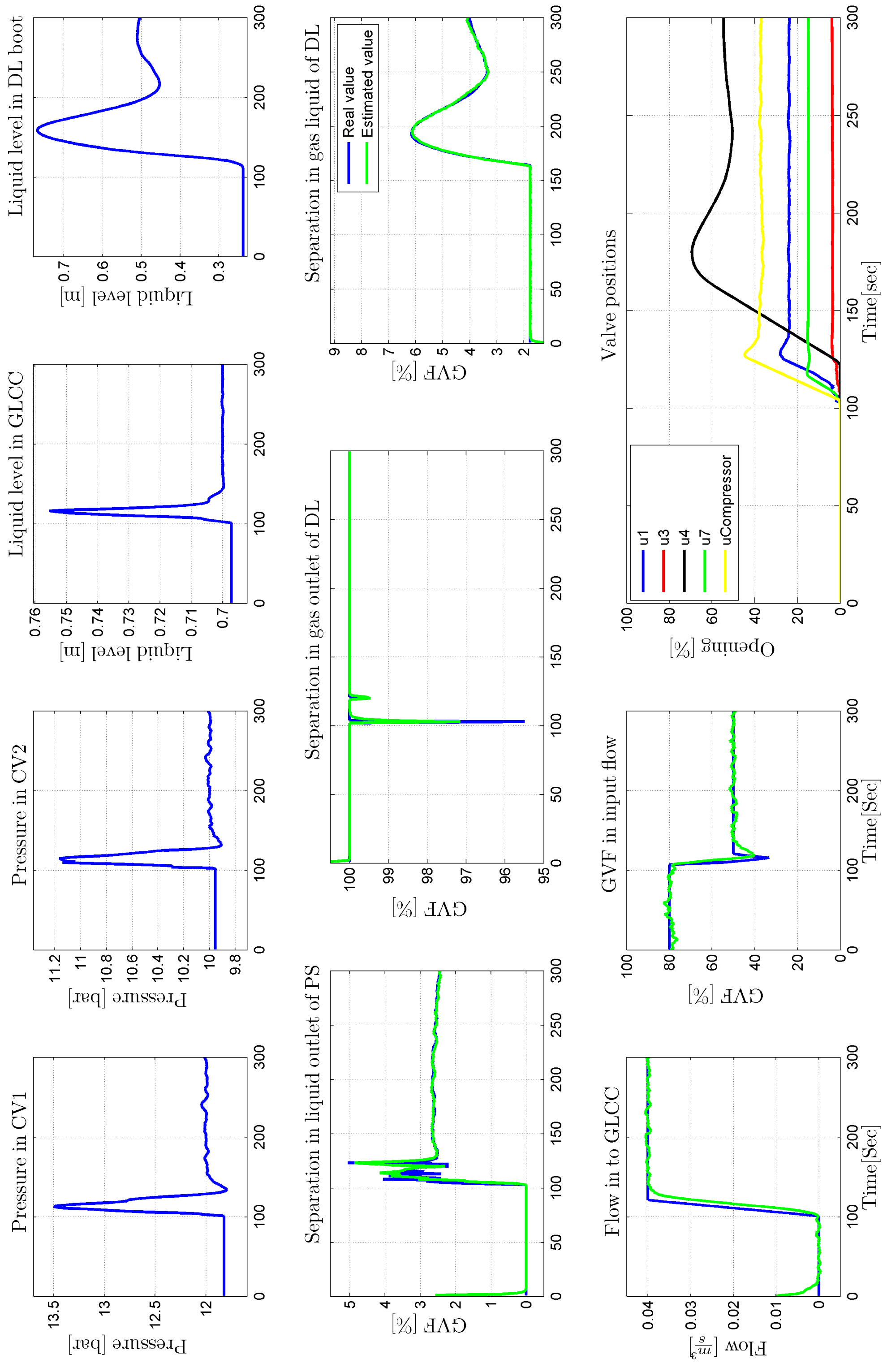

Figure A.1: Planned start-up using NMPC with estimated states from EKF

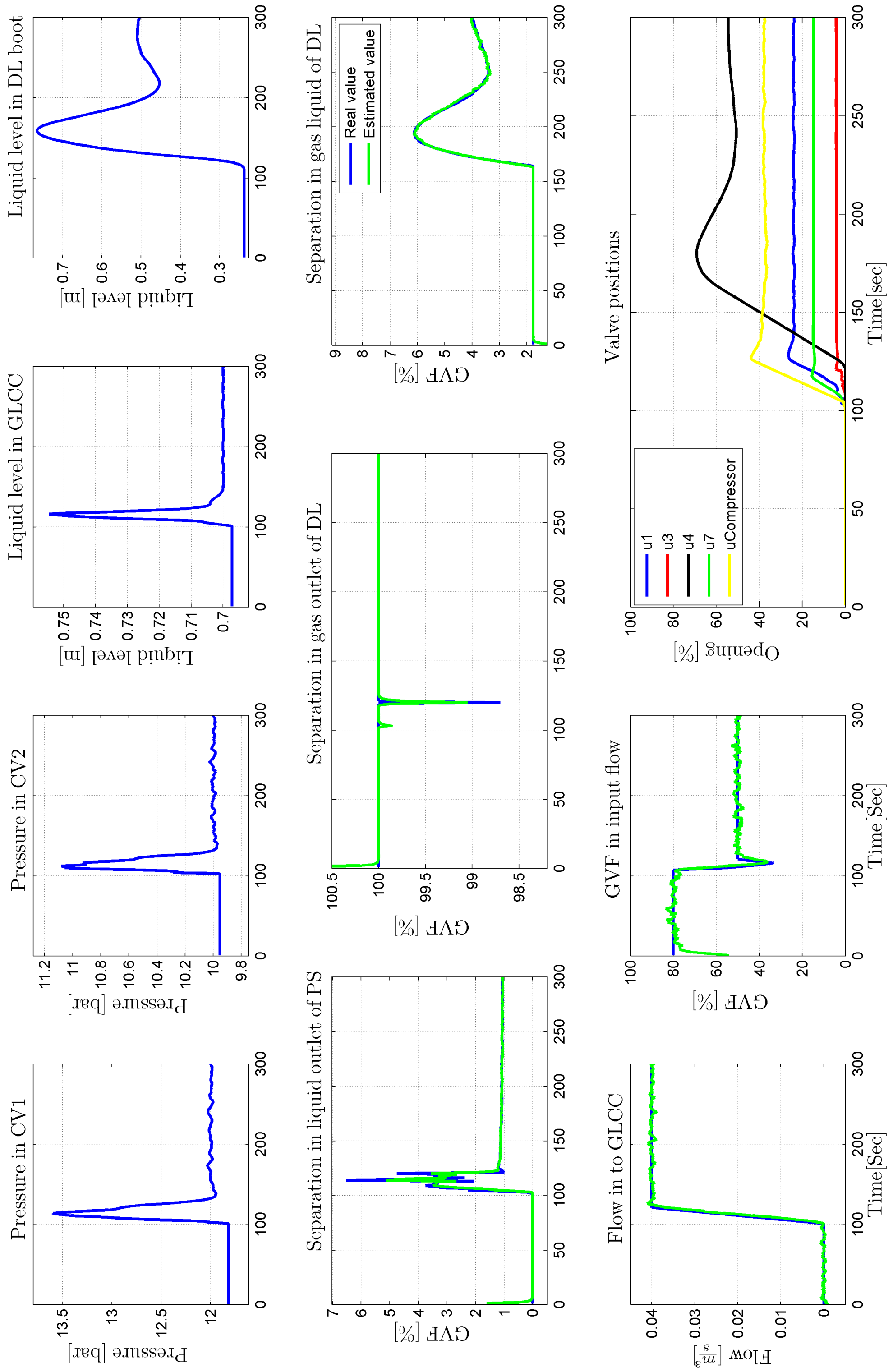

Figure A.2: Planned start-up using NMPC with estimated states from UKF

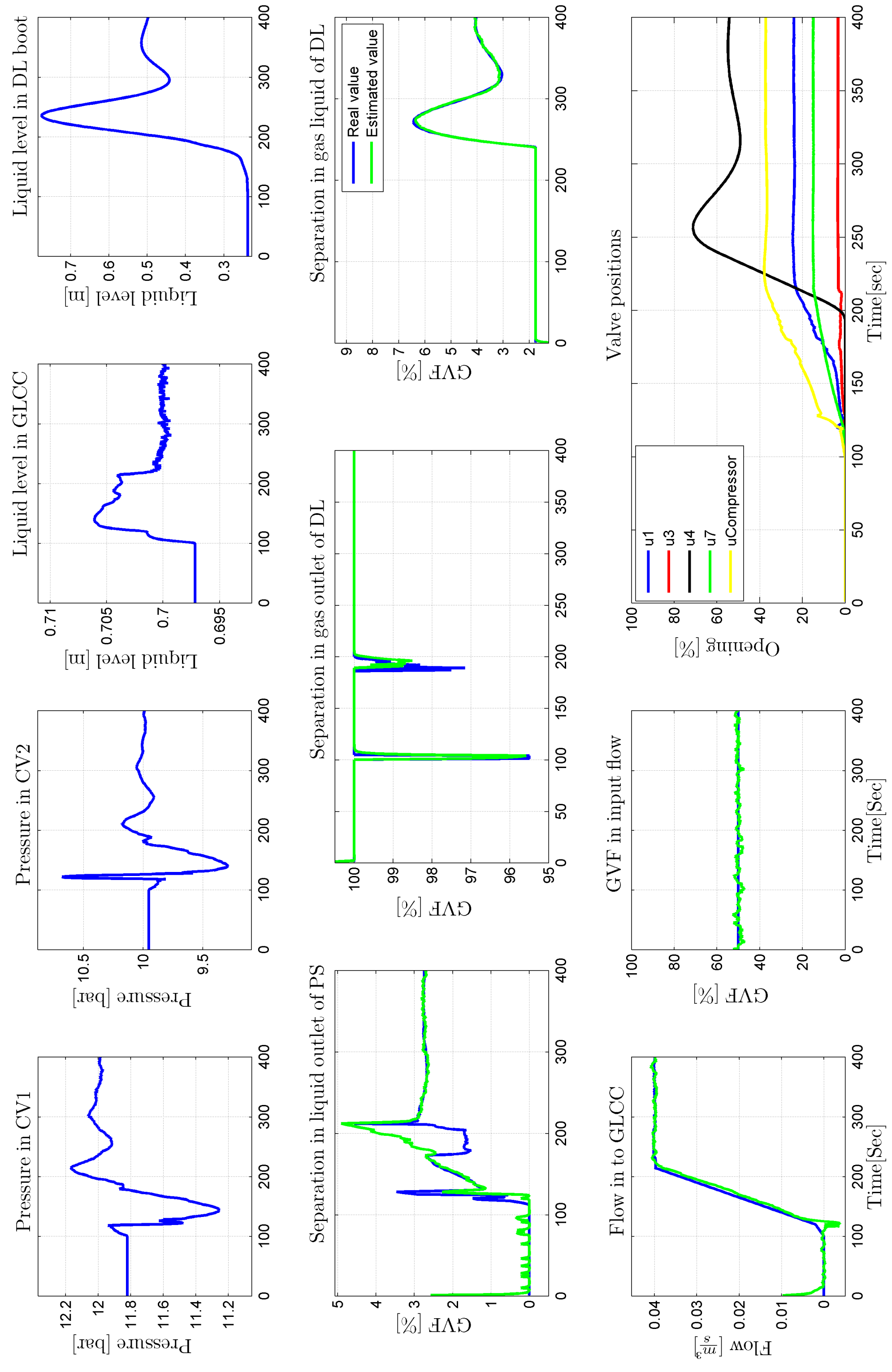

Figure A.3: Start-up using modifed NMPC with estimated states from EKF

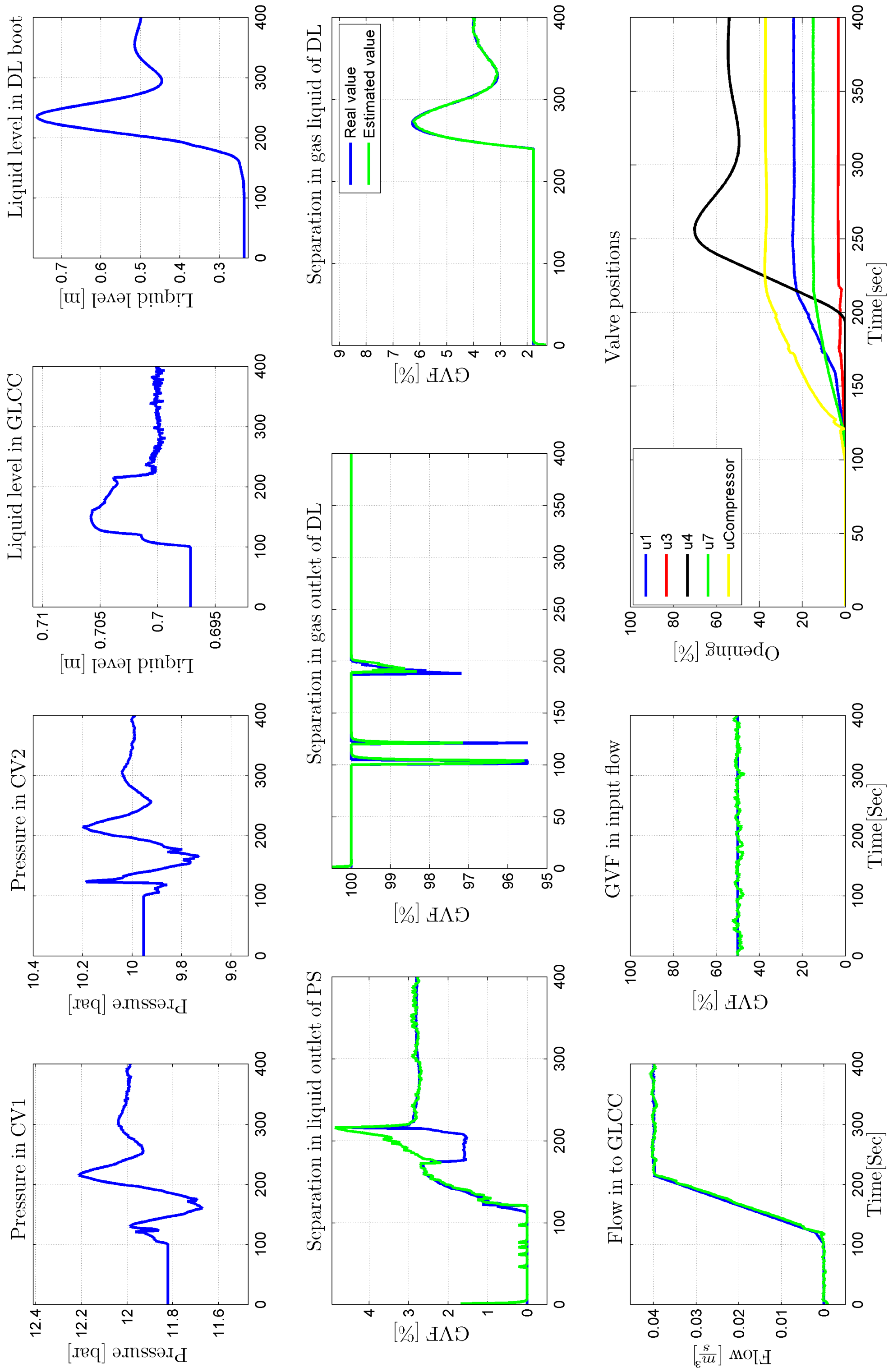

Figure A.4: Start-up using modifed NMPC with estimated states from UKF

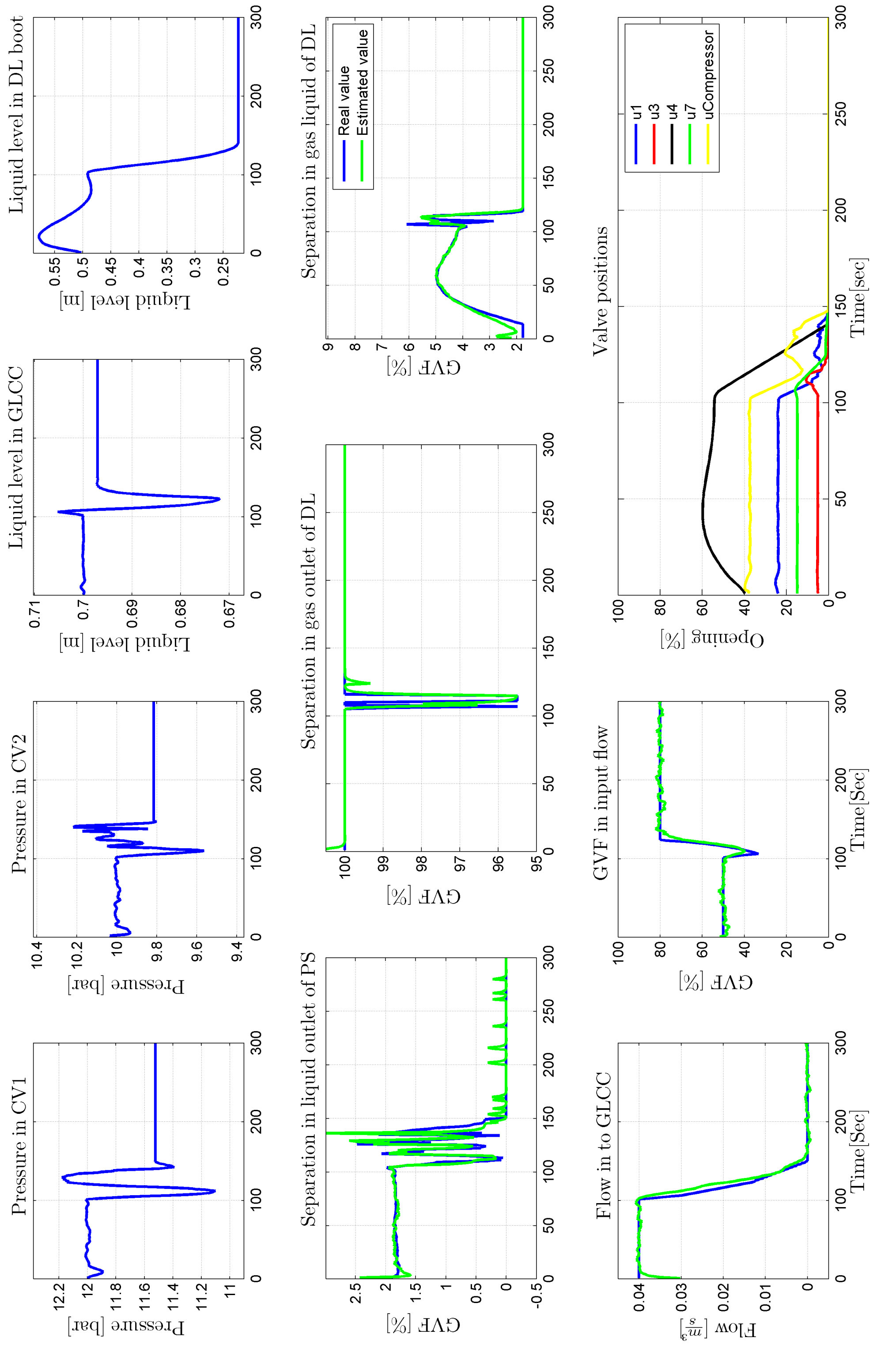

Figure A.5: Planned shut-down using NMPC with estimated states from EKF

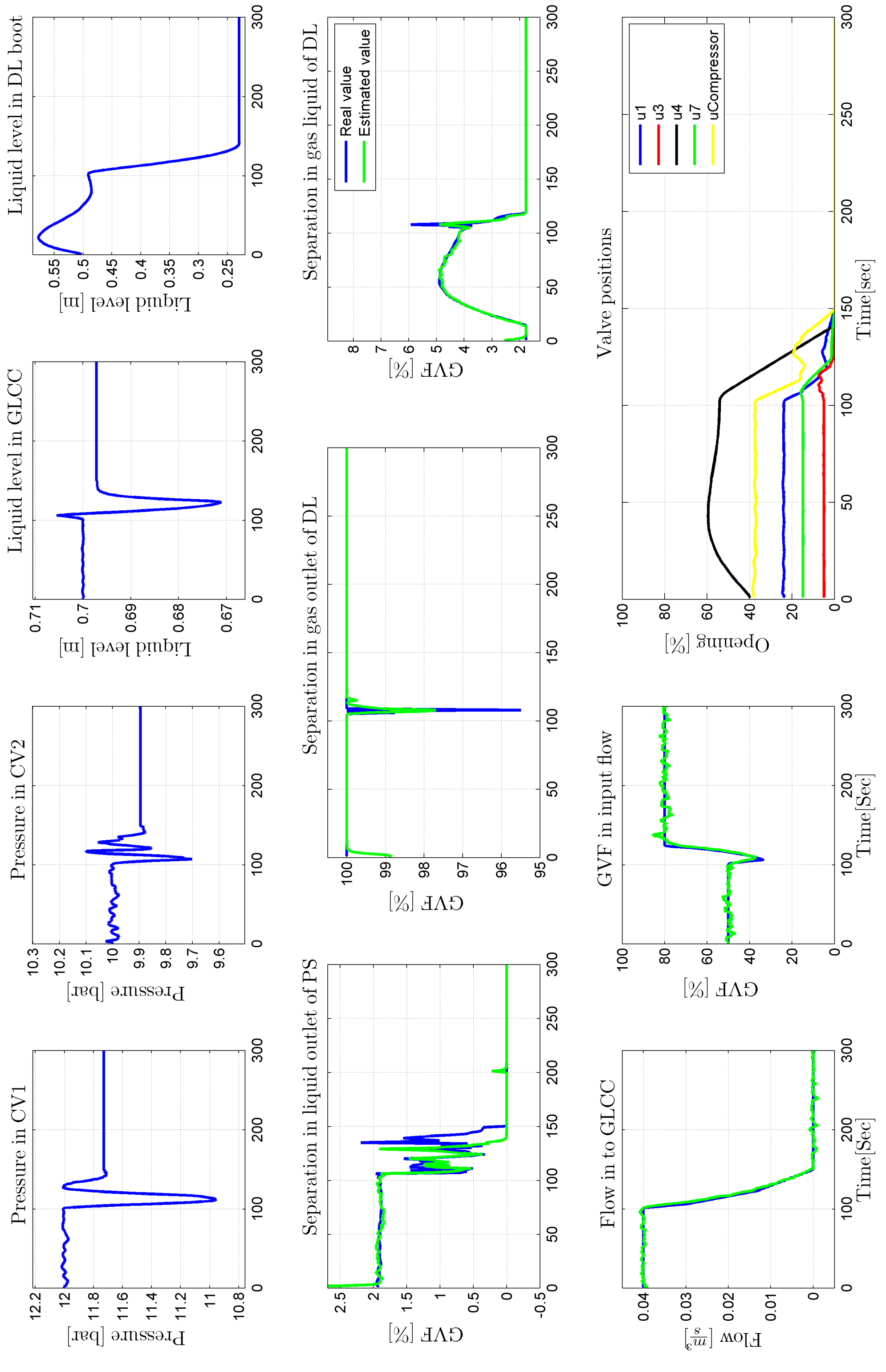

Figure A.6: Planned shut-down using NMPC with estimated states from UKF

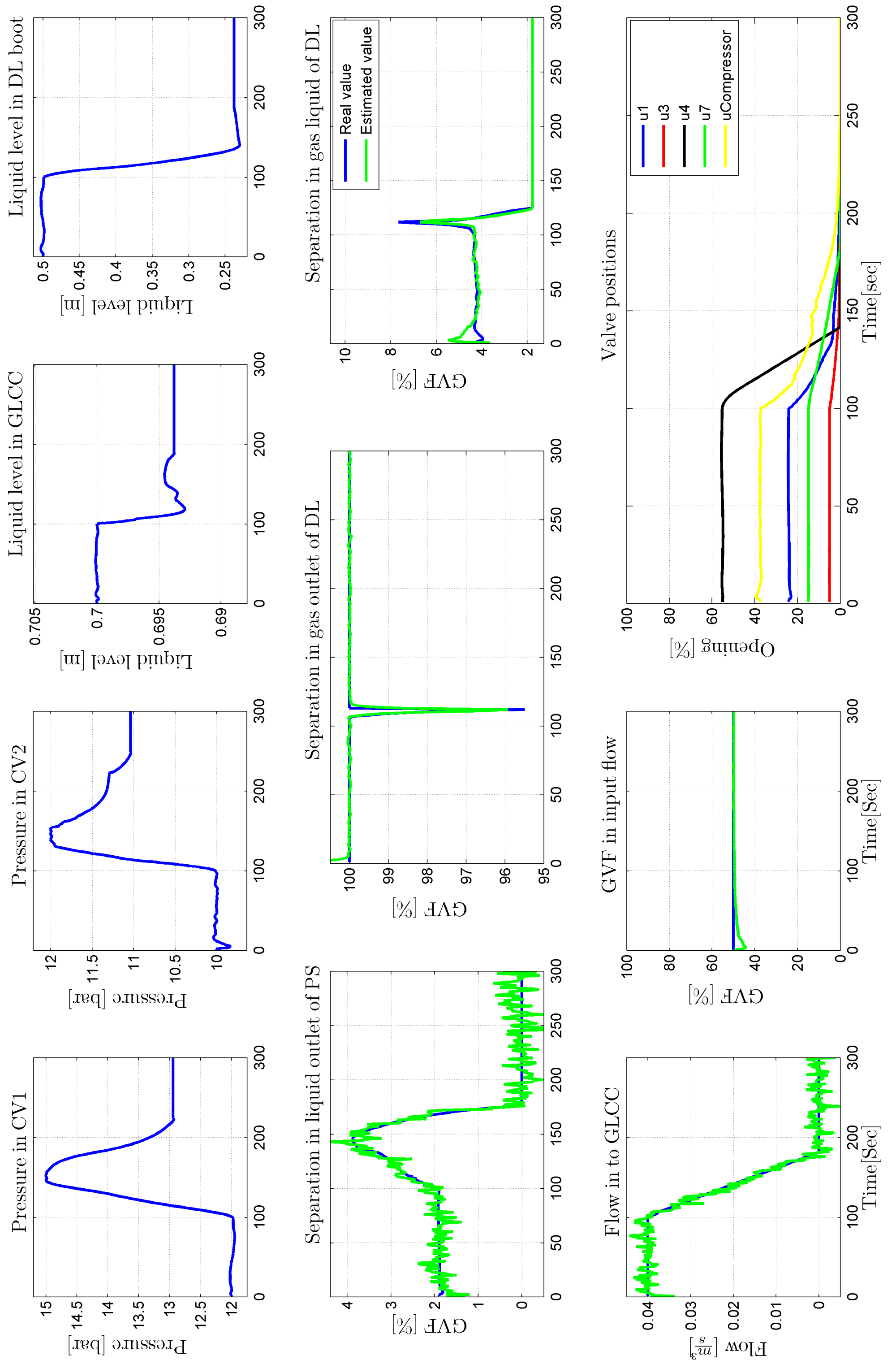

Figure A.7: Shut-down using modifed NMPC with estimated states from EKF

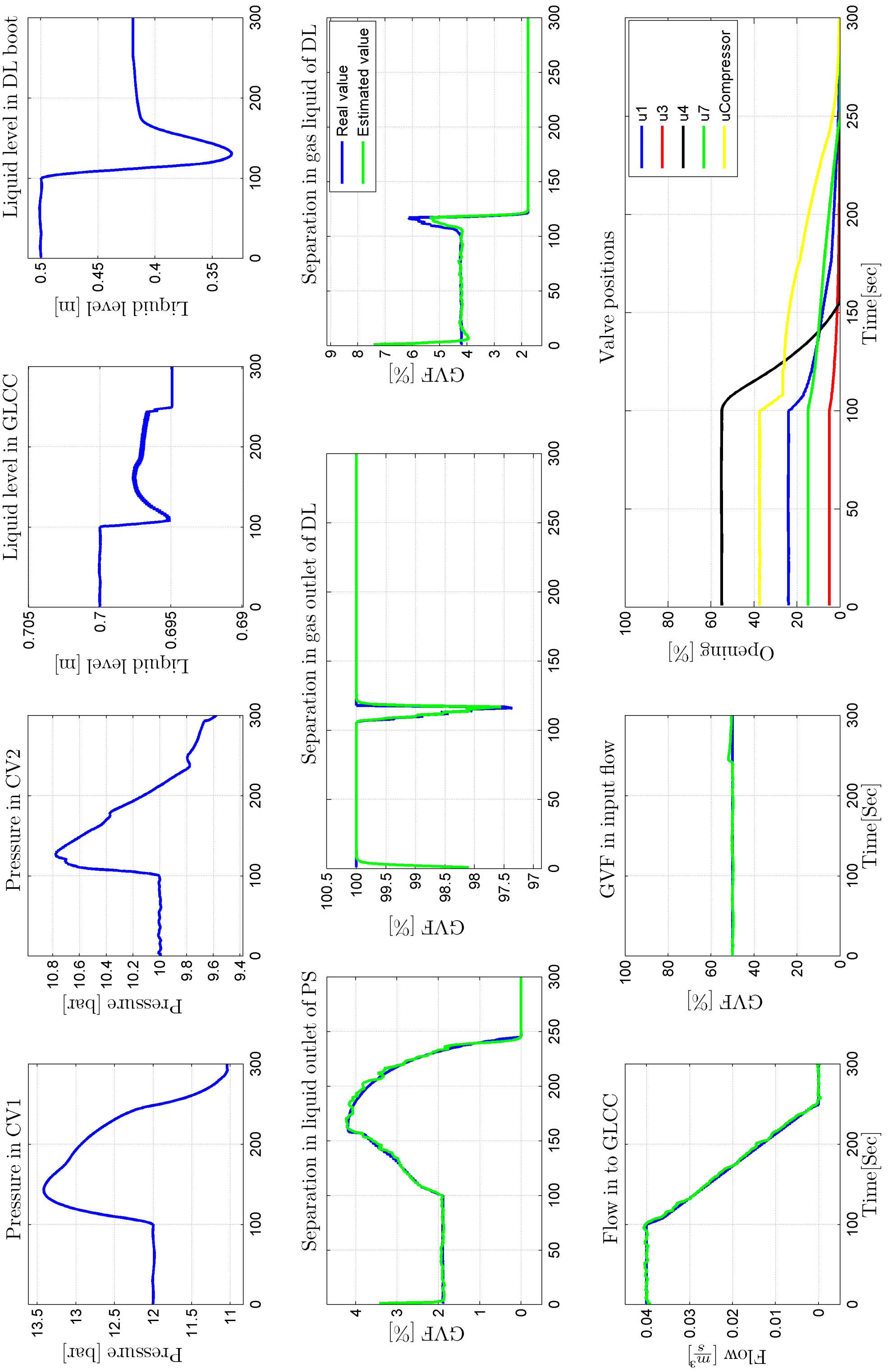

Figure A.8: Shut-down using modifed NMPC with estimated states from UKF